

手排齒輪箱換檔過程之動態模擬分析

研究生：劉彥辰

指導教授：曾錦煥

國立交通大學機械工程學系

摘要

同步器最主要用於手排(MT)與自手排(AMT)汽車變速齒輪箱，其功能在於避免換檔時會產生不正常的齒輪撞擊；此裝置可以確保齒輪於嚙合前，嚙合的齒輪與同步軸套間達同樣轉速，而使嚙合動作能夠平順，並減少齒輪嚙合時未同步所造成的撞擊。因為應用手排齒輪箱的汽車無論是手排或自手排的市場都已漸漸成熟，所以對一個高傳動效率、高換檔性能與低成本同步器的需求，也漸漸受到重視。

本論文針對排檔過程中用於避免齒輪間不正常撞擊的同步器，提出了一個動態模擬分析的模型。此建立於 ADAMS™ 的模型，除了模擬出完整的排檔過程外，更將此完整的排檔過程分割成兩個各別的模組，以協助了解同步軸套與離合齒輪間隨機嚙合的情形，並改善同步器因為機構原件複雜與作動時間短所產生無法在一般實驗過程中完整了解其詳細作動的問題。最後，本論文使用田口設計法進行排檔過程中同步器性能的最佳化，而這樣的結果，除了可以更仔細的協助了解同步器作動過程外，也提供於改善車輛對於手排齒輪箱操作舒適性與同步器使用壽命上的兩大需求。

Dynamic Simulation and Analysis of Shifting Process on Manual Transmission Gearbox

Student: Yen-Chen Liu

Advisor: Ching-Huan Tseng

Department of Mechanical Engineering

National Chiao Tung University

ABSTRACT

The synchronizer is mainly used to avoid the abnormal impact during shifting for manual transmission (MT) and automated manual transmission (AMT) system. This device makes sure that the rotational velocity of transmission gear equals to that of synchronizer sleeve after the synchronization process in order to smooth the process of engagement, and avoid the abnormal impact from different rotational velocity during engaging. Since the development of MT as well as AMT, using manual transmission gearbox, gradually mature recently, a high transmission efficiency, high shifting capability, and low cost of synchronizer is necessary.

The thesis presents dynamic analysis and simulation on synchronizer, which is used to avoid the abnormal impact between different gear ratio during shifting on manual transmission gearbox. Because the complicated mechanism and random engagement of synchronizer are all shrouded in a short time, it is difficult to realize the synchronization process by experiment. Using ADAMS™, the entire shifting process and two minor phase modules, separated from entire shift process, are all constructed for realizing synchronized action and random mesh between sleeve and clutch gear. After verifying results from the simulation model, Taguchi method was used by the thesis to optimize the performance of synchronization. Consequently, the results on this thesis can help to not only understand synchronization process but also provide for improving two major demands on manual transmission gearbox, which are vehicle operational comfort and lifespan of synchronizer.

ACKNOWLEDGEMENT

當得知自己很幸運的可以進入應用最佳化設計實驗室的那天起，我就知道我會有個獨特、充實且難忘的研究所生活；的確，在實驗室學習與生活的兩年中，都證實了我當初的預感是正確的，而我之所以會有這麼充實的兩年，最主要的，都是因為有你們的存在。

碩士論文與學業的完成，首先要感謝的是實驗室的大家長 曾錦煥教授；感謝老師在這幾年間的教導與協助，讓學生無論在課業、生活或是待人處事上都有相當的進步；此外，老師時常將自己的生活經驗與學習過程傳授給學生，讓學生獲益良多，相信這樣的影響將延續到學生往後的求學與生活，謝謝老師。最後，希望老師往後的日子，身體能夠跟心理一樣的自由自在，以將這樣好的實驗室基因傳承給更多的學生。

接下來要感謝在求學過程中，不斷給我鼓勵的父母；上研究所後，回家的時間少了，但家人還是一直不斷的支持我、包容我，此外更提供了一個穩定無虞的求學環境，讓我可以把所有的心力都放在課業上；如今，順利的完成碩士學位，這些成就都將歸功於我的父母，謝謝你們。

應用最佳化設計實驗室，一個充滿笑容與溫暖的實驗室，在這些日子裡，我們留下了很多難忘的回憶，相信這些記憶，都將在畢業之後永遠深藏在我的心中。感謝實驗室的大家，感謝你們的包容，感謝你們的指導，感謝你們帶來的歡笑，更感謝你們的協助，讓我可以快樂、順利的度過研究所兩年的生活，謝謝你們。

感謝論文的口試委員：清華大學蕭教授德瑛、清華大學宋教授震國與交通大學洪教授景華，不辭辛勞的撥冗來擔任學生的論文口試委員，並對學生的論文提出了寶貴的建議與修正，讓學生的論文內容更加充實完整，謝謝你們。

最後，感謝在這兩年來，不斷聽我訴苦與開導我的高中同學們，每當情緒不好時，都是你們不厭其煩的聽我抱怨、跟我談心，讓我能順利的度過每個生活中的不順遂，謝謝你們。此外，更感謝L與S小姐，妳們的出現除了充實了我的生活與讓我有成長外，更趨使我順利的達成了當初在進研究所時所訂下在課業上的目標，謝謝你們。

在兩年的研究所生活中，遇到了之前求學與生活過程中未經歷過的體驗，有歡笑、開心、榮耀，更有挫折、傷心、難過；但還好有你們的存在，我都順利的度過了，謝謝。

TABLE OF CONTENTS

ABSTRACT (IN CHINESE).....	i
ABSTRACT	ii
ACKNOWLEDGEMENT	iii
TABLE OF CONTENTS.....	iv
LIST OF TABLES	vii
LIST OF FIGURES	ix
NOTATIONS	xiii
CHAPTER 1 INTRODUCTION.....	1
1.1 Synchronization Mechanism	1
1.2 Motivations	4
1.3 Thesis Outlines	6
CHAPTER 2 STRUTLESS SYNCHRONIZER.....	8
2.1 Introduction	8
2.2 Components.....	8
2.2.1 Sleeve	10
2.2.2 Hub	11
2.2.3 Annular Spring.....	12
2.2.4 Outer Ring	13
2.2.5 Cone.....	14
2.2.6 Inner Ring	15
2.2.7 Clutch Gear.....	15
2.3 Action of Synchronization	16
2.3.1 Start of Shifting	19
2.3.2 Contact between Sleeve and Annular Spring	19
2.3.3 Yielding Synchronized Torque	23
2.3.4 Synchronizing Relative Rotational Velocity.....	26
2.3.5 Mesh between Sleeve and Outer Ring.....	29

2.3.6 Mesh between Sleeve and Clutch Gear	29
CHAPTER 3 SIMULATION MODEL AND RESULTS	34
3.1 Introduction	34
3.2 Simulation Assumptions	34
3.3 Dynamic Model Creation	36
3.3.1 Units Setting	36
3.3.2 Component	36
3.3.3 Mass and Inertia	37
3.3.4 Joint	37
3.3.5 Contact.....	38
3.3.6 Force	39
3.3.7 Parameter	40
3.4 Entire Model	41
3.4.1 Simulation Conditions and Parameters	42
3.4.2 Simulation Results	45
3.5 Separating Modules	55
3.5.1 Synchronized Module.....	57
3.5.2 Mesh Module.....	59
CHAPTER 4 PARAMETERS ANALYSIS.....	68
4.1 Introduction	68
4.1 Durability on Synchronizer	68
4.1.1 Lubrication and Wear	68
4.1.2 Variation in Coefficient of Friction on Cone	71
4.2 Synchronization Analysis	72
4.2.1 Sleeve Force	73
4.2.2 Cone Angle	74
4.2.3 Stiffness of Annular Spring	75
4.2.4 Coefficient of Friction on Cone Surface.....	78
4.2.5 Remark	84
4.3 Engagement Analysis	84

4.3.1 Tooth Angle	84
4.3.2 Sleeve Force	86
4.3.3 Remark	90
CHAPTER 5 OPTIMIZATION BY TAGUCHI METHOD.....	91
5.1 Overview of Taguchi Method.....	91
5.1.1 Introduction	91
5.1.2 Steps.....	93
5.1.3 Response.....	95
5.2 Formulation of the Problem.....	98
5.2.1 Objective Function/Response.....	98
5.2.2 Factors and Levels.....	100
5.2.3 Orthogonal Array.....	102
5.3 Results and Discussions	104
5.3.1 Simulation Results.....	104
5.3.2 Analysis of Mean (ANOM).....	105
5.3.3 Analysis of Variance (ANOVA).....	108
5.3.4 Confirmation Run and Discussions.....	110
5.3.5 Synchronized Time.....	112
CHAPTER 6 CONCLUSIONS AND FUTURE WORKS.....	115
6.1 Conclusions	115
6.2 Future Works	116
REFERENCES.....	118

LIST OF TABLES

Table 2.3-1 Process of engaged possibilities	32
Table 3.3-1 Units setting on simulation model.....	36
Table 3.3-2 Restrictive relations between all components	37
Table 3.3-3 Contact and coefficient of friction setting.....	39
Table 3.3-4 List of parameters assigning in the model.....	41
Table 3.4-1 Parameters on all gear and shaft.....	42
Table 3.4-2 Reflected inertia transferring from different gear ratio	43
Table 3.4-3 Gear ratio and reflected inertia on each shift	44
Table 3.4-4 Experiment data from Industrial Technology Research Institute (ITRI).....	46
Table 3.4-5 Parameters for simulating shift from gear ratio 1 st to 2 nd	46
Table 3.4-6 List of distinct points during shifting on the parameters as Table 3.4-5	47
Table 3.5-1 Parameters assigned to mesh module.....	59
Table 3.5-2 Parameters assigned to mesh module for shifting from 1 st to 2 nd	60
Table 3.5-3 List of descriptions	64
Table 4.2-1 Parameter study on sleeve force.....	73
Table 4.2-2 Parameter study on cone angle.....	74
Table 4.2-3 Parameter study on stiffness of annular spring.....	76
Table 4.2-4 Parameter study on coefficient of friction.....	78
Table 4.2-5 Parameter study on sleeve force at $\mu_c = 0.61$	80
Table 4.3-1 Simulation results in different tooth angle	85
Table 4.3-2 Simulation results in different sleeve force while tooth angle = 90°	87
Table 4.3-3 Simulation results in different sleeve force while tooth angle = 100°	88
Table 4.3-4 Simulation results in different sleeve force while tooth angle = 80°	89
Table 5.2-1 Control factors and their level of settings for the experiment.....	102
Table 5.2-2 L ₁₆ (4 ⁵) orthogonal array	103
Table 5.3-1 Factors, levels, experimental results and S/N ratio for durability	104
Table 5.3-2 S/N ratio of ANOM at different labels and levels for durability.....	106
Table 5.3-3 Analysis of variance for durability	110
Table 5.3-4 Optimization result for durability.....	110

Table 5.3-5 Experimental result for discussing synchronized time..... 112
Table 5.3-6 S/N ratio of ANOM at different labels and levels for synchronized time 113
Table 5.3-7 Analysis of variance for synchronized time 114



LIST OF FIGURES

Figure 1.1-1 Manual transmission gearbox (Crouse and Anglin, 1985)	1
Figure 1.1-2 Pin type synchronizer (Ore et al., 1995)	2
Figure 1.1-3 Strut type synchronizer (Ore et al., 1995).....	2
Figure 1.1-4 Strutless type synchronizer (Razzacki and Holbrook, 1988).....	3
Figure 1.1-5 Single and double cone synchronizer (Komatsuzaki and Okazaki, 1990)	3
Figure 1.1-6 Single and triple cone synchronizer (Komatsuzaki and Okazaki, 1990).....	4
Figure 2.2-1 A disassembled strutless double cone synchronizer	9
Figure 2.2-2 Sleeve.....	10
Figure 2.2-3 Larger spline on sleeve	11
Figure 2.2-4 Smaller spline on sleeve	11
Figure 2.2-5 Hub	12
Figure 2.2-6 Annular spring	13
Figure 2.2-7 Outer ring.....	13
Figure 2.2-8 Cone.....	14
Figure 2.2-9 Inner ring	15
Figure 2.2-10 Clutch gear.....	16
Figure 2.3-1 Inner structure of transmission gearbox (Crouse and Anglin, 1985).....	17
Figure 2.3-2 Processes of synchronization on strutless synchronizer (Fujiwara, 1991)	18
Figure 2.3-3 General deflection of beam (Fujiwara, 1991).....	19
Figure 2.3-4 Deformation of annular spring (Fujiwara, 1991).....	21
Figure 2.3-5 Section of projecting on larger spline	21
Figure 2.3-6 FBD of sleeve contact with annular spring.....	22
Figure 2.3-7 FBD on cone torque (Socin and Walters, 1968)	23
Figure 2.3-8 FBD of contact between outer ring and sleeve (Socin and Walters, 1968)	25
Figure 2.3-9 Cone and index torque exerting on outer ring and clutch gear	26
Figure 2.3-10 Sketch of synchronization.....	27
Figure 2.3-11 Sketch on transmission gears with number of teeth and inertia.....	28
Figure 2.3-12 Mass and radius of drive wheel on vehicle.....	29
Figure 2.3-13 Processes of sleeve pass through clutch gear (Socin and Walters, 1968).....	30

Figure 2.3-14 Parameters influence different mesh possible	33
Figure 3.2-1 Analytical model of annular spring.....	35
Figure 3.3-1 Coefficient of friction varying with slip velocity (ADAMS™, 2003)	38
Figure 3.4-1 Contour of analytic model on ADAMS™ in different visual angle.....	41
Figure 3.4-2 Generative structure analysis of annular spring.....	44
Figure 3.4-3 Distance of sleeve movement	48
Figure 3.4-4 Relative rotational velocity between hub and transmission gear.....	50
Figure 3.4-5 Relative rotational velocity between outer ring and transmission gear.....	50
Figure 3.4-6 Torque yielded between cone and rings.....	51
Figure 3.4-7 Deformation on annular spring.....	52
Figure 3.4-8 Cone torque and index torque.....	52
Figure 3.4-9 Relative rotational displacement between hub and outer ring.....	54
Figure 3.4-10 Coefficient of friction between cone and rings.....	54
Figure 3.5-1 Distance of sleeve movement with the same conditions in different situation.....	55
Figure 3.5-2 Relative rotational velocity with the same conditions in different situation	55
Figure 3.5-3 Procedure on separating modules.....	56
Figure 3.5-4 Sleeve velocity on synchronized module.....	58
Figure 3.5-5 Angular velocity of clutch gear on synchronized module	58
Figure 3.5-6 Geometric shape on splines of sleeve, outer ring, and clutch gear.....	59
Figure 3.5-7 Mesh angle between sleeve and clutch gear	60
Figure 3.5-8 Scale view on displacement of sleeve for different mesh angle.....	61
Figure 3.5-9 Mesh time with different mesh angle	61
Figure 3.5-10 Mesh description of section 1	62
Figure 3.5-11 Mesh description of section 2	62
Figure 3.5-12 Mesh description of section 3	63
Figure 3.5-13 Mesh description of section 4.....	63
Figure 3.5-14 Displacement of sleeve on sections 1 and 2	65
Figure 3.5-15 Relative rotational velocity on sections 1 and 2	65
Figure 3.5-16 Displacement of sleeve on sections 2 and 3	66
Figure 3.5-17 Relative rotational velocity on sections 2 and 3	66
Figure 4.1-1 Wear rate for various lubrication regimes (Hamrock et al., 1999)	69

Figure 4.1-2 Showing coefficient of friction for various lubrication conditions (Hamrock et al., 1999).....	69
Figure 4.1-3 Cycle #500 of endurance test (Sigl and Höhn, 2003).....	71
Figure 4.1-4 Cycle #100,000 of endurance test (Sigl and Höhn, 2003).....	72
Figure 4.2-1 Cone torque versus time at different sleeve force.....	73
Figure 4.2-2 Relative rotational velocity versus time at different sleeve force.....	73
Figure 4.2-3 Cone torque versus time at different cone angle.....	75
Figure 4.2-4 Relative rotational velocity versus time at different cone angle.....	75
Figure 4.2-5 Cone torque versus time at different stiffness of annular spring	76
Figure 4.2-6 Relative rotational velocity versus time at different stiffness of annular spring .	76
Figure 4.2-7 Sleeve movement versus time at different stiffness of annular spring	77
Figure 4.2-8 Scale view of sleeve movement in Figure 4.2-7.....	77
Figure 4.2-9 Cone torque versus time at different coefficient of friction.....	79
Figure 4.2-10 Coefficient of friction versus time at different coefficient of friction	79
Figure 4.2-11 Relative rotational velocity versus time at different coefficient of friction.....	79
Figure 4.2-12 Cone torque versus time at different sleeve force while $\mu_c = 0.61$	81
Figure 4.2-13 Index torque versus time at different sleeve force while $\mu_c = 0.61$	81
Figure 4.2-14 Difference between cone and index torque.....	81
Figure 4.2-15 Coefficient of friction versus time at different sleeve force while $\mu_c = 0.61$..	82
Figure 4.2-16 Sleeve movement versus time at different sleeve force while $\mu_c = 0.61$	82
Figure 4.2-17 Deformation of annular spring versus time at different sleeve force while $\mu_c = 0.61$	82
Figure 4.2-18 Relative rotational velocity versus time at different sleeve force while $\mu_c = 0.61$	83
Figure 4.3-1 Mesh time versus different mesh angle with different tooth angle.....	85
Figure 4.3-2 Plot the data in Table 4.3-1	86
Figure 4.3-3 Mesh time versus different sleeve force while tooth angle = 90°	87
Figure 4.3-4 Plot the data in Table 4.3-2	88
Figure 4.3-5 Mesh time versus different sleeve force while tooth angle = 100°	88
Figure 4.3-6 Plot the data in Table 4.3-3	89
Figure 4.3-7 Mesh time versus different sleeve force while tooth angle = 80°	89

Figure 4.3-8 Plot the data in Table 4.3-4	90
Figure 5.1-1 Quadratic loss function (Peace, 1993)	92
Figure 5.1-2 Flowchart of the Taguchi method	93
Figure 5.1-3 Smaller-the-better analysis (Phadke, 1989)	97
Figure 5.1-4 Larger-the-better analysis (Phadke, 1989)	97
Figure 5.1-5 Nominal-the-best analysis (Phadke, 1989)	97
Figure 5.3-1 Plots of factor effects in different labels and levels for durability.....	106
Figure 5.3-2 Plots of factors effects in different labels and levels for synchronized time	113

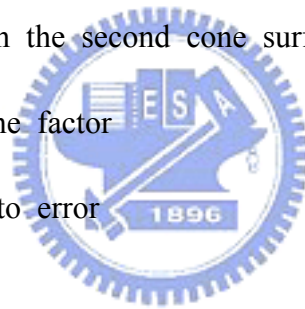


NOTATIONS

A	factor name of ANOM
c	constant on annular spring deformation
CF	correction factor
DV_i	design variable
E	Young's modulus
f	degree of freedom
f_{sa}	friction force between sleeve and annular spring
F	variance ratio
F_{ar}	reaction force acting from outer ring on annular spring
F_{as}	force pushing on larger spline
F_k	pushing force from driver or actuator
F_o	force to over annular spring
F_s	force acting on sleeve for shifting
F_{sM}	maximum shifting force
F_l	force acting on tooth
F_R	force acting on outer ring from sleeve
g_a	gear ratio after shifting
g_b	gear ratio before shifting
i	name of factor
I	sectional secondary moment

I_c	sectional secondary moment inertia of counter shaft and gear
I_d	sectional secondary moment inertia of clutch disk
I_i	sectional secondary moment inertia of i_{th} gear
I_{or}	reflected inertia on objective gear ratio
I_r	reflected initial apply on clutch gear
I_v	total inertia reflected from whole vehicle
k	stiffness coefficient of annular spring
k_s	stiffness coefficient of annular spring on simulation model
K	loss coefficient
l	distance between projection
L	lever ratio from handball to sleeve
m	average of all S/N ratio
m_i	experimental number on p_{th} of factor i
m_{Ai}	average of the i_{th} level of factor A
M	total number of cases on Taguchi method
M_v	mass of the vehicle
n	number of objective function on Taguchi method
n_A	number of the i_{th} level of factor A appear on the orthogonal array
N	normal force between splines
N_i	number of gear teeth on i_{th} gear
N_i'	number of gear teeth on counter shaft of i_{th} gear

N_{sa}	normal force between sleeve and annular spring
N_G	relative rotational velocity
O_i	objective value
P	number of level
P	deflection strength acting on annular spring
r_v	radius of drive wheel
R_b	mesh radius between coupling sleeve and synchronizer ring
R_c	mean cone radius
R_{m1}	mean cone radius on the first cone surface
R_{m2}	mean cone radius on the second cone surface
S	sum of square on the factor
S_e	sum of square due to error
S_i	sensitivity value
S_m	mean of the square sum
S_T	total sum of square
t_{mm}	time on mesh module
t_s	synchronized time
t_{sm}	time on synchronized module
T	target value
T_c	cone torque
T_d	drag torque



T_s	synchronized torque
T_I	index torque
v_s	linear velocity of sleeve
V	moving velocity of sleeve on direction of axis
V_d	friction transition velocity at contact point
V_e	experimental variance
V_i	variance
V_s	stiction transition velocity at contact point
x	distance between sleeve and clutch gear parallel to moving direction of sleeve
y	distance between sleeve and clutch gear vertical to moving direction of sleeve
y_1	objective function on 100 N
y_2	objective function on 200 N
y_i	response of each experimental case
Y	actual measurement
δ	deflection of beam or annular spring
α_o	angular acceleration of output shaft
α_r	angular acceleration of reflected inertia
η	S/N ratio
η_{A_i}	S/N ratio of the i th level of factor A
η_j	S/N ratio at the j th experiment
ρ_i	contribution on factor i

θ_{as}	angle of chamfer on projecting
θ_c	cone angle
θ_g	tooth angle on clutch gear
θ_m	mesh angle between sleeve and clutch gear
θ_r	angle of synchronizer ring chamfer
θ_s	angle of sleeve chamfer
μ_1	lowest coefficient of friction making synchronization finish on 100 N
μ_2	lowest coefficient of friction making synchronization finish on 200 N
μ_{as}	friction coefficient between larger spline and annular spring
μ_b	static coefficient of friction between chamfers of splines
μ_c	coefficient of friction between cone and rings
μ_{cs}	static friction coefficient on cone
μ_d	dynamic coefficient of friction
μ_{de}	difference in coefficient of friction on cone surface
μ_{md}	dynamic coefficient of friction between teeth
μ_{ms}	static coefficient of friction between teeth
μ_s	static coefficient of friction
ω_a	rotational velocity of objective gear ratio after synchronization
ω_b	rotational velocity of objective gear ratio before synchronization
ω_c	rotational velocity of clutch gear
ω_e	engine rotational velocity while starting shift

ω_s rotational velocity on synchronized side

ω_v rotational velocity on vehicle side



CHAPTER 1 INTRODUCTION

1.1 Synchronization Mechanism

Synchronizer is mainly used for lower the abnormal impact during shifting. Both manual transmission (MT) and automated manual transmission (AMT) use this device in vehicle transmission system. This device, used to switch the driving power from one gear ratio to another, is set up on transmission gearbox, as showing in Figure 1.1-1. The synchronized action starts proceeding synchronization while the driver on manual transmission or the actuator on automated manual transmission shifts the gear shift level, and then finish the shifting after sleeve engage with clutch gear (Crouse and Anglin, 1985).

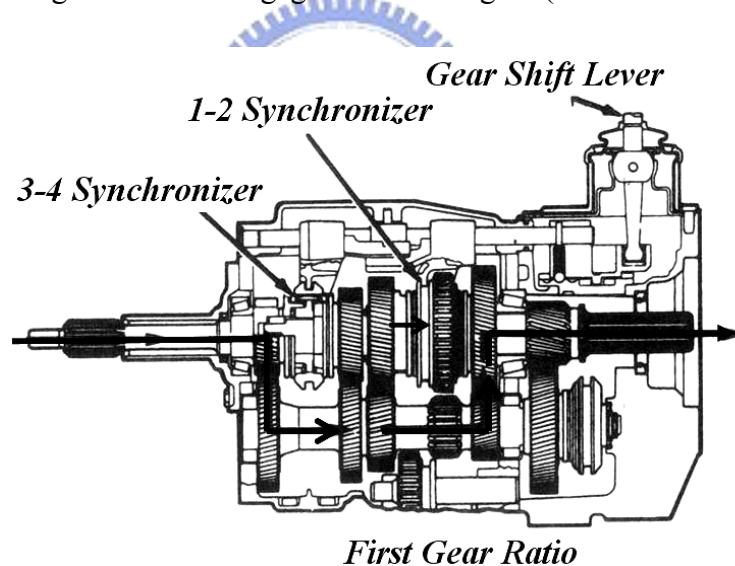


Figure 1.1-1 Manual transmission gearbox (Crouse and Anglin, 1985)

While shifting, driver moves shift knob, which connects to shift part through linkage mechanism, and prompts the starting of synchronization in order to yield synchronized torque to synchronize different rotational velocity. Meanwhile, the rotational velocity of hub, shift part and ring differs from that of cone and clutch gear. The torque, yielded from cone, will diminish the different rotational velocity between these two groups of components. Shifting finishes until splines of shift part engage with clutch gear.

There is a torque that is yielded from contact surface between cone and synchronizer ring while shift. This torque is used to synchronize the relative rotational velocity between transmission output shaft and objective gear as shifting. After finishing synchronization, the relative rotational velocity approach zero, and then the mesh between sleeve and clutch gear occurs for finishing the gear ratio shift.

Seeing that the device had been invented for a long time, there are a lot kinds of synchronizer have already been developed and used in different kinds of transmission gearboxes. Pin type, strut type (Fernandez, 2003; Jackson, 2004) and strutless type (Youk, 2005), shown in Figure 1.1-2, Figure 1.1-3 and Figure 1.1-4 respectively, are the three main types of synchronizer often seen in vehicle market.

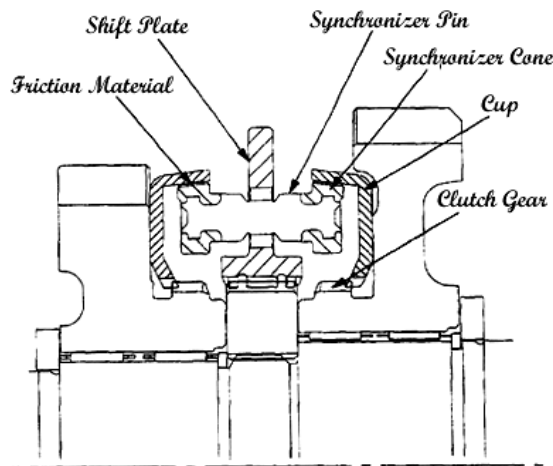


Figure 1.1-2 Pin type synchronizer (Ore et al., 1995)

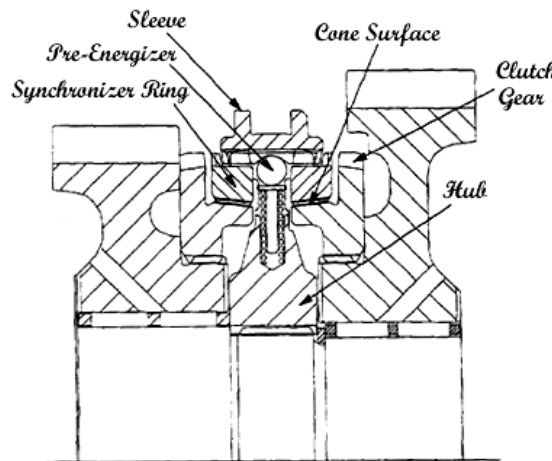


Figure 1.1-3 Strut type synchronizer (Ore et al., 1995)

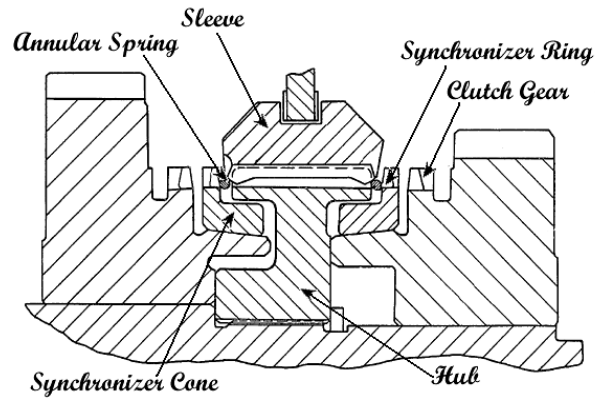


Figure 1.1-4 Strutless type synchronizer (Razzacki and Holbrook, 1988)

These three types of synchronizer only differ from their principle of action; however, reducing the relative rotational velocity and finishing shift are their main purpose in common. Besides, in these different types of synchronizer, there are some components such as hub, shift part (shift plate or sleeve), cone and clutch gear in common within.

In addition to these different kinds of synchronizer, it can be classified into three other types, which are single cone, double cone and multiple cone. These different kinds of synchronizer are separated according to their torque capacity, shown in Figure 1.1-5 and Figure 1.1-6. Generally, the torque capacity of double cone synchronizer is larger than that of single cone synchronizer based on the same size, but the cost of double cones synchronizer is higher than that of single cone synchronizer.

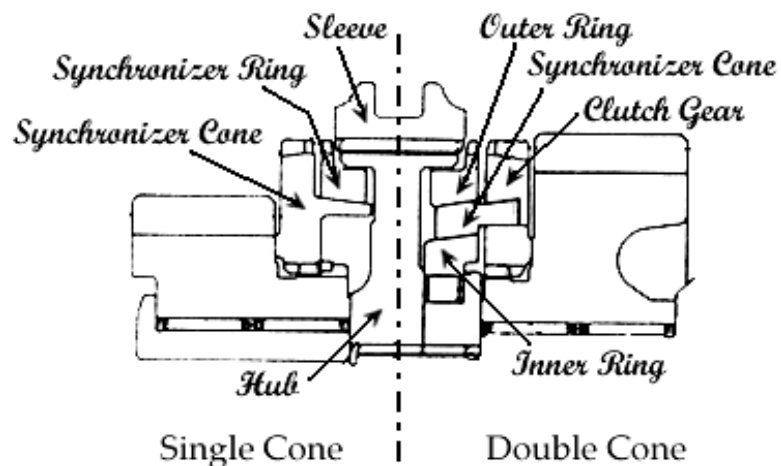


Figure 1.1-5 Single and double cone synchronizer (Komatsuzaki and Okazaki, 1990)

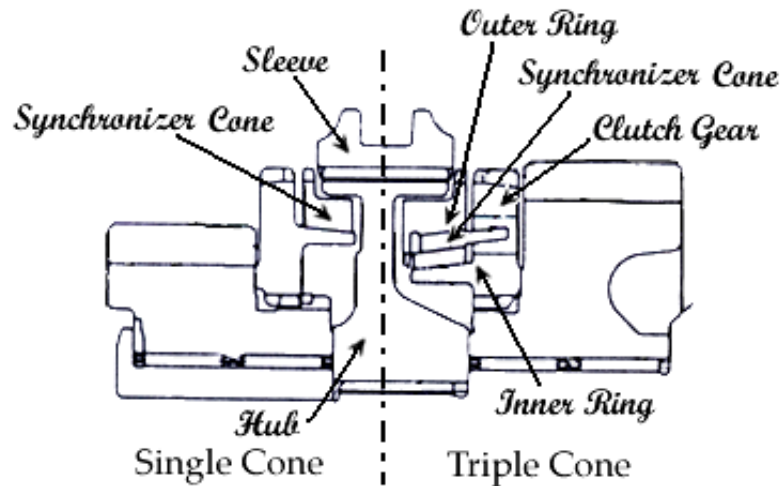


Figure 1.1-6 Single and triple cone synchronizer (Komatsuzaki and Okazaki, 1990)

1.2 Motivations

Synchronizer is mainly used for lower the abnormal impact during shifting on manual transmission gearbox. Both manual transmission (MT) and automated manual transmission (AMT) use this device in vehicle transmission system. For market needs, drivers' demands have risen every year for a better shift ability from the transmission. Feeling of transmission shift influences shift ability directly, and it is one of important elements, which influences the evaluation of vehicle operational comfort. Furthermore, lifespan of synchronizer and shifting time are another aspects that have to pay much attention on while dealing with the research of synchronization. Therefore, the action of synchronization needs to be developed and improved to achieve driver's increasing demands and market needs.

This device, using on manual transmission gearbox, has already been invented for a long time. However, there still exist some aspects on synchronization that need to be developed and investigated, because its complicated mechanism and random mesh all happen in a short time. In order to find out the shifting process, which is complicated and randomized, some researches had dealt with simulation of synchronization in prior studies.

An analytical model of synchronizer was established on ADAMS™ by Hoshino (1998, 1999). This study simulated synchronization process and found out three different shifting speeds that will bring out different process of spline meshing. However, the mesh process between sleeve and clutch gear does not only relate to shifting speed. Besides, the drivetrain, which will also influence synchronization and mesh between sleeve and clutch gear, was not included in this paper.

Another study, discussing with gearshift model simulator in MATLAB®/Simulink®, was developed by Kelly and Kent (2000). This paper divided entire shifting process into five stages, where stage 3 to stage 5 described shifting from neutral to objective gear ratio. This gearshift dynamic modeling gave a picture of the interactions of transmission components influence the shift quality.

Kim et al. (2002) developed a shift feeling simulator for a manual transmission by dividing the whole process into eleven steps which depend on the relative displacement of components. This simulator provided only one possible situation among the mesh possibilities between sleeve and clutch gear from step 9 to step 10.

In this thesis, the model of synchronized mechanism on transmission will be built to find out relationships between components and action of synchronization. This entire shifting process has been divided into six distinct events while sleeve moves from neutral forward to objective gear ratio. Each event will be simulated and checked out the result first, and then the all events were combined to form an entire analysis model. After verifying the tendency of the simulation model, the entire model was divided into synchronized phase and mesh phase module, which were used to simulate the synchronization and the random mesh between sleeve and clutch gear respectively. Moreover, the synchronized phase module can also simulate the phenomenon that when abrasion, which lead into a lower coefficient of friction, happened on cone surface. The results and study of simulation and analysis on

synchronizer, which was presented and constructed by the thesis, can provide a way for improving the performance of shifting and synchronization in the future.

1.3 Thesis Outlines

The simulation model will be constructed on ADAMSTM in this thesis for improving the performance of synchronization mechanism on manual transmission gearbox. Furthermore, the model can simulate all processes, and help to find out the influence on synchronized performance with parameters. Finally, Taguchi method was chosen by the thesis to engage in the design optimization of synchronizer for providing a further clear understanding on synchronization. The brief description of outlines on this thesis contents were given as below.

Chapter 2 proposes the dynamic analysis of synchronization, which will divide the whole process of synchronization into several minor processes and describe these mathematical models respectively for assistance of construction on simulation model.

Chapter 3 will construct a simulation model on ADAMSTM. There are some assumptions assuming in the model that was built by ADAMSTM, and this model can be used to show the action during synchronization. In the end of this chapter, the simulation results will be mentioned and confirmed by matching for phenomenon of physics.

Chapter 4 chooses some parameters to look for the influence of these parameters on the performance of synchronization. The results in this chapter can not only realize the influence of parameters, but also provide the selection of parameters in Chapter 5.

Chapter 5 optimizes the synchronization to find out a better design that can bear a lower coefficient of friction on cone surface, which can raise the lifespan of synchronizer. Taguchi method is used to be engaged in the optimization in the chapter.

Finally, Chapter 6 contains the conclusions and further works, which could assist some aspects for following works, on this study.



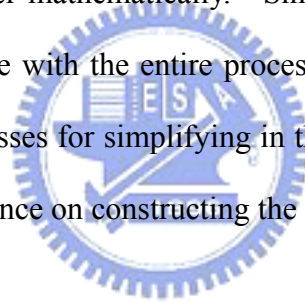
CHAPTER 2

STRUTLESS SYNCHRONIZER

2.1 Introduction

There are so many kinds of synchronizer, which have already been described above, using on different transmission gearboxes for different needs and vehicles. In this study, the simulation model will focus on strutless double cone synchronizer, whose components were shown in Figure 1.1-4. Moreover, the synchronized action and components of this synchronizer will be introduced in this chapter.

After talking about the action and components, the dynamic analysis on shifting process will be discussed in the chapter mathematically. Since the synchronization process is very complicated and hard to debate with the entire process altogether, the entire process will be divided into some minor processes for simplifying in the thesis. These minor processes will be mentioned for giving assistance on constructing the simulation model.



2.2 Components

The system of a strutless double cone synchronizer consists of seven components; all of these components have their respective different functions, which will be introduced in this subsection.

These seven components, shown in Figure 2.2-1, are listed as below with the simple description of their general function.

- (1) Sleeve – Moveable element on the transmission that accomplishes gear lockup to the output shaft, and leads outer ring through the chamfers.
- (2) Hub – External spline element that is attached to the output shaft where sleeve and cone pilot.

- (3) Annular spring – Initial energizing element that mounts on outer ring, and provides the initial load from sleeve to obtain synchronized torque.
- (4) Outer ring – Element that includes external teeth and friction surface, this is used for yielding synchronized torque while shifting, and is that used for contacting and engaging with spline on sleeve.
- (5) Cone – Element, which rotates with clutch gear, being used to provide synchronized torque.
- (6) Inner ring – Friction element, which can yield synchronized torque while contact with cone, rotating with outer ring.
- (7) Clutch gear – Element connecting with cone and providing drive power through gear on final lockup after sleeve engage with it.

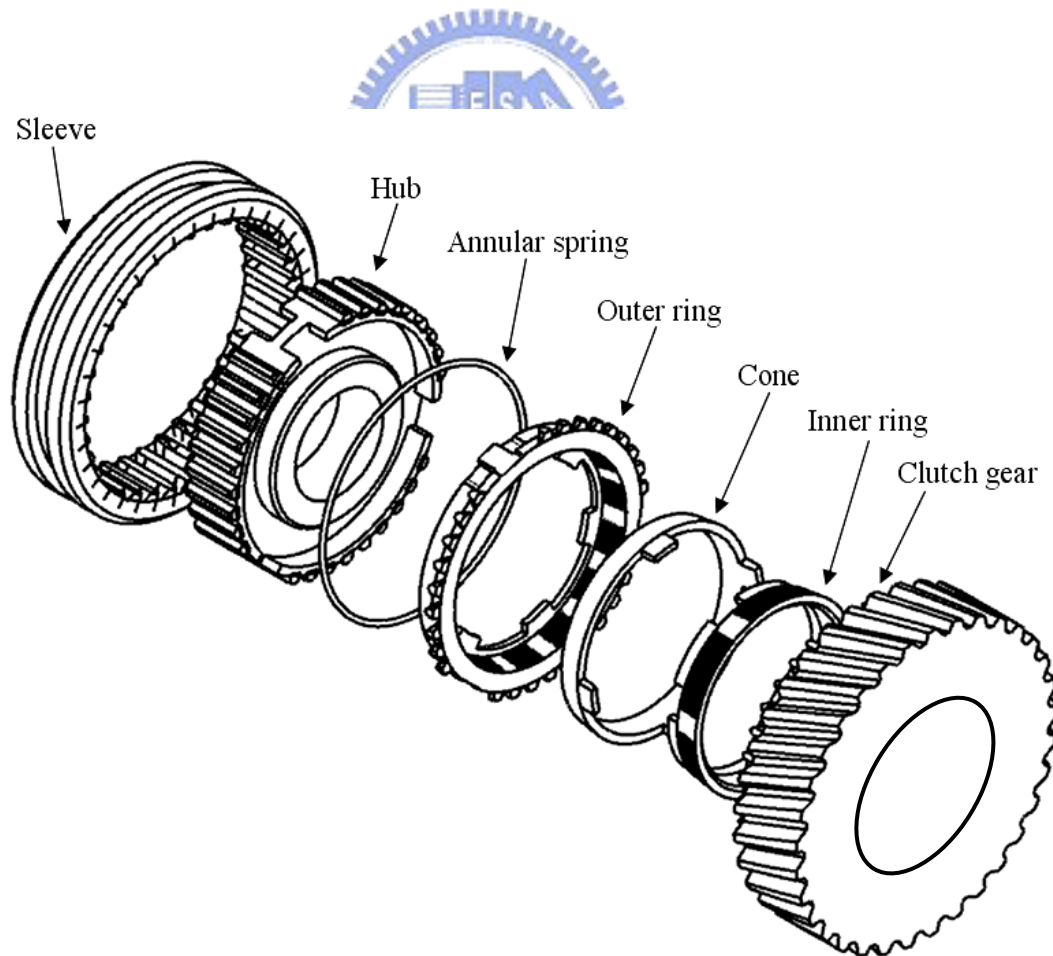


Figure 2.2-1 A disassembled strutless double cone synchronizer

2.2.1 Sleeve

Sleeve is the most significant component on synchronizer, because most of other components all relate to sleeve during the shifting process. There are 36 splines, which are divided into smaller spline, normal spline, and larger spline, arranging on sleeve with 10 degrees included angle. All these three kinds of splines on sleeve and larger spline are shown in Figure 2.2-2 and Figure 2.2-3 respectively. These three kinds of spline are arranged on inner surface of circular ring with a sequence of two larger splines, four normal splines, two smaller splines, four normal splines, and two larger splines, and then repeating this order until splines fill up the ring.

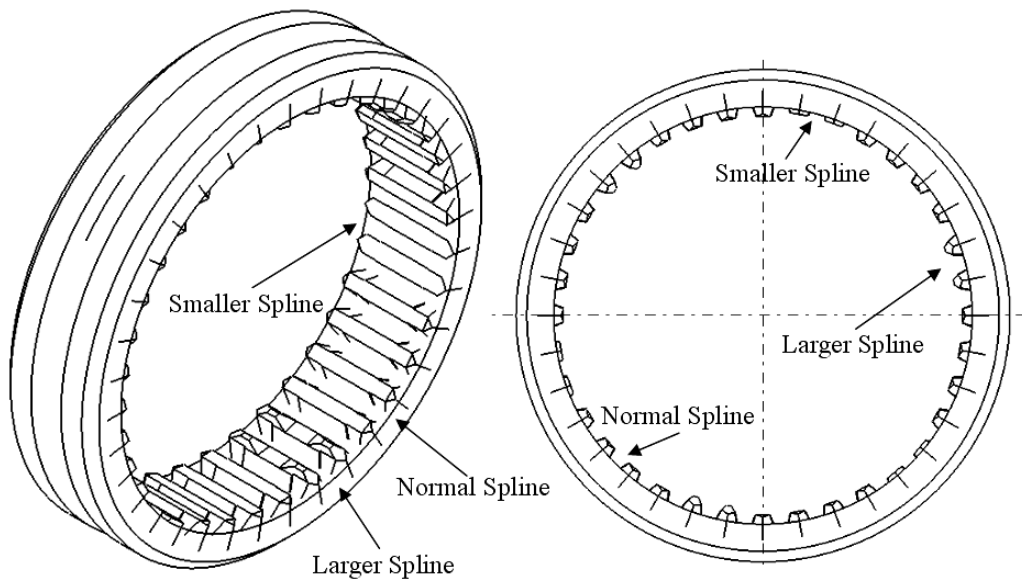


Figure 2.2-2 Sleeve

Engaging with hub, teeth of outer ring and clutch gear are the main and identical function of these three kinds of splines. Besides, the projecting on larger spline are used to contact with annular spring; it is used to push outer ring to move toward to the objective gear ratio, and yield synchronized torque to reduce the relative rotational velocity between sleeve and clutch gear. There is only larger spline has projecting, which can be clearly and easily recognized between Figure 2.2-3 and Figure 2.2-4.

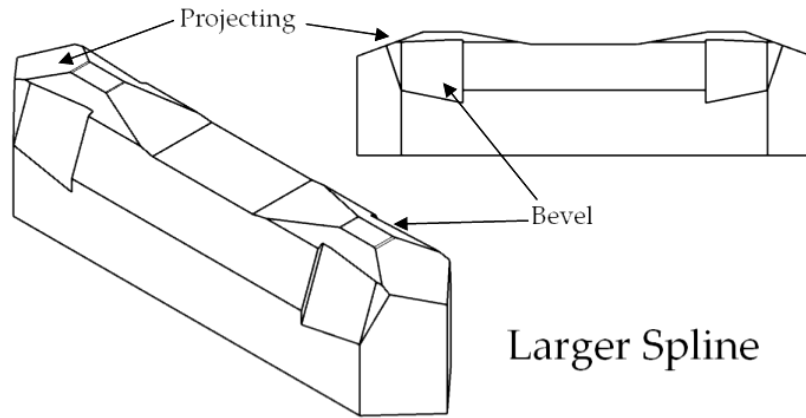


Figure 2.2-3 Larger spline on sleeve

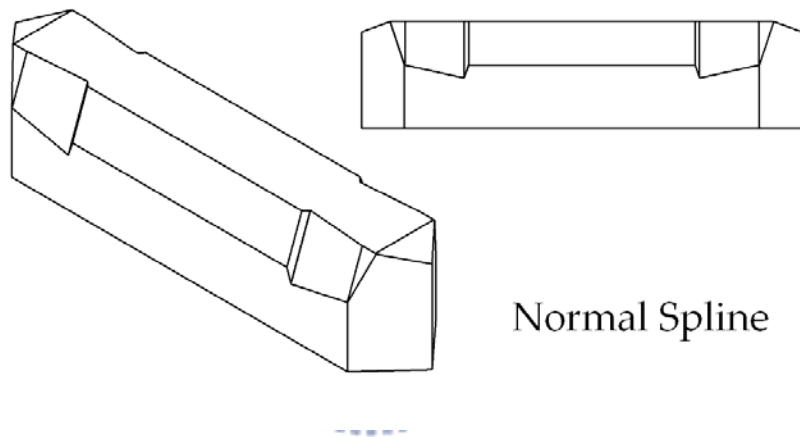


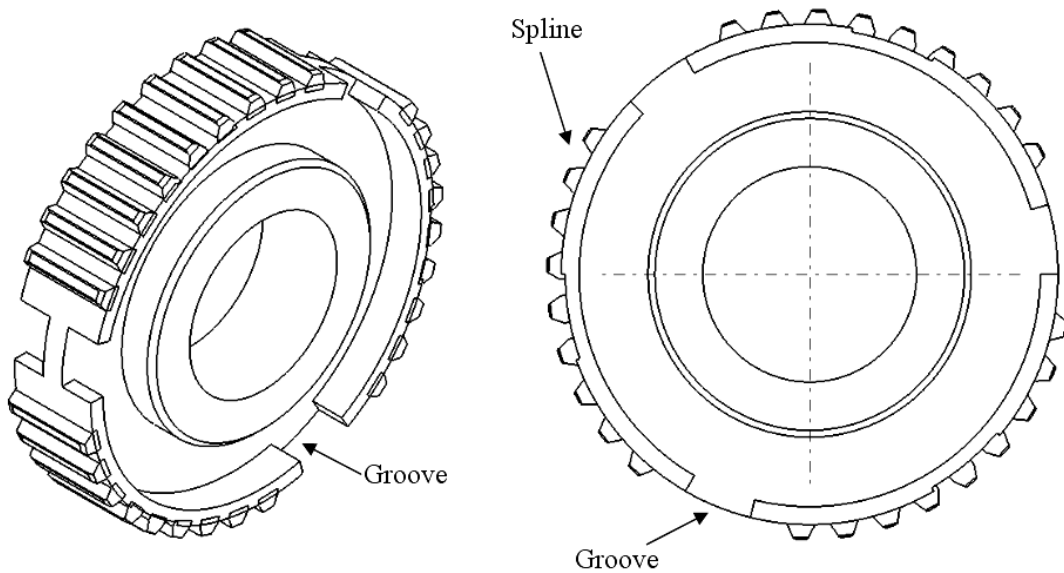
Figure 2.2-4 Smaller spline on sleeve

Furthermore, there is a bevel, used to avoid sleeve sliding out and coming up transmission jumps out of gear after finishing shift, arranged on each side and head of splines on these three kinds of splines. Besides, there is an annular groove, which provides fork to fix on it and transfers the moving force exerting from shift knob by driver, on the outside of sleeve.

2.2.2 Hub

Hub is fixed on output shaft for transferring power from each gear to differential for driving the vehicle. Moreover, there are 27 splines and 6 grooves, which are arranged on annular outer surface and each side of hub respectively, mounted on a hub, as showing in

Figure 2.2-5. Splines, being used to engage with sleeve, are all similar to each other on hub. Besides, these grooves fit for projections on outer ring to confirm that outer ring can only rotate in certain limited angle with hub, and translate in direction of axis on output shaft.



2.2.3 Annular Spring

Annular spring, which can move in direction of axis, is mounted on outer ring and shown in Figure 2.2-6. To transfer moving force from sleeve to outer ring, and prompt to yield synchronized torque are main functions of annular spring. This phenomenon, due to annular spring, can increase the time of sleeve passing through outer ring for keeping synchronized torque to reduce the relative rotational velocity, and avoid sleeve pass through outer ring without finishing synchronization.

While the projecting on larger spline of sleeve contacts with annular spring, the contact force between them causes the deformation of annular spring and action of annular spring, then it forces outer ring to move forward clutch gear for yielding synchronized torque, which is used to synchronize different rotational velocity.

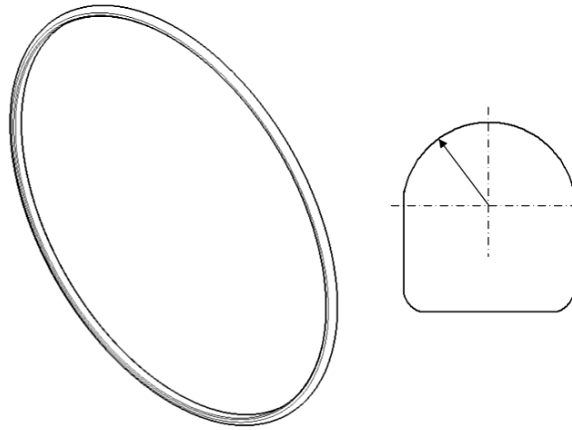


Figure 2.2-6 Annular spring

2.2.4 Outer Ring

As showing in Figure 2.2-7, an outer ring includes three projections and 27 external teeth, which are used to contact and engage with sleeve while synchronization. These three projections are collocated with three grooves of hub for limiting the rotational angle of outer ring, and reducing the impact of engaging between sleeve and outer ring.

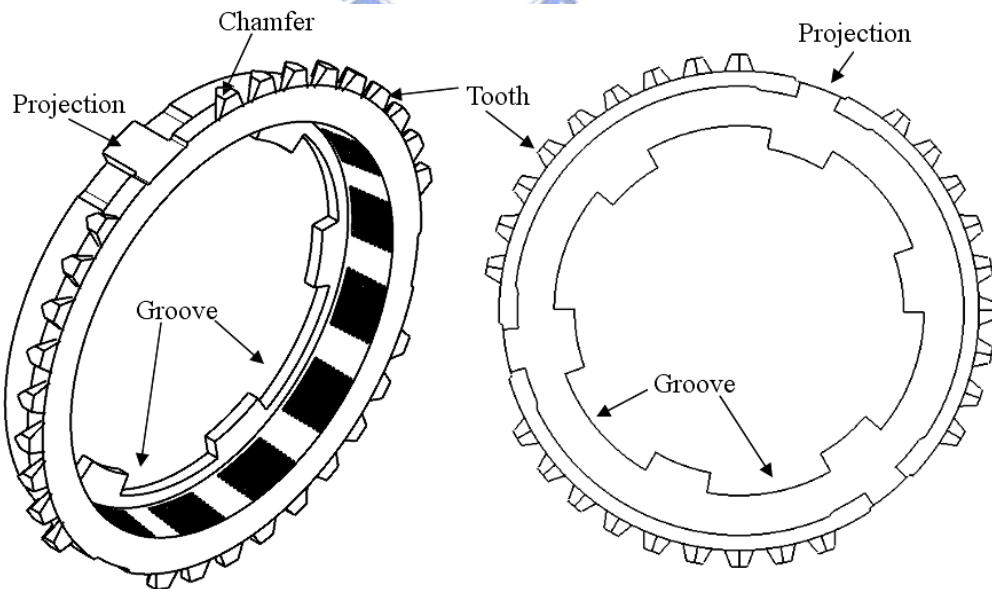


Figure 2.2-7 Outer ring

There are two chamfers, facing to sleeve and hub, mounted on every tooth of outer ring. These chamfers are used to contact with spline on sleeve for yielding index torque, which can

force sleeve not to engage with outer ring before finishing synchronization. In addition to teeth and projections, there are six grooves, which are used for arranging inner ring on its inside, and limiting inner ring to rotate with it, are disposed on outer ring. Besides, there are a number of threads collocated on the inner surface of outer ring for contacting with cone to yield synchronized torque.

The gap between inner surface of outer ring and outer surface of cone will decrease while outer ring moves toward cone; meanwhile, lubricant will be brained out along these threads to make the coefficient of friction rise rapidly to yield a higher synchronized torque. The detail process of contacting between cone and rings will be particularity mentioned in the following chapters.

2.2.5 Cone

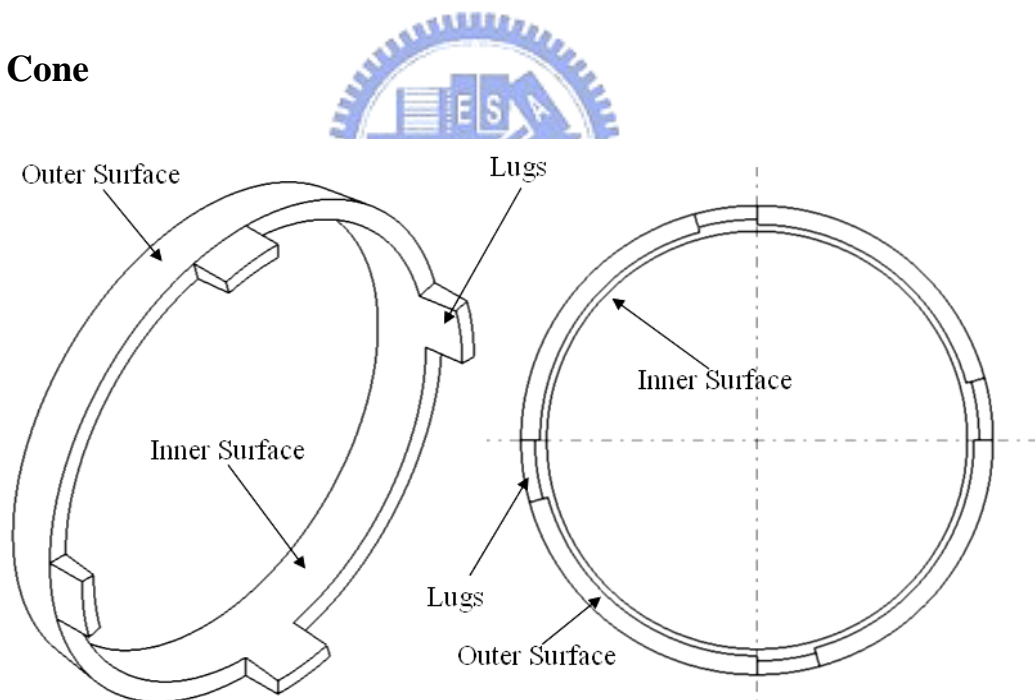


Figure 2.2-8 Cone

A cone includes three different portions, which are outer surface, inner surface and lugs, as showing in Figure 2.2-8. Outer and inner surface are used to contact with outer ring and inner ring for yielding cone torque respectively. Moreover, lugs can ensure cone rotating with clutch gear, and moving in direction of axis on it by putting on holes of clutch gear.

2.2.6 Inner Ring

An inner ring includes six lugs that are collocated to six grooves of outer ring for keeping outer ring rotating with inner ring and moving in direction of axis, shown in Figure 2.2-9. Besides, there is an outer surface, on which a number of threads arrange, used to contact cone for yielding cone torque. These threads, many tiny long grooves, can drain lubricant away, and provide a higher coefficient of friction for cone torque just like the function in outer ring.

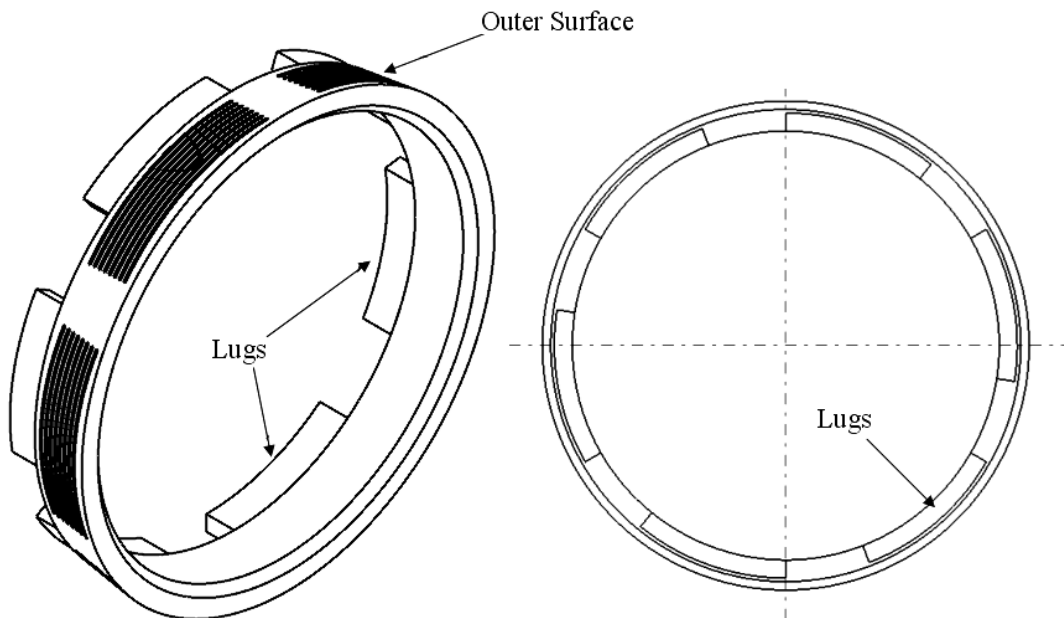


Figure 2.2-9 Inner ring

2.2.7 Clutch Gear

The last component, named as clutch gear, consists of transmission gear, four holes and clutch gear, where the clutch gear is used to engage with spline on sleeve, as showing in Figure 2.2-10. Engaging with counter gear for transferring power from it to output shaft through specific gear ratio is the main purpose of transmission gear. Furthermore, the action of shifting finishes while clutch gear accomplishes the engagement with sleeve.

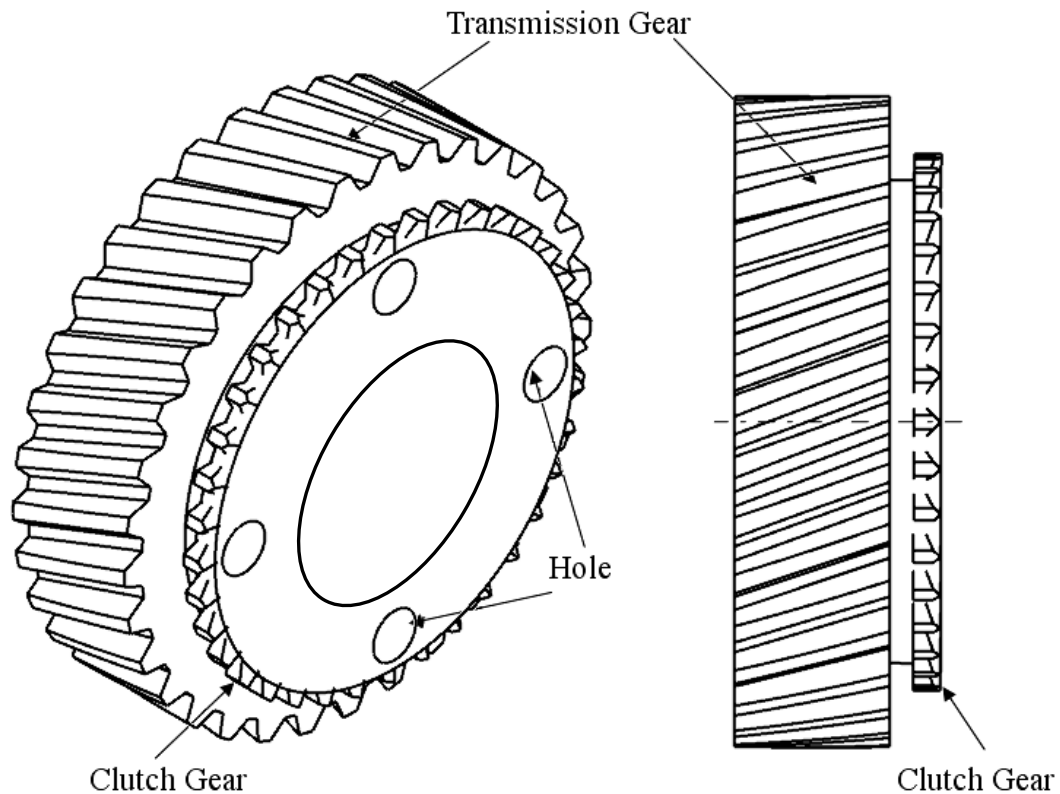


Figure 2.2-10 Clutch gear

2.3 Action of Synchronization

After talking about the descriptions of all components on strutless double cone synchronizer, the action of synchronization will be discussed in this section.

Reducing the relative rotational velocity between output shaft and input gear ratio is the major function of synchronizer. Until sleeve engages with clutch gear of objective gear ratio, synchronizer starts transferring power from input shaft to output shaft through the objective gear. The inner structure of a manual transmission gearbox is shown in Figure 2.3-1.

In a gearbox, the gear and other moving metal parts must not touch. A thin film of lubricant must continuously separate them; this prevents excessive wear and early failure. Therefore, a gearbox runs partially filled with a lubricant or gear oil. However, the lower coefficient of friction due to lubricant is too low to yield enough torque for synchronization, so a synchronizer needs to drain lubricant out while yielding cone torque.

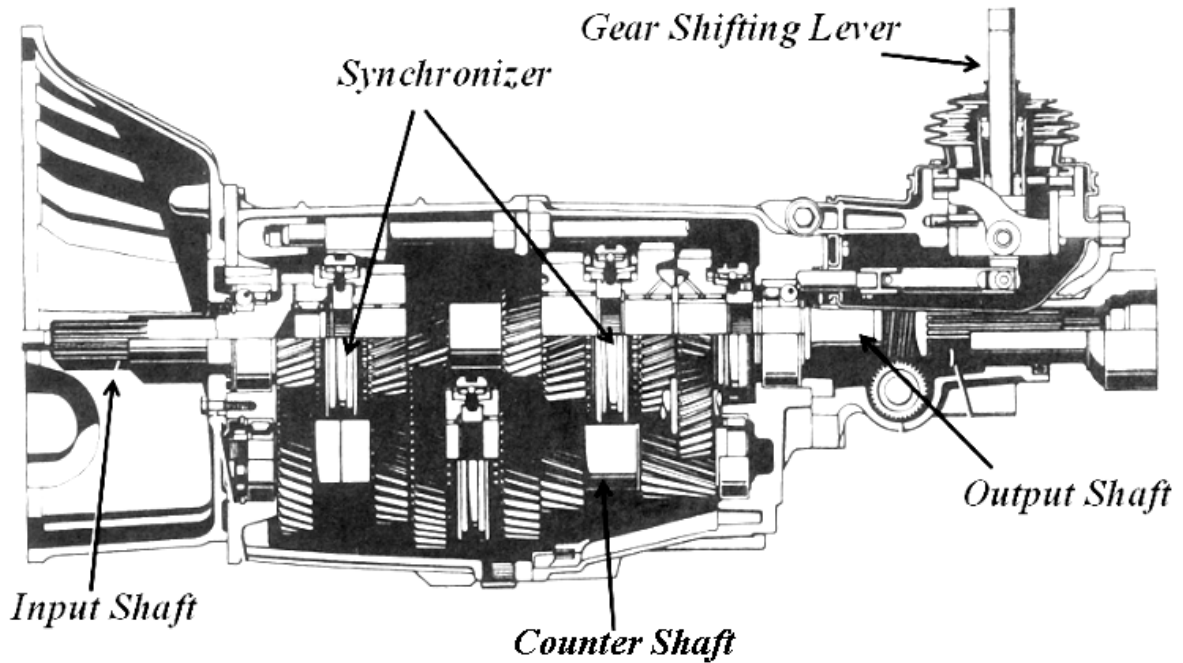


Figure 2.3-1 Inner structure of transmission gearbox (Crouse and Anglin, 1985)

In the process of synchronization, driver moves gear shifting lever from neutral position toward the objective gear ratio position. The movement of gear shifting lever will push sleeve moving from neutral position toward clutch gear, because of fork that connects gear shifting lever with sleeve, as showing in Figure 2.3-1. Besides, sleeve can only rotate with hub and move in the direction of axis, since spline of sleeve meshes with hub.

Firstly, sleeve moves until larger splines contact with annular spring, then annular spring will push outer ring to contact with cone on the contact surface between outer ring and cone, and yield the first synchronized torque. At the same time, cone will immediately move toward inner ring and decrease the gap between them for yielding second synchronized torque. A double cone synchronizer can yield torque twice as larger as a single cone synchronizer, since there exists two contact surfaces that are used to provided synchronized torque.

As the continued move of sleeve, splines of sleeve will contact the teeth of outer ring for yielding index torque, which is used to obstructed sleeve for avoiding abnormal impact occurring between sleeve and clutch gear before finishing synchronization. Until sleeve and

clutch gear achieve synchronous rotational velocity, sleeve moves forward to engage with outer ring and pass through it. Then, sleeve continues moving forward to clutch gear, and engaging with it for transferring power from engine to wheel, and then drive the vehicle. The whole synchronization processes is shown in Figure 2.3-2, and these similar actions take place in synchronizer as being used for other gears.

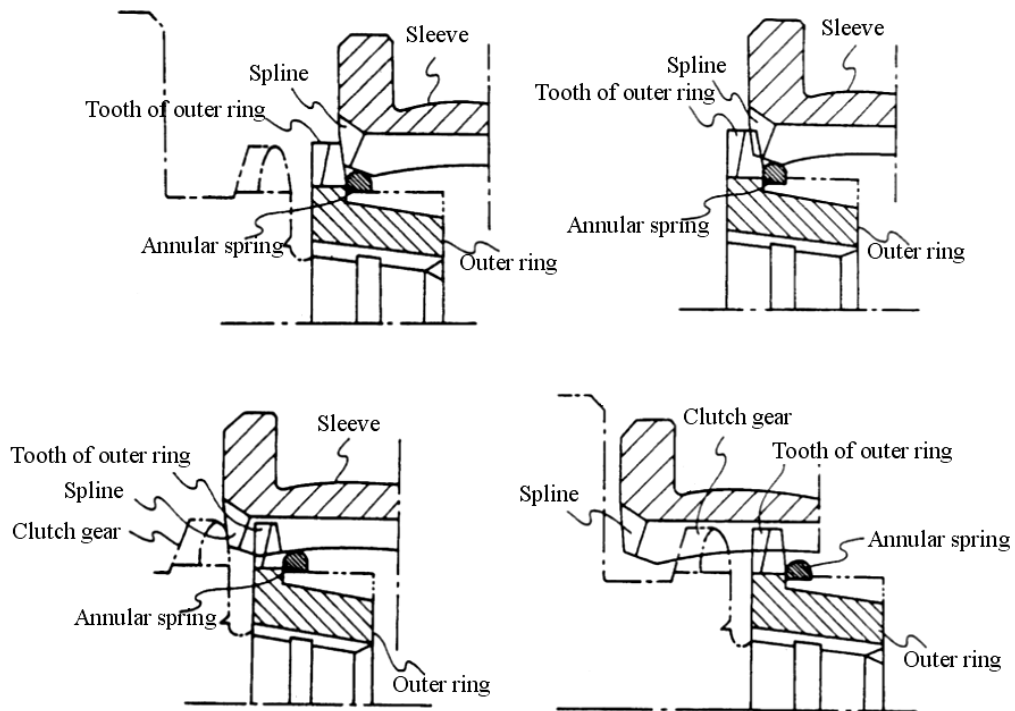


Figure 2.3-2 Processes of synchronization on strutless synchronizer (Fujiwara, 1991)

The process of synchronization can be divided into several distinct minor processes while driver pushes the shift knob from neutral position to the objective gear ratio until the finish of synchronization (Razzacki, 2004).

- (1) Start of shifting
- (2) Contact between sleeve and annular spring
- (3) Yielding synchronized torque
- (4) Synchronizing relative rotational velocity
- (5) Mesh between sleeve and outer ring
- (6) Mesh between sleeve and clutch gear

The following subsections in this chapter will mention about the dynamic analytic model mathematically.

2.3.1 Start of Shifting

Driver pushes shift knob from neutral position toward objective gear ratio for starting the action of synchronization. The pushing force F_h will be transferred through lever ratio L to yield sleeve force F_s , which acts on sleeve for proceeding the shifting process, as showing in Eq. (2.3-1).

$$F_h = \frac{F_s}{L} \quad (2.3-1)$$

Sleeve force F_s will lead the entire action of synchronization, and it will be often considered in the following subsections of minor processes.

2.3.2 Contact between Sleeve and Annular Spring

After sleeve moves a certain distance from neutral position, the projectings on larger spline of sleeve will contact with annular spring first. This contact results in movement of outer ring, and drives to yield synchronized torque for synchronization. In this subsection, annular spring will be discussed before the discussion about the relation between annular spring and sleeve.

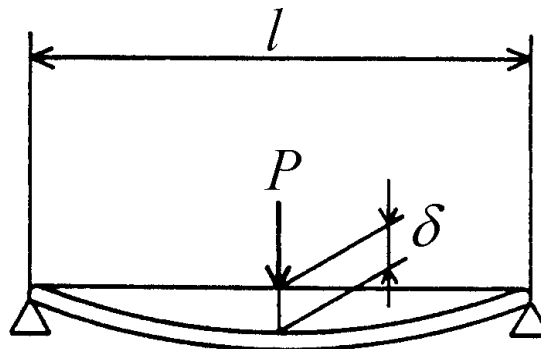


Figure 2.3-3 General deflection of beam (Fujiwara, 1991)

Annular spring can be simplified as deflection strength P of the beam, which is generally expressed and shown in Figure 2.3-3. The equation is

$$P = 48 \times \frac{EI\delta}{l^3} \quad (2.3-2)$$

where E is Young's modulus, I is sectional secondary moment, δ is deflection and l is distance between fulcrums.

If the same deflection amount is applied to the beam, having the same cross section, the deflection strength P is inversely proportional to a triple ratio, so that the variation of the deflection strength P caused by varying the distance between the fulcrums becomes excessively large. Annular spring is mounted on outer ring through three projections, which can divide annular spring into three equal parts, as showing in Figure 2.3-4. According to the force diagram and deformation of annular spring, it can be simplified as Figure 2.3-4, and the equation can be established as

$$P = c \times \frac{EI\delta}{l^3} = k\delta \quad (2.3-3)$$

where c is constant, and k is the stiffness coefficient of annular spring.

The force, that annular spring pushes outer ring, is according to the deformation of annular spring. Moreover, there are only larger splines can contact and push annular spring because of its projecting. The projecting on larger spline can be divided into three different parts and shown as Figure 2.3-5. The deformation of annular spring increases as the distance between sleeve and outer ring approaches along front section on projecting. In addition, the more the deformation of annular spring does, the higher the spring force is yielded.

While sleeve moves to the position that annular spring moves to middle section, annular spring suffers form friction force. Since the movement of sleeve dose not stop, annular spring will keep moving toward the back section after passing through middle section. In

back section, annular spring will move in the opposite direction of the movement of sleeve, and finish its function during synchronization.

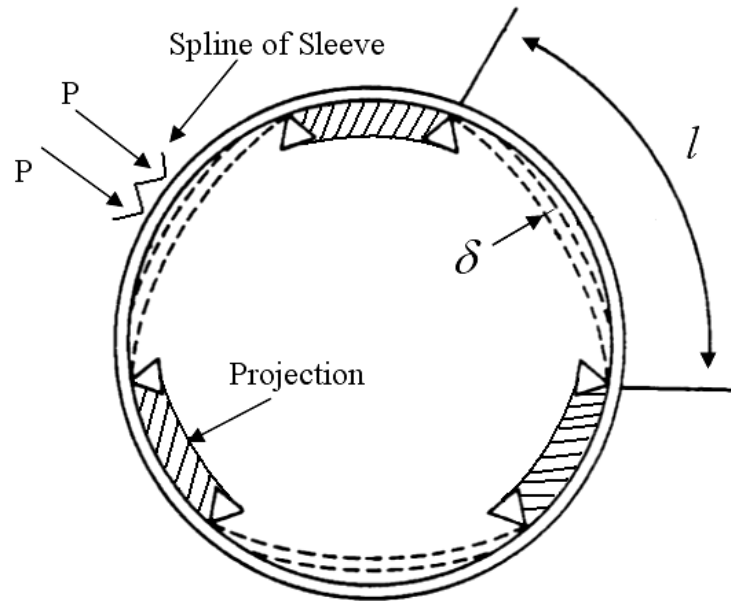


Figure 2.3-4 Deformation of annular spring (Fujiwara, 1991)

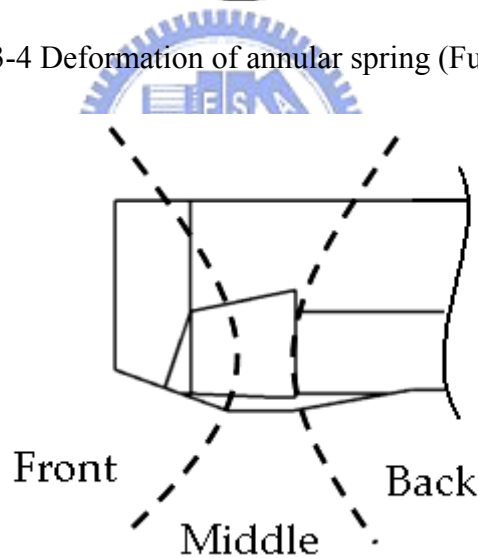


Figure 2.3-5 Section of projecting on larger spline

If here focus on one larger spline, the free body diagram can be drawn in Figure 2.3-6; moreover, combining Figure 2.3-5 and Figure 2.3-6 can yield an equation that relates to F_o and δ as

$$F_o = \frac{(\mu_{as} \cos \theta_{as} + \sin \theta_{as})}{(\cos \theta_{as} - \mu_{as} \sin \theta_{as})} \times \frac{cEI\delta}{l^3} \quad (2.3-4)$$

where F_o is force for over annular spring, θ_{as} is angle of chamfer on projecting, μ_{as} is

coefficient of friction between larger spline and annular spring, N_{sa} is the normal force on the contact surface, f_{sa} is friction force on contact surface, F_{ar} is reaction force acting on outer ring from annular spring, and F_{as} is pushing force from larger spline equaling to $\frac{F_s}{6}$, because there are six larger splines on a sleeve.

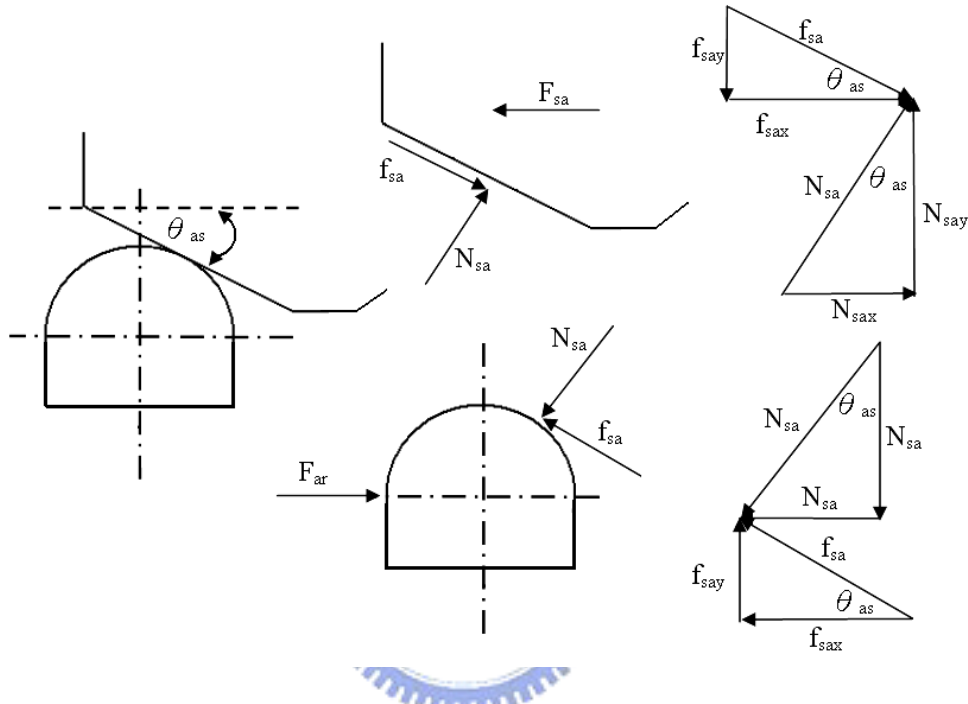


Figure 2.3-6 FBD of sleeve contact with annular spring

There are six contact points between larger splines of sleeve and annular spring, so the relation of F_s and F_o can be shown as

$$F_s \geq 6F_o \quad (2.3-5)$$

The sleeve force, generally speaking, should be larger than the over force for six times, so that the sleeve can stride over annular spring after finishing synchronization, just like the equation shown in Eq. (2.3-5). Even though, a larger force difference may lead sleeve crossing outer ring directly without finishing synchronization, and due to the abnormal collision, occurring between teeth of clutch gear and splines of sleeve. This phenomenon, which will result in a worse lifespan of synchronizer, has to be avoided in gear ratio shift.

The combination of Eqs. (2.3-4) and (2.3-5) can find out some parameters, which will influence the process of sleeve passing through annular spring, synchronized time, and performance of synchronization. These parameters are angle of projecting chamfer on larger spline, friction coefficient between spline of sleeve and annular spring, distance between projections, and deflection and material characteristic of annular spring.

2.3.3 Yielding Synchronized Torque

There are two kinds of torque, which are cone torque and index torque, yielded in this process. Cone torque is yielded from contact friction force between outer ring and cone, and inner ring and cone, whereas index torque is yielded from the contact between splines of sleeve and teeth of outer ring.

If the restitution coefficient between sleeve and annular spring is very small, here assumes that the force, applied from sleeve, without losing while it passes through annular spring. Consequently, the force from sleeve can be transmitted to outer ring through annular spring completely, namely, the loss of force on annular spring is negligible.

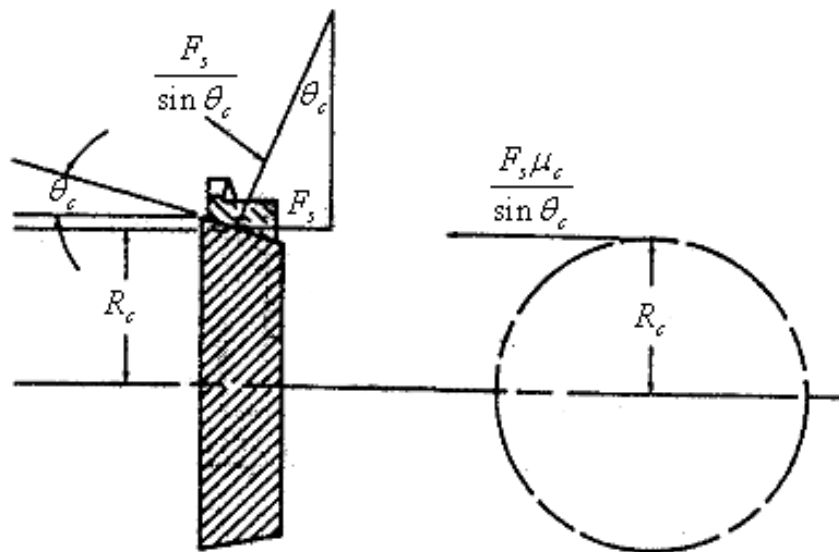


Figure 2.3-7 FBD on cone torque (Socin and Walters, 1968)

Annular spring pushes outer ring, and then yields cone torque as the following equation and Figure 2.3-7.

$$T_c = \frac{F_s \mu_c R_c}{\sin \theta_c} \quad (2.3-6)$$

where T_c is torque yielded from cone, μ_c is dynamic coefficient of friction between rings and cone, R_c is mean cone radius, and θ_c is cone angle in degree.

A double cone synchronizer has two cone torques, yielding from outer ring and cone, and inner ring and cone. If that these two cone torques are equal is assumed, the total cone torque can take as two times of Eq. (2.3-6).

As Figure 2.3-8, index torque can be established as

$$T_I = F_I R_b = \left(\frac{1 - \mu_b \tan \frac{\theta_r}{2}}{\mu_b + \tan \frac{\theta_r}{2}} \right) F_s R_b \quad (2.3-7)$$

where F_I is force acting on tooth, T_I is index torque, μ_b is static coefficient of friction between chamfers, θ_r is angle on chamfer of outer ring that equals to chamfer angle on sleeve θ_s , N is normal force between splines, and R_b is radius of mesh between coupling sleeve and outer ring.

As Figure 2.3-9, outer ring suffers from cone torque and index torque at the same time. If index torque is larger than cone torque without in the time that the synchronization finished, sleeve will pass through outer ring directly, and lead into abnormal collision between clutch gear and sleeve. In order to avoid this situation, cone torque needs to be larger or equal than index torque as Eq. (2.3-8) before the different rotational velocity achieving synchronization.

$$T_c \geq T_I \quad (2.3-8)$$

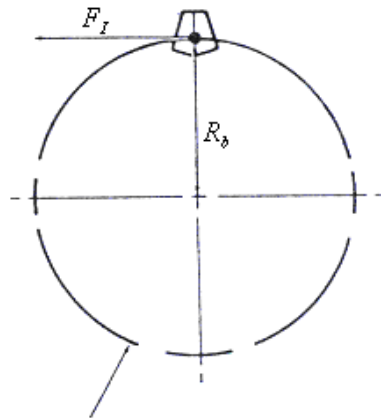
Eqs.(2.3-6), (2.3-7), and (2.3-8) can obtain the following equation.

$$\mu_c \geq \frac{R_b \sin \theta_c \left(1 - \mu_b \tan \frac{\theta_r}{2} \right)}{R_c \left(\mu_b + \tan \frac{\theta_r}{2} \right)} \quad (2.3-9)$$

For preventing rings and cone lock together after synchronization, the static coefficient of friction needs to match Eq. (2.3-10).

$$\mu_{cs} \leq \tan \theta_c \quad (2.3-10)$$

where μ_{cs} is static coefficient of friction on cone.



Radius of mesh between coupling sleeve and synchronizer ring

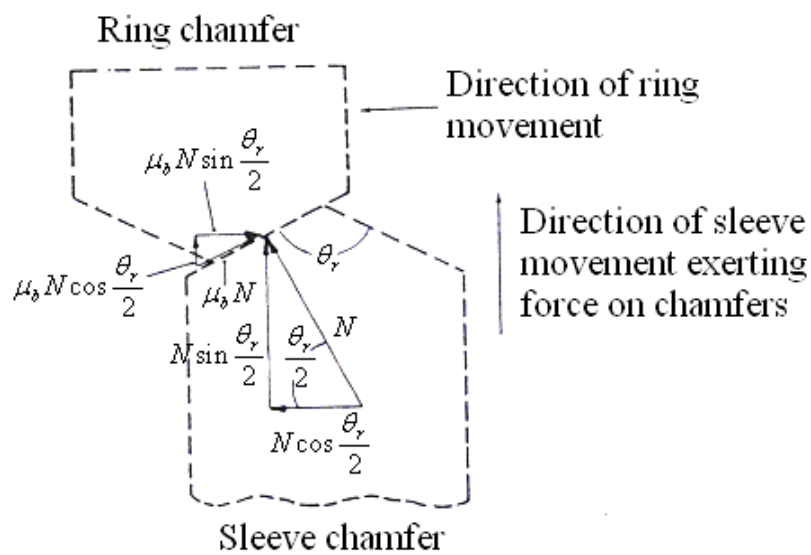


Figure 2.3-8 FBD of contact between outer ring and sleeve (Socin and Walters, 1968)

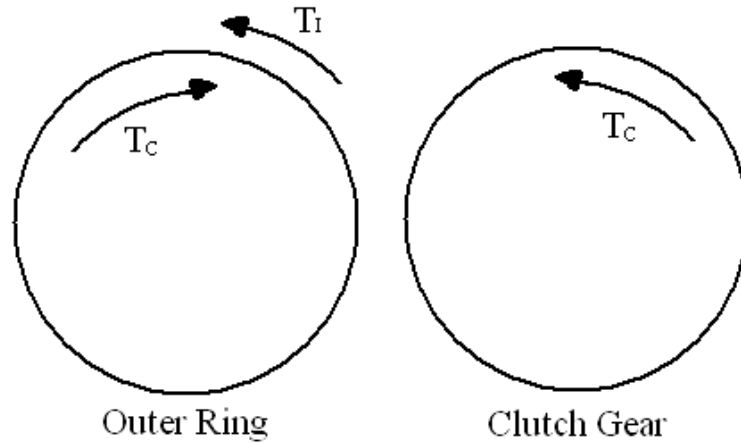


Figure 2.3-9 Cone and index torque exerting on outer ring and clutch gear

After talking about cone torque and index torque, the synchronized torque is yielded and shown in Eq. (2.3-11).

$$T_s = T_c \pm T_d \quad (2.3-11)$$

where T_s is synchronized torque, and T_d is drag torque.

The cone torque T_c , in double cone synchronizer is almost twice as large as in single cone synchronizer. Furthermore, drag torque always acts to slow down transmission components, so it adds to cone torque while upshifts, and subtracts from cone torque while downshifts.

2.3.4 Synchronizing Relative Rotational Velocity

As showing in Figure 2.3-10, the synchronized torque, acting on rings and clutch gear, is used to synchronize different rotational velocity between output shaft and input gear ratio, which are ω_v and ω_s respectively. Moreover, the torque T_s acts on output shaft, whose reflected inertia is I_v , and input gear ratio, whose reflected inertia is I_{or} , in the meantime. In addition, this subsection will talk about the relation between synchronized torque and different rotational velocity.

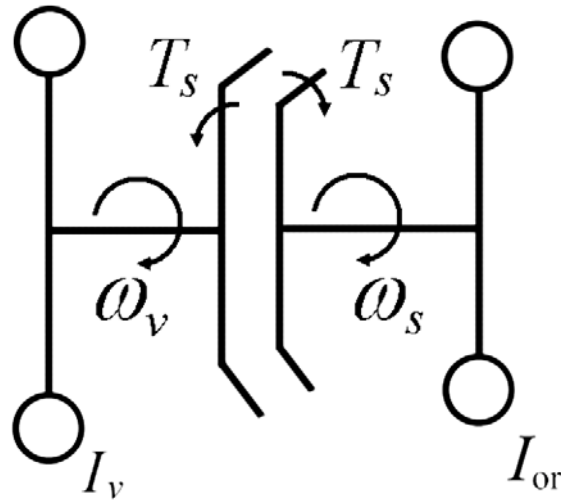


Figure 2.3-10 Sketch of synchronization

On the side of transmission gear, the synchronized torque that acts on clutch gear is shown in Eq. (2.3-12).

$$T_s = I_r \alpha_r \quad (2.3-12)$$

where I_r is reflected inertia, and α_r is angular acceleration of reflected inertia.

As the definition of annular acceleration, Eq. (2.3-12) can be transferred to obtain synchronized time in Eq. (2.3-13).

$$t_s = \frac{(\omega_a - \omega_b) I_r}{T_s (avg.)} \quad (2.3-13)$$

where t_s is synchronized time, ω_a is rotational velocity of objective gear ratio after synchronization, and ω_b is rotational velocity of objective gear ratio before synchronization.

Sleeve, hub, outer ring, annular spring and inner ring rotate in ω_b before synchronizing; meanwhile, cone and clutch gear rotate in ω_a . Diminishing the different rotational velocity between ω_b and ω_a is the purpose of synchronization.

The variation of objective gear ratio will influence the rotational velocity of all the other gears, which are the total number of items that depend on the layout of transmission. Therefore, the inertia mass of other gear ratio need to transfer to the objective gear ratio while

shifting. This inertia, transferring from all the others, is called reflected inertia.

If the objective gear ratio is 2nd, the reflected inertia can be shown in Eq. (2.3-14) and illustrated in Figure 2.3-11.

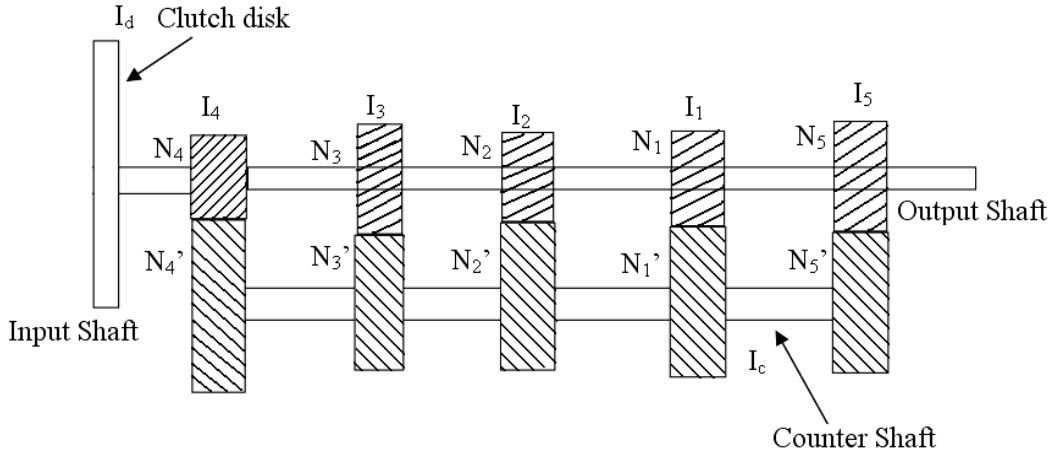


Figure 2.3-11 Sketch on transmission gears with number of teeth and inertia

$$I_{2r} = I_2 + \left(\frac{N_2}{N_2'} \right)^2 \left[I_c + \left(\frac{N_4'}{N_4} \right)^2 (I_d + I_4) + \left(\frac{N_5'}{N_5} \right)^2 I_5 + \left(\frac{N_3'}{N_3} \right)^2 I_3 + \left(\frac{N_1'}{N_1} \right)^2 I_1 \right] \quad (2.3-14)$$

where I_i is sectional secondary moment inertia of i^{th} gear, N_i is number of gear teeth on i^{th} gear, N_i' is number of gear teeth on counter shaft of i^{th} gear, I_c is sectional secondary moment inertia of counter shaft and gear, and I_d is sectional secondary moment inertia of clutch disk.

Opposite of synchronized torque acting on clutch gear, this torque acts on rings to synchronize the rotational velocity on output shaft, whose equation is established in Eq. (2.3-15).

$$T_c = I_v \alpha_o \quad (2.3-15)$$

where I_v is the total inertia reflected from whole vehicle, and α_o is the angular acceleration of output shaft.

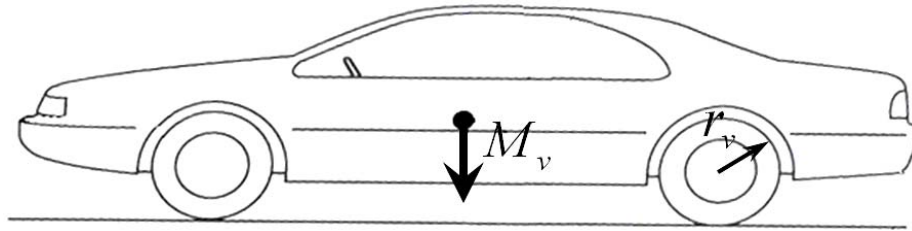


Figure 2.3-12 Mass and radius of drive wheel on vehicle

The inertia of vehicle can be approximate established from Figure 2.3-12, and is shown in following equation.

$$I_v = r_v^2 M_v \quad (2.3-16)$$

where r_v is the radius of wheel, and M_v is the mass of the vehicle.

2.3.5 Mesh between Sleeve and Outer Ring

Because of the projections on outer ring and the grooves on hub, the angular position of outer ring and hub is restricted in a certain angle. And so on, the angle, which influences contact between sleeve and outer ring, is also restricted.

Based on these restrictions, there is only a lower abnormal impact, which will be happened between sleeve and outer ring. The most important function of outer ring is to yield index torque, and keep off sleeve passes through outer ring before the relative rotational velocity between sleeve and clutch gear lower enough.

The function has already discussed before in Figure 2.3-8, so the detail will not be discussed in this subsection again.

2.3.6 Mesh between Sleeve and Clutch Gear

After finishing the synchronization, the relative rotational velocity between clutch gear and sleeve approaches to zero, as shown in Figure 2.3-13, where N_G is relative rotational

velocity, F_R is the force acting on outer ring from sleeve, and V is the moving velocity of sleeve on direction of axis.

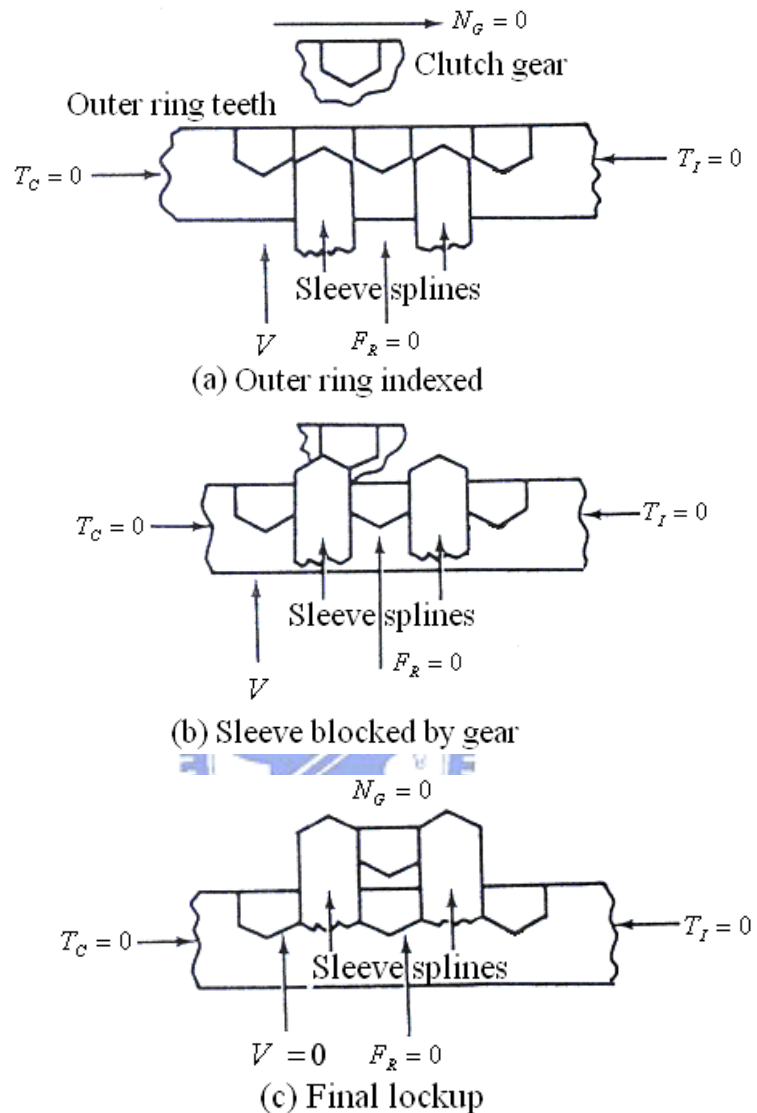


Figure 2.3-13 Processes of sleeve pass through clutch gear (Socin and Walters, 1968)

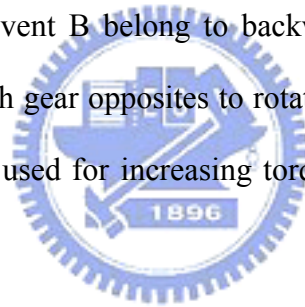
In Figure 2.3-13 (a), when the relative rotational velocity between outer ring and clutch gear approaches zero, the cone torque will diminish. Meanwhile, index torque is larger than cone torque, so that outer ring rotates for allowing the sleeve splines passing and engaging with it. Synchronization completes at the same time.

In Figure 2.3-13 (b), when synchronization is completed, and the sleeve has passed beyond outer ring, the chamfer of sleeve contacts with splines of clutch gear, and yields a new

index torque on the contact surface, between spline and clutch gear, until sleeve passes through clutch gear. In Figure 2.3-13 (c), after the index torque on clutch gear approaches zero, sleeve passes through clutch gear along the chamfer of sleeve and clutch gear, and finishes the final lockup and gear shift (Murata et al., 1989).

Mesh between sleeve and clutch gear is an important part that needs to be discussed because the contact point between splines of sleeve and clutch gear is unable to forecast. It is impossible to accurately predict the engaged possibility, so it will first mention the compendium of all these engaged possibilities in this chapter in the thesis. These possibilities of engagement have been divided into five events, which include backward, forward and just engage conditions, which are shown as Table 2.3-1.

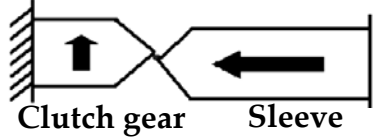
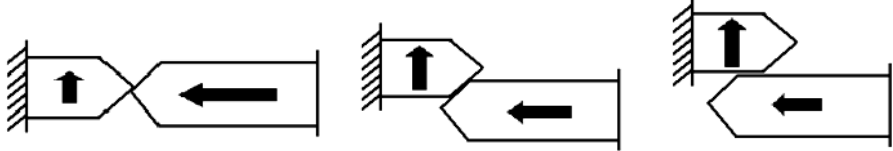
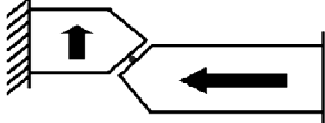
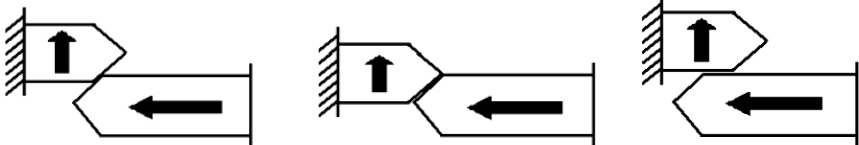
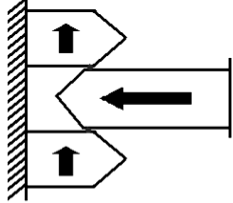
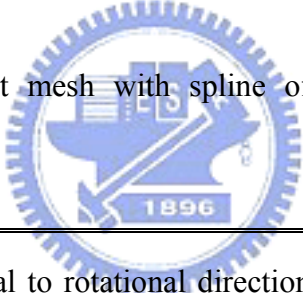
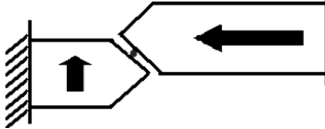
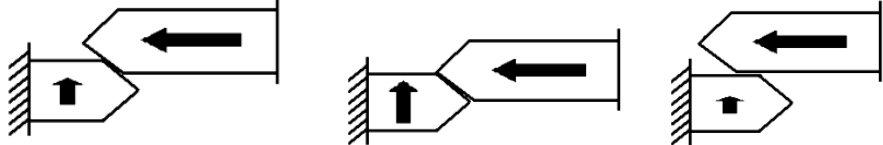
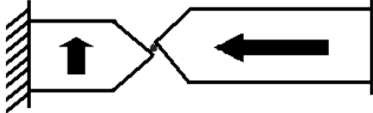
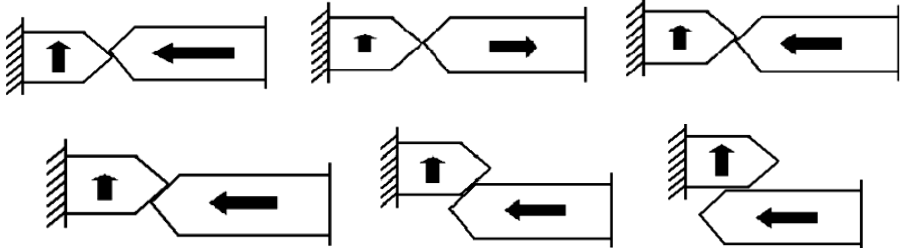
Table 2.3-1 event A and event B belong to backward condition, since the first contact point between sleeve and clutch gear opposites to rotational direction of clutch gear. In this condition, the contact force is used for increasing torque to rotate clutch gear in its original rotational direction.



The possibility of engaging belong to event C only if sleeve just engages with clutch gear exactly, shown as Table 2.3-1 event C. The mesh time and contact force on this event is the least among all these situations. The latest event is forward condition, which includes Table 2.3-1 event D and event E. In this condition, the first contact point between sleeve and clutch gear is identical to rotational direction of clutch gear. The contact force is used for reducing relative rotational velocity between sleeve and clutch gear.

Backward and forward conditions can be further separated into two possible cases, which are contact point near tip of spline and far from tip of spline. Different contact point will bring out different possible result; moreover, these engaged processes of five events not only is shown in Table 2.3-1, but also will be mentioned in the simulation model.

Table 2.3-1 Process of engaged possibilities

<p>A. Contact point opposite to rotational direction of clutch gear and near tip of spline</p>	 <p>Clutch gear Sleeve</p>
	
<p>B. Contact point opposite to rotational direction of clutch gear and far from tip of spline</p>	
	
<p>C. Spline of sleeve just mesh with spline of clutch gear exactly</p>	
	
<p>D. Contact point identical to rotational direction of clutch gear and far from tip of spline</p>	
	
<p>E. Contact point identical to rotational direction of clutch gear and near tip of spline</p>	
	

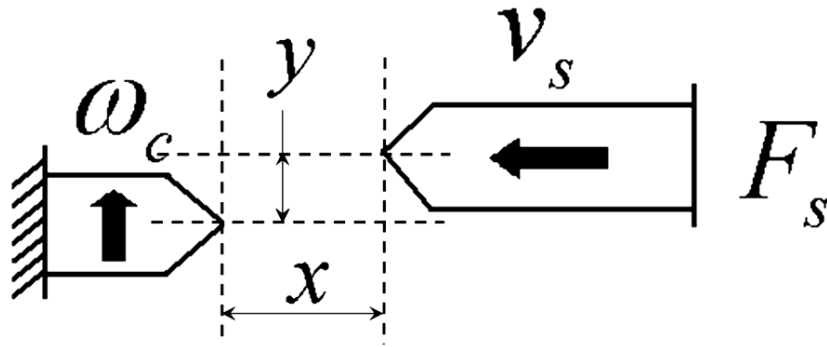


Figure 2.3-14 Parameters influence different mesh possible

Different force and synchronizer performance is not the main criteria for these five different situations. Because it is a random process that cannot be controlled by driver or designer which mesh situation will occur. The parameters, which will influence different possible results, are associated to Figure 2.3-14, where ω_c is rotational velocity of clutch gear, F_s is sleeve force, v_s is linear velocity of sleeve, x is distance between tip of sleeve and clutch gear parallel to moving direction of sleeve, and y is distance between tip of sleeve and clutch gear vertical to moving direction of sleeve.

Even the possibilities of engagement cannot be governed by driver or designer, these random processes will lead a certain extent influences on shift time and lifespan. Therefore, the following chapters will discuss this phenomenon in detail from the simulation model building on ADAMS™.

CHAPTER 3

SIMULATION MODEL AND RESULTS

3.1 Introduction

In this chapter, the simulation model will be built up on commercially available software, ADAMSTM, for analyzing mechanical dynamics. Soon afterwards, the assumptions, constraints and conditions for simulation will be discussed in this chapter; this is an important part that needs to be claimed before building simulation model.

Because the synchronization process can be roughly divided into synchronized process and mesh process, this is the engagement situation between sleeve and clutch gear, and that describes synchronized torque, making sleeve and clutch gear achieve synchronous rotational velocity. The model will be constructed not only entire model, but also synchronized module and mesh module, which correspond to synchronized process and mesh process respectively. In addition, the results of entire model and both modules will be confirmed with literatures or experiment data to make sure that the exactitude of simulation model.

Synchronized module and mesh module are separated from entire model, because these two minor modules will influence complete shifting time respectively, and separating entire process on synchronization is a better method to analysis it. Prior researches always talked only about the entire model of this technique or the geometric action of the final mesh; however, they did not pay much attention on the mesh period about time that will be discussed and simulated in the thesis.

3.2 Simulation Assumptions

In this simulation model, all components are assumed to solid, and rotational freedom around the rotational axis and/or movement freedom along the rotational axis are given to

each component.

Input and output shaft transfers power through gear and hub respectively, so transmission gear connects on ground with a revolutionary joint, whereas hub is fixed on ground because the reflected inertia from whole vehicle is much higher than it is reflected from transmission gearbox. The reflected inertia reflected from vehicle and gearbox will be mentioned in this chapter later.

Some geometric restriction between, sleeve and hub, outer ring and inner ring, clutch gear and cone, are simplified by translation joint, which can make both components move in direction of axis and rotate with each other. This simplified model on components can also diminish the simulation time that uses for calculation the contact between components mounted together.

The annular spring is also simplified in the simulation model. An annular spring will yield larger deformation during the process of synchronization, and the components are assumed to be solid in this model on ADAMS™, so annular spring is transferred to another type of model that can also express the original function that is shown as below.

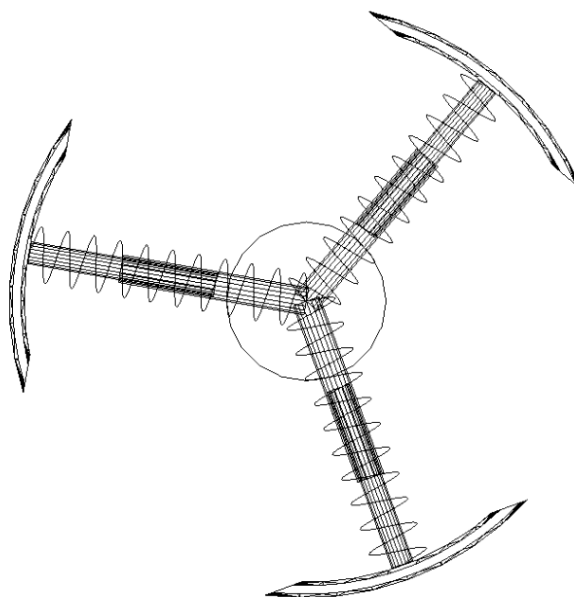


Figure 3.2-1 Analytical model of annular spring

The annular spring is divided into three parts, and respectively connected to the core of spring through a helical spring, which is an available element in ADAMSTM. The stiffness coefficient of spring can be yielded by FEM from regular annular spring, or experiment data.

In addition to the assumption of this model about joint, solid and annular spring, it is also neglected on heat, gravity, vibration and wear. Besides, the model only talks about the influence of lubricant on coefficient of friction, and a slight influence about viscosity, instead of considering coefficient of viscosity in this model accurately.

3.3 Dynamic Model Creation

3.3.1 Units Setting

Because the dimensions on all components are marked in millimeter, and for convenient to express and calculate, this model uses MMKS unit for setting all components and all other quantity such as force, speed, and etc. The units setting is listed as Table 3.3-1 and shown below.

Table 3.3-1 Units setting on simulation model

Length	Mass	Force	Time	Angle	Frequency
Millimeter(mm)	Kilogram(kg)	Newton(N)	Second(sec)	Degree(deg)	Hertz(Hz)

3.3.2 Component

The whole model, building here, includes all components in a strutless type synchronizer. All these components are built up in CATIA according to the layout originating from Mitsubishi Motors Corporation, and then exported these CAD models into STEP (Standard for the Exchange of Product model data), which is an undeniable need to transfer product data in computer-readable form from one site to another. The export files will finally be imported

into ADAMS™ for the following processes to construct model in ADAMS™.

3.3.3 Mass and Inertia

Mass and inertia mass will be assigned to all these components in ADAMS™ after importing. The mass of components are set according to the layout, but inertia mass, except inertia on clutch gear, is automatically calculated by ADAMS™ from geometric shape on each component. The inertia on clutch gear equals to reflected inertia from gearbox, which will be mentioned in the following section.

3.3.4 Joint

Joints on this model are used not merely to restrict the movement between all components, but also to simplify model on geometric restriction, which had already been described in the previous section. The joints between every two relevant components are all represented as Table 3.3-2.

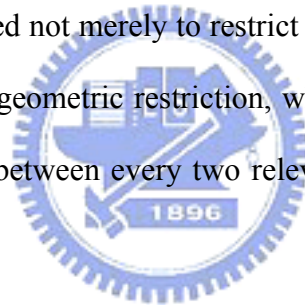


Table 3.3-2 Restrictive relations between all components

1 st component	2 nd component	Joint
Ground	Hub	Fixed
Ground	Outer Ring	Cylindrical
Ground	Transmission Gear	Translation
Sleeve	Hub	Translation
Outer Ring	Inner Ring	Translation
Outer Ring	Annular Spring Core	Fixed
Annular Spring Fragment	Annular Spring Core	Translation
Transmission Gear	Cone	Translation

In this table, the translation joints between, sleeve and hub, outer ring and inner ring, transmission gear and cone, are used to restrain the movement on these components according to the restriction of geometric shape between them. Besides, the three annular spring

fragments, and annular spring core are used to simplify annular spring as Figure 3.2-1. Hub transfers power, and connects with output shaft for driving vehicle; the reflected inertia from vehicle is much higher than that from gearbox, so hub is fixed on ground as the assumption that the reflected inertia is infinite.

3.3.5 Contact

The contact from ADAMSTM allows modeling how free-moving bodies interact with one another when they collide during a simulation. There are two contact force algorithms available in ADAMSTM that are restitution-based contact and impact-function-based contact. Impact-function-based was chosen for calculating contact force in the analytic model in this thesis, because this algorithm spends less simulation time than restitution-based contact, and the force is essentially modeled as a nonlinear spring-damper.

ADAMSTM uses a relatively simple velocity-based friction model for calculating contacts. Specifying the frictional behavior is optional. Figure 3.3-1 shows how the coefficient of friction varies with slip velocity.

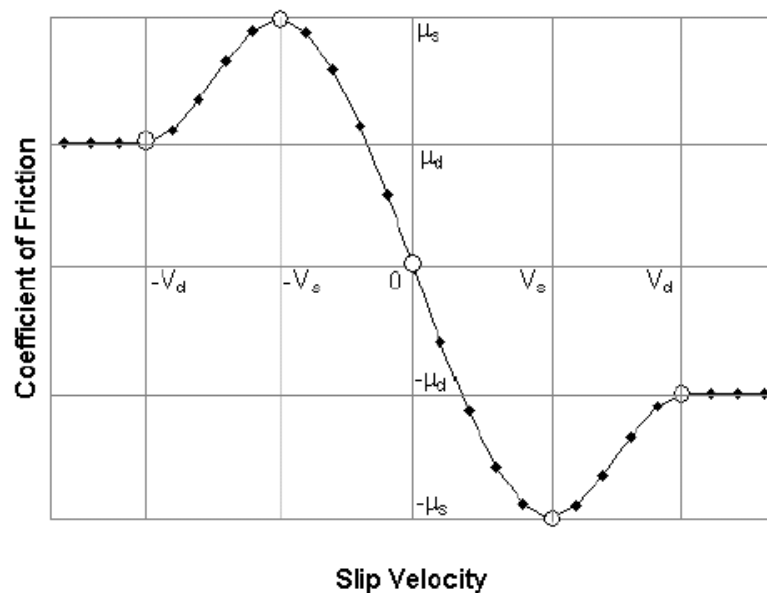


Figure 3.3-1 Coefficient of friction varying with slip velocity (ADAMSTM, 2003)

where V_s is stiction transition velocity at contact point, V_d is friction transition velocity at contact point, μ_s is static coefficient of friction, and μ_d is dynamic coefficient of friction.

All these contact factors that need to be assigned to this model are in accordance with a table, which lists value in varied factors on different contact situation, released from MSC.Software Corporation. Moreover, all components on gearbox are separated by a thin lubricant from other components, and the coefficient of friction between these components, which are surrounded by lubricant, is very low. Therefore, a lower coefficient of friction is set on all contacts, excluding cone surface. The coefficient of friction on cone surface is varied as the thickness of lubricant between cone and rings, because the lubricant will be drained out through a lot tiny grooves, mounted on rings. The draining out process of lubricant will be discussed in Chapter 4. The contact setting on this model is listed as Table 3.3-3.

Table 3.3-3 Contact and coefficient of friction setting

1 st component	2 nd component	Coefficient of friction	
		Static	Dynamic
Sleeve	Clutch Gear	8.5E-2	5E-2
Sleeve	Outer Ring	8.5E-2	5E-2
Sleeve	Transmission Gear		
Sleeve	Annular Spring Fragment	8.5E-2	5E-2
Hub	Outer Ring		
Hub	Annular Spring Fragment		
Cone	Outer Ring	Variable	Variable
Cone	Inner Ring	Variable	Variable
Inner Ring	Transmission Gear		

3.3.6 Force

The sleeve force, which acts on sleeve for driving whole process through synchronization, is simplified by step function. If the sleeve force is pushed by driver on manual transmission,

according to technical literature, this force is similar to step function (Bansbach, 1998). However, if the sleeve force was pushed by actuator on automated manual transmission, this force can also be simplified to step function. Consequently, this analytic model utilizes step force, which sets the maximum sleeve force, to simulate the shifting force.

About spring force, because the annular spring in a strutless synchronizer is replaced to a linear spring as assumption before. The stiffness of spring needs to be defined and assigned in this simulation model. Here, the stiffness is gotten from CATIA module, called Generative Structural Analysis.

3.3.7 Parameter

In the analytic model, there are some parameters such as the gear ratio before shifting, gear ratio after shifting, the reflected inertia transferring from transmission gearbox, rotational velocity of engine while shifting, stiffness of annular spring, coefficient of friction on cone surface, difference in coefficient of friction on cone surface, and maximum sleeve force. These parameters need to be assigned to analytical model, and these descriptions and unit of parameters are listed on Table 3.3-4.

There are some coefficients of friction, which are coefficient of friction between cone and rings, and coefficients of friction between all contacts of teeth need to assign in this model. The coefficient of friction between cone and rings will change the value of cone torque, influencing the value of synchronized torque a lot.

Because cone surface is the easiest place that might yield wear while synchronization, the analytic model simulate this phenomenon by use difference in coefficient of friction on cone surface. The detailed variation on coefficient of friction will be stated in the next chapter.

Table 3.3-4 List of parameters assigning in the model

Description	Unit	Notation
Reflected initial apply on clutch gear	$kg \cdot mm^2$	I_r
Gear ratio before shifting	None	g_b
Gear ratio after shifting	None	g_a
Engine rotational velocity while starting shift	RPM	ω_e
Maximum shifting force	nt	F_{sM}
Stiffness of annular spring	nt/mm	k_s
Coefficient of friction between cone and rings	None	μ_c
Static coefficient of friction between teeth	None	μ_{ms}
Dynamic coefficient of friction between teeth	None	μ_{md}
Cone angle	$^\circ$	θ_c
Difference in coefficient of friction on cone surface	None	μ_{dc}
Mean cone radius of first cone surface	mm	R_{m1}
Mean cone radius of second cone surface	mm	R_{m2}

The geometric model and relation between all components had already been constructed, and discussed in this section. In the following sections, simulation conditions and parameters, applying to this model, will be discussed in the thesis, and from the results of entire model.

3.4 Entire Model

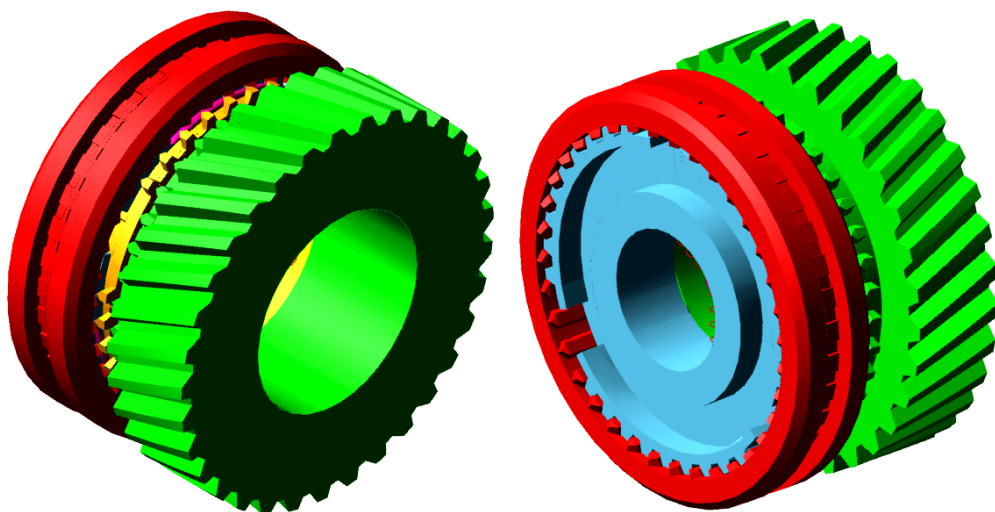


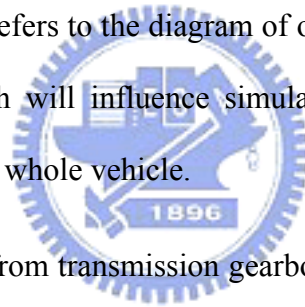
Figure 3.4-1 Contour of analytic model on ADAMS™ in different visual angle

During construction of analytical model, the results of simulation model will be logically checked on separation from Chapter 2, and then a simulation model on the entire system was made as below.

In the entire model, all minor processes are simulated from the movement of sleeve until it finishes meshing with clutch gear. The simulation conditions, parameters, and results will be described in this section. The entire model, built up in ADAMS™, is shown in Figure 3.4-1, which includes all seven components, in different viewpoint.

3.4.1 Simulation Conditions and Parameters

The first part that will be discussed in this section is mass and inertia mass. The mass of all components on this model refers to the diagram of original layout. Besides, there are two most important inertias, which will influence simulation enormously, are reflected inertia from transmission gearbox and whole vehicle.



The first inertia, reflected from transmission gearbox, can be calculated from Eq. (2.3-14) and Table 3.4-1.

Table 3.4-1 Parameters on all gear and shaft

	Gear ratio		Mass(kg)	Radius(mm)	I(kg-mm ²)
1 st Gear	$g_1 = \left(\frac{33}{13} \times \frac{28}{18}\right)$	3.95	0.75	47.2	835.44
2 nd Gear	$g_2 = \left(\frac{29}{19} \times \frac{28}{18}\right)$	2.37	0.65	41.05	547.65831
3 rd Gear	$g_3 = \left(\frac{27}{28} \times \frac{28}{18}\right)$	1.50	0.38	34.72	229.0409
5 th Gear	$g_5 = \left(\frac{17}{31} \times \frac{28}{18}\right)$	0.85	0.109	26	36.842
Main drive	$g_4 = 1$	1	0.9	27.45	339.07613
Clutch disk					2300
Counter shaft					1215

The gear ratio, mass and radius on Table 3.4-1 are referred to original layout, and the inertial is calculated from the mass and radius.

The result of reflected inertia I_r was shown in Table 3.4-2. If the simulation model wants to simulate from 1st gear ratio to 2nd gear ratio, just need to input $I_r = 1.9423 \times 10^4 \text{ kg} \cdot \text{mm}^2$ on the parameter of reflected inertia on the component of clutch gear.

Another important inertia is the total inertia, transferred from whole vehicle I_v . As Eq. (2.3-16), if the mass of vehicle is 1835kg and radius of wheel is 343.3mm, basing on one available sedan, the inertia from whole vehicle reflection to transmission gearbox can be obtained, and the value is $I_v = 2.1626 \times 10^8 \text{ kg} \cdot \text{mm}^2$.

Even different vehicle will bring out different I_v ; however, seeing that I_v is always much higher than I_r , and following the assumption that has been discussed before, the hub can be fixed on the ground, and the model just needs to apply the reflected inertia of transmission gearbox on the analytic model.

Table 3.4-2 Reflected inertia transferring from different gear ratio

	$\frac{N_1'}{N_1}$	$\frac{N_2'}{N_2}$	$\frac{N_3'}{N_3}$	$\frac{N_4'}{N_4}$	$\frac{N_5'}{N_5}$	Objective gear ratio	Reflected Inertia (kg-mm²)
1 st to 2 nd	13/33	19/29	28/27	28/18	31/17	2 nd	1.9423×10^4
2 nd to 3 rd	13/33	19/29	28/27	28/18	31/17	3 rd	0.7749×10^4
3 rd to 4 th	13/33	19/29	28/27	28/18	31/17	4 th	0.3784×10^4
4 th to 5 th	13/33	19/29	28/27	28/18	31/17	5 th	0.2507×10^4
5 th to 4 th	13/33	19/29	28/27	28/18	31/17	4 th	0.3784×10^4
4 th to 3 rd	13/33	19/29	28/27	28/18	31/17	3 rd	0.7749×10^4
3 rd to 2 nd	13/33	19/29	28/27	28/18	31/17	2 nd	1.9423×10^4
2 nd to 1 st	13/33	19/29	28/27	28/18	31/17	1 st	5.3725×10^4

The gear ratio before and after shifting is according to Table 3.4-1. This gear ratio can be just assigned to the parameter in simulation model while simulating. The values on Table

3.4-1 are also according to the layout from Mitsubishi Motors Corporation; if the values differ from this table, it can be changed while input the gear ratio into analytic model. Besides, the reflected inertia, assigned to the parameter on simulation model, can be referred to Table 3.4-2. As the gear ratio that was discussed before, if the gear ratio of each gear ratio differs from Table 3.4-1, one can recalculate it and assign the result to the model.

Table 3.4-3 Gear ratio and reflected inertia on each shift

	Gear Ratio Changing	Reflected Inertia (kg-mm²)
1 st to 2 nd	3.95 to 2.37	1.9423×10^4
2 nd to 3 rd	2.37 to 1.50	0.7749×10^4
3 rd to 4 th	1.50 to 1	0.3784×10^4
4 th to 5 th	1 to 0.85	0.2507×10^4
5 th to 4 th	0.85 to 1	0.3784×10^4
4 th to 3 rd	1 to 1.50	0.7749×10^4
3 rd to 2 nd	1.50 to 2.37	1.9423×10^4
2 nd to 1 st	2.37 to 3.95	5.3725×10^4

All these parameters of gear ratio, and reflected inertia for shifting between different gear ratio are shown as Table 3.4-3. There is an important aspect that the value of reflected inertia only depends on the objective gear ratio in this table.

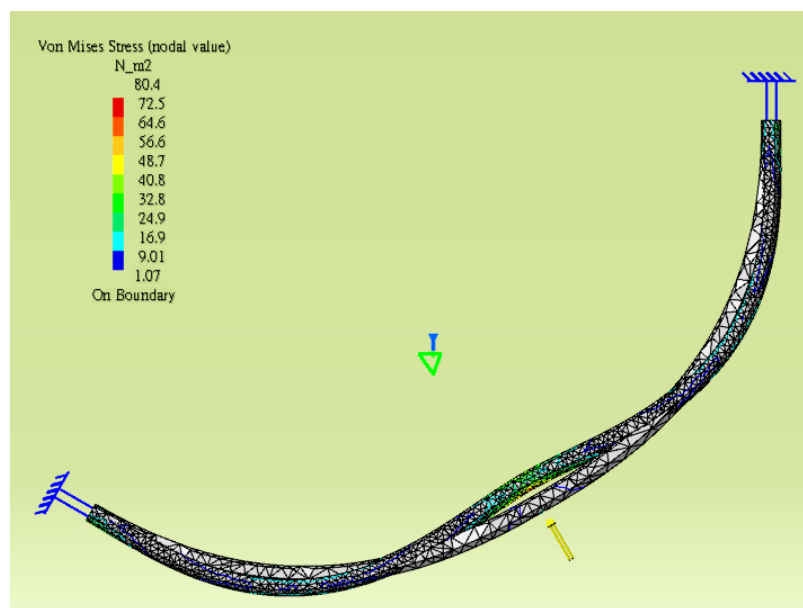


Figure 3.4-2 Generative structure analysis of annular spring

The stiffness of annular spring was obtained from CATIA module Generative Structure Analysis. Because annular spring is partitioned into three parts by three projections, setting on outer ring, the finite element model only construct one-third of completely annular spring. Moreover, because the contact point between projection and annular spring suffer from two efforts on both sides, the both end sides of finite element model are fixed on ground. After applying force on the center of the finite element model, the stiffness of linear spring replaced to annular spring can be yielded as equaling to the value that force divided by maximum displacement. The displacement of this finite element model is shown as Figure 3.4-2, and the result is used for simulation in next section.

3.4.2 Simulation Results

After discussing the simulation conditions and parameters, the simulation results will be expounded in this section. There are so many different states of affairs for shifting, say, shifting from 1st gear ratio to 2nd gear ratio, 1st gear ratio to 3rd gear ratio, 3rd gear ratio to 4th gear ratio and 4th gear ratio to 1st gear ratio, and etc. The analytic model can simulate all these cases; moreover, the section only chooses one of these cases for discussing the simulation results.

Shifting from 1st gear ratio to 2nd gear ratio is the most often switching gear ratio in common use. In addition, it suffers from higher reflected inertia, and needs more shifting time and force while shifting. So, the case was chosen by the thesis for talking about simulation results in this section.

There are some methods for setting the system parameters in this research, which are design parameters, experiment data, table data, and calculation data. Most dimensions are referred to layout origination from synchronizer and gearbox design, such as gear ratio and cone angle. The other parameters, say, rotational velocity of engine while shifting, and

maximum sleeve force refer to experiment data, as shown in Table 3.4-4, an experiment data about synchronized time. The value that sleeve force and rotational velocity on engine were provided from ITRI on a single cone synchronizer. The engine experiment and synchronized type for gaining on the table differ from the synchronizer and gearbox studies in this thesis, so there only refer to the rotational velocity on engine and sleeve force on the analytic model, and compare the tendency of simulation model with this table.

Table 3.4-4 Experiment data from Industrial Technology Research Institute (ITRI)

	Gear ratio	Reflected Inertia	Engine RPM	Sleeve Force	Synchronized time
1 st to 2 nd	3.95 to 2.37	18494.23	2500	116N	0.275
2 nd to 3 rd	2.37 to 1.49	7563.70	3000	117N	0.2
3 rd to 4 th	1.49 to 1	3182.14	3000	65N	0.2
4 th to 5 th	1 to 0.85	2524.61	3000	27N	0.2
5 th to 4 th	0.85 to 1	3182.14	3500	39N	0.2
4 th to 3 rd	1 to 1.49	7563.70	3000	153N	0.2
3 rd to 2 nd	1.49 to 2.37	18494.23	2500	190N	0.25
2 nd to 1 st	2.37 to 3.95	50451.16	2000	254N	0.275

Another property of these parameters, like coefficient of friction on cone surface, static and dynamic coefficient of friction between teeth, is according to table data. The last kind of parameters such as reflected inertia, and stiffness of annular spring are yielding from formula calculating and FEM, respectively.

The simulation parameters, which are used for simulating shift from 1st gear ratio to 2nd gear ratio, is listed as Table 3.4-5.

Table 3.4-5 Parameters for simulating shift from gear ratio 1st to 2nd

I_r	g_b	g_a	ω_e	F_{sM}	k_s
$1.9423 \times 10^4 \text{ kg} \cdot \text{mm}^2$	3.95	2.37	2500 RPM	120 nt	17 nt/mm

R_{m1}	R_{m2}	μ_c	μ_{ms}	μ_{md}	θ_c	μ_{dc}
30.559 mm	28.059 mm	0.11	8.5E-2	5E-2	7.5°	0

The simulation of this model was set to end time at 0.25 seconds with calculation interval of 0.0001 seconds that included 2500 steps in the duration on it. According to the simulation results, the logical validity is studied about the figures of sleeve movement, rotational velocity, and rotational displacement and force affect on components. These representative results and phenomena are described below to confirm the tendency of the simulation model.

For picturing the simulation results easier and clear, the entire shifting process was divided into several distinct points to describe every detail phase that help to understand more detail about the action of synchronization in the thesis, listed as the table below.

Table 3.4-6 List of distinct points during shifting on the parameters as Table 3.4-5

Point	Description	Time(sec)
A	Start of synchronization	0.0060
B	Outer ring obstructs sleeve	0.0110
C	End of synchronization	0.1467
D	Synchronizing transmission gear and sleeve	0.1490
E	Sleeve over strides over annular spring/ Sleeve engage with outer ring	0.1600
F	Sleeve finishes engaging with outer ring	0.1707
G	Sleeve contacts with clutch gear	0.1736
H	End of engagement	0.2131
I	Sleeve contacts with bevel	0.2155
J	End of shifting	0.2205

Movement of sleeve

The movement of sleeve, while shifting from neutral position to objective gear ratio, can be divided into several segments showing as Figure 3.4-3, for concerning with tendency of the result, and the characteristics on sleeve movement.

First, sleeve starts moving while driver moves shift knob. This action prompts sleeve to move forward objective gear ratio for starting the synchronization. At point A, projectings

on sleeve contact with annular spring, and push it moves toward 2nd gear ratio. Meanwhile, outer ring also moves forward cone due to the movement on annular spring, and synchronized torque starts increasing at the same time. Sleeve keeps moving until it contacts with teeth of outer ring, at point B, and then outer ring obstructs sleeve, because cone torque is higher than index torque at that time. The index torque was yielded from the contact force between sleeve and outer ring.

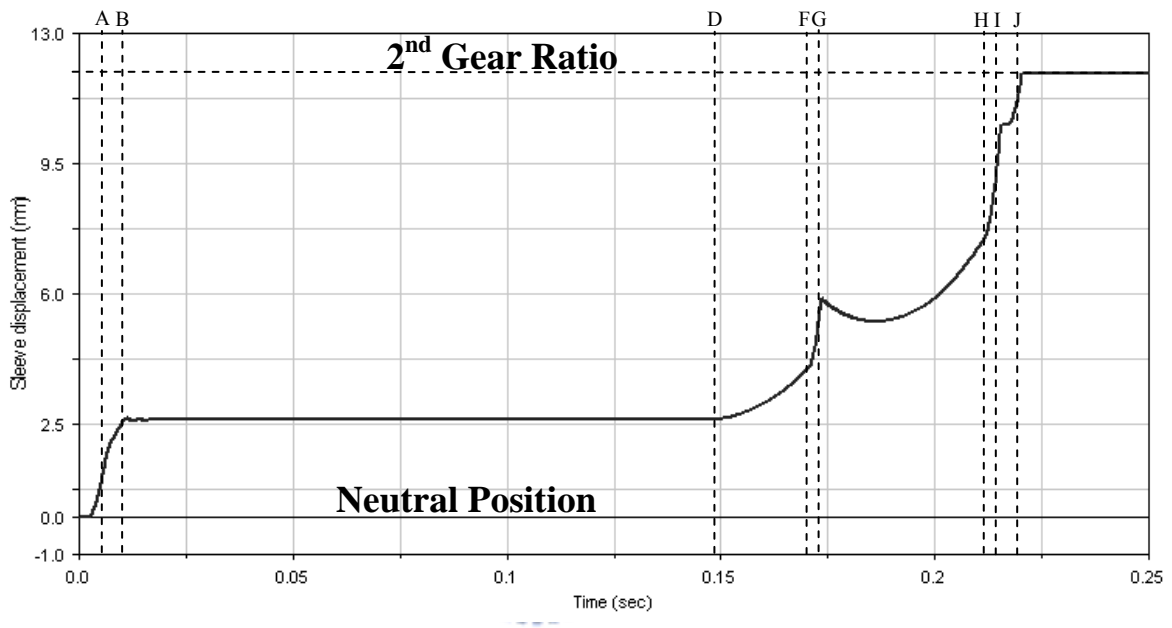


Figure 3.4-3 Distance of sleeve movement

The synchronized torque continuing acts for reducing the relative rotational velocity between sleeve and transmission gear on the interval between point B and D, equaling to the synchronized time as Eq. (2.3-13). While sleeve moves to point F, it totally engages with outer ring, and then keeps proceeding to finish the final engagement with clutch gear, whose first contact point located on point G. The interval between point G and H is a random process, as showing in the Section 2.3.6 and Table 2.3-1. Different mesh situation will lead into not only different mesh process and circumstance, but also different curve and time on this interval. After sleeve finishes engaging with clutch gear, there is an unsmooth curve between point I and J, because of the contact between sleeve and bevel, which was shown on

Figure 2.2-3. The entire shifting on changing gear ratio is finished while sleeve moves to point J.

Here, defining two time on shifting, which are shifting time and synchronized time; this means the interval between start and end of synchronization, point A to J, and that means the interval between start and end of shifting, point B to D. The definition of both these time will be mentioned later, and used for building separating modules.

In Figure 3.4-3, it can be realized that the shifting time equals to 0.2145 sec, and synchronized time is 0.1407 sec. To calculate from Eqs. (2.3-6) and (2.3-13) as the parameters in Table 3.4-5, and the mean cone radius, which are 30.56mm and 28.06mm based on the layout originating from Mitsubishi Motors Corporation, the calculation synchronized time is 0.14296 sec, in which the inaccuracy is lower than 1.58%.

Rotational velocity of transmission gear

The rotational velocity of transmission gear on the simulation model was shown in Figure 3.4-4. Because hub is fixed on ground, as the assumption in this analytic model, this rotational velocity equals to relative rotational velocity between transmission gear and output shaft in reality. The relative rotational velocity between outer ring and transmission gear, which is shown in Figure 3.4-5, deals with the action of cone torque.

There is a tiny decrease before the start of synchronization, yielding from resistance and drag torque act on transmission gear. If shifting up, this resistance torque will decrease the relative rotational velocity; on the contrary, it was used to increase the relative rotational velocity while shifting down.

The relative rotational velocity starts decreasing quickly when the start of synchronization, at point A. The decrease keeps until point D, when the relative rotational velocity approaches zero; meanwhile, index torque becomes higher than cone torque. So sleeve starts

moving forward again for engaging with outer ring, and results in the clutch gear rotating in reverse relative, which results from the engagement on sleeve and outer ring, as showing in the interval between point D and F.

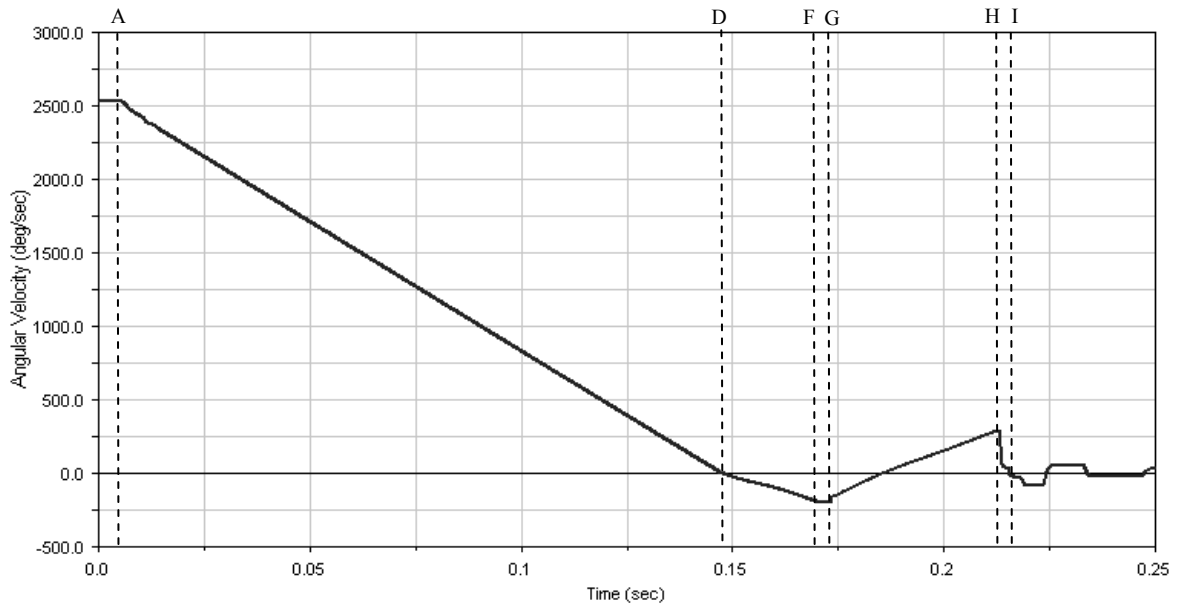


Figure 3.4-4 Relative rotational velocity between hub and transmission gear

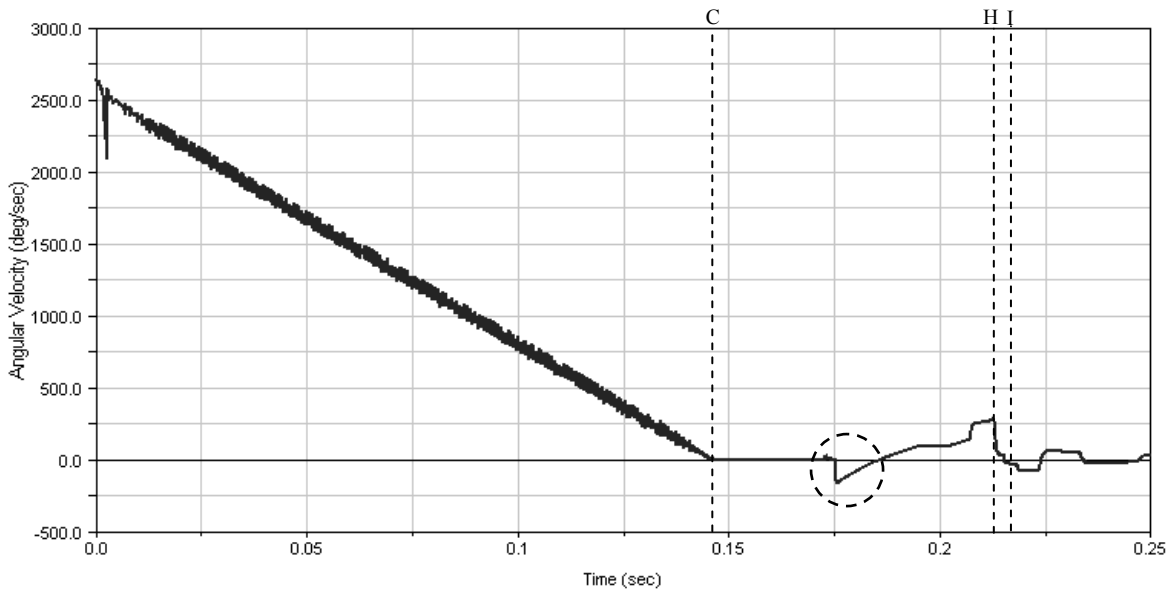


Figure 3.4-5 Relative rotational velocity between outer ring and transmission gear

At the interval between point F and G, sleeve finishes engaging with outer ring, so the relative rotational velocity between sleeve and transmission gear keep in a certain value. After point G, sleeve contacts and starts engaging with clutch gear; consequently, it yields the

transmission gear rotates again. The phenomenon that was shown on the circle, showing in Figure 3.4-5, is due to this contact force between sleeve and clutch gear. The simulation result between point G and H in Figure 3.4-4 depends on different mesh possibility, which will be discussed in next section.

Point D and C, in Figure 3.4-4 and Figure 3.4-5 respectively, is different. At point C, the relative rotational velocity between outer ring and transmission gear reaches zero, and the cone torque starts decreasing; meanwhile, the rotational velocity on transmission gear is still higher than hub and sleeve. That will approach zero only when sleeve keeps proceeding until point D. Besides, there is several unregulated variation from negative to positive, resulting from bevel and the contact between sleeve and clutch gear after engagement, after point H.

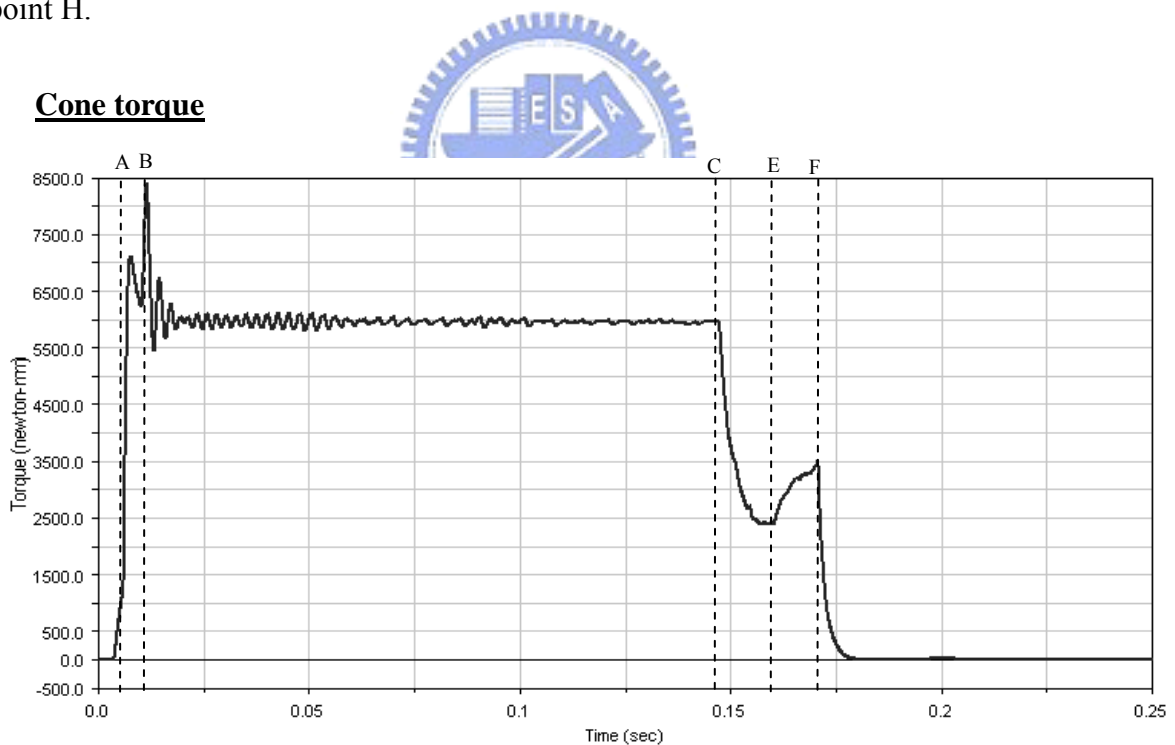


Figure 3.4-6 Torque yielded between cone and rings

Figure 3.4-6 shows the cone torque, acting on outer ring, during the shifting. This torque starts increasing as the distance between outer ring with cone, and inner ring with cone decrease, at point A, because lubricant was drained out, and lead to the increase of both

contact force and coefficient of friction on cone surface. The cone torque yields a peak at the first time when sleeve contacts with outer ring, at point B.

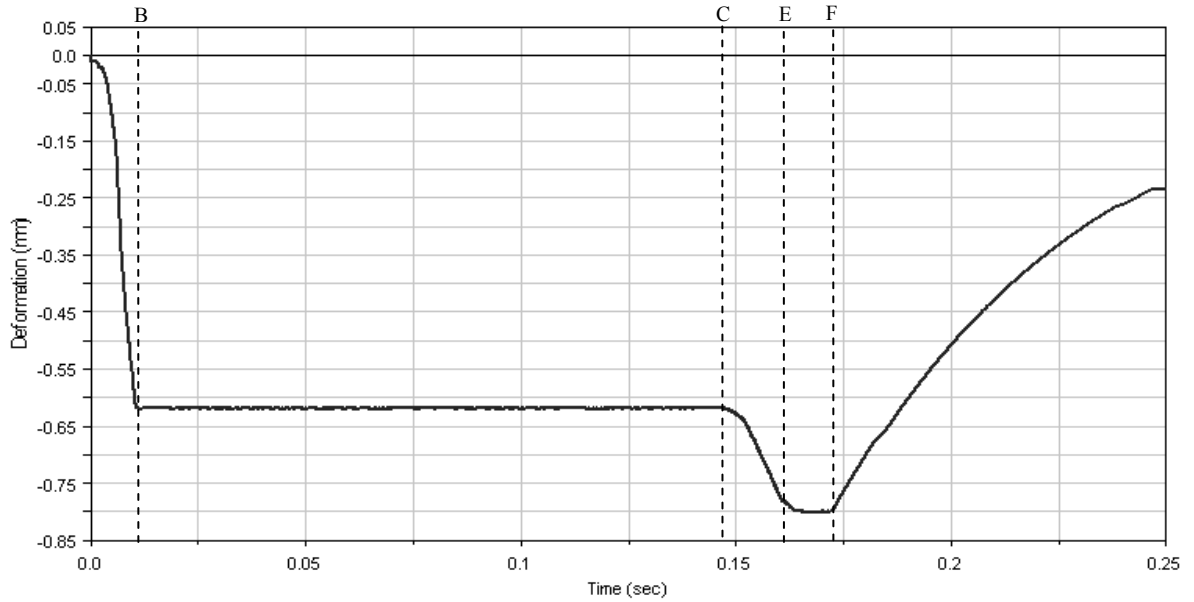


Figure 3.4-7 Deformation on annular spring

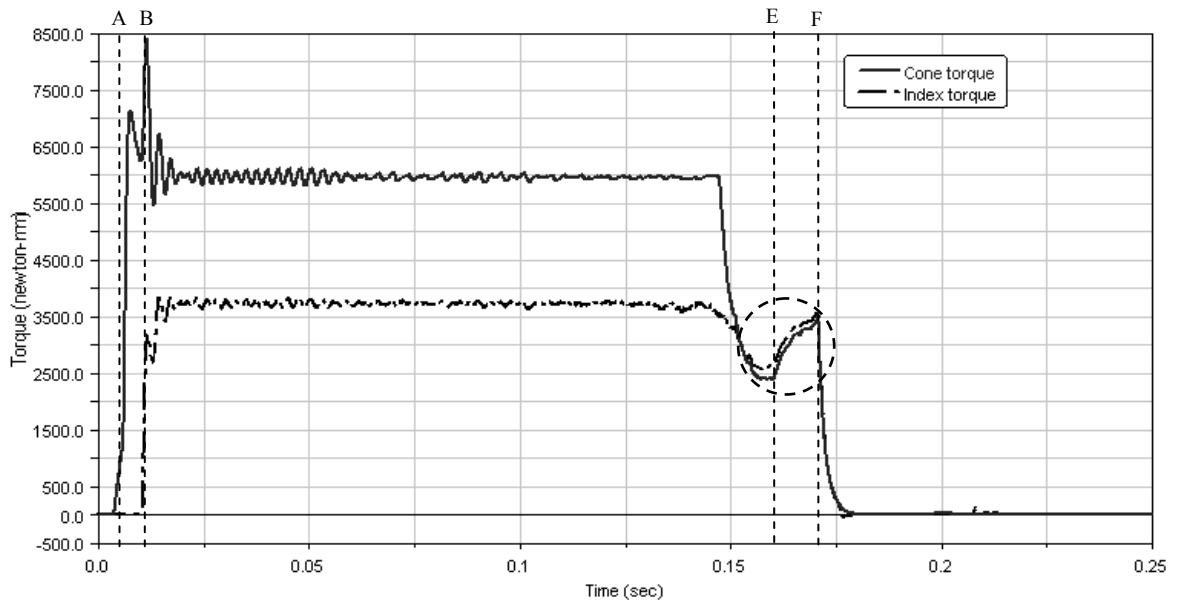


Figure 3.4-8 Cone torque and index torque

After finishing synchronization, at point C, sleeve moves to engage with outer ring that leads to the decrease of cone torque as the contact force on outer ring is decreasing.

Meanwhile, annular spring stays in the front section in Figure 2.3-5 that was shown in Figure 3.4-7. As sleeve moves to point E, annular spring reaches the middle section, where causes the maximum spring force and resistant force, acting on sleeve from annular spring to impede the movement of sleeve. Therefore, the cone torque rises again until the sleeve finishes engaging with outer ring, because the contact force action from sleeve to outer ring is increasing, and then the cone torque starts to fall approach to zero, after point F.

As Eq. (2.3-8), the result of index and cone torque was shown in Figure 3.4-8, where cone torque is always larger than index torque only as the relative rotational velocity between transmission gear and sleeve approaches to zero. Index torque was yielded at point B, and then it keeps in a certain value until the end of synchronization, right after that, it begins to become larger than cone torque, and results in the engagement between sleeve and outer ring. This situation of index torque larger than cone torque brings out sleeve moving in forward, and leads on sleeve engaging with outer ring. In this simulation, the average cone torque is about 6000 N-mm, which almost equals to the value 5927.967 N-mm, calculated from Eq. (2.3-6).

Angular displacement of outer ring

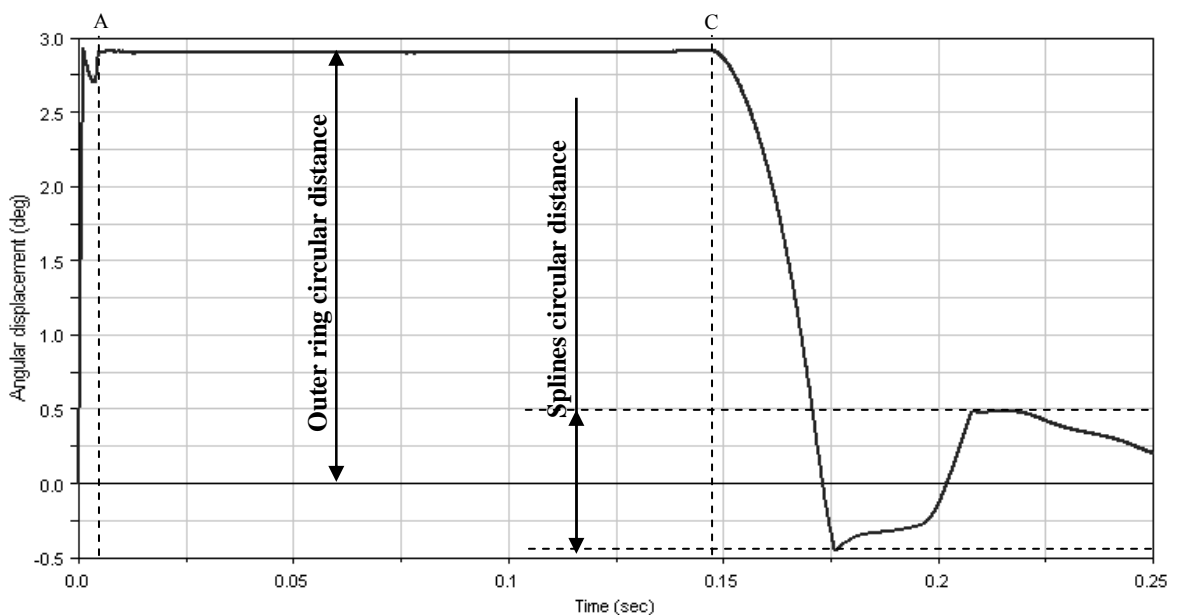


Figure 3.4-9 Relative rotational displacement between hub and outer ring

The relative rotational displacement between hub and outer ring was shown in Figure 3.4-9. While spline of sleeve begins to contact with outer ring, index torque was yielded and leads outer ring rotating in reverse direction, then it reverts to contact with sleeve for synchronization, as in point A. Until the finish of synchronization, sleeve keeps moving and pushes outer ring rotating in reverse direction again. After the mesh of outer ring and sleeve, sleeve is vibrating in the rotational direction according to the clearance, which is in the rotational direction between splines.

Coefficient of friction on cone

The coefficient of friction on cone, which was shown in Figure 3.4-10, is increasing suddenly at point A, while the sleeve force prompts outer ring to move forward cone for draining lubricant out. It is decreasing after finishing synchronization, because the sleeve force acting on outer ring is also reduce, and leads outer ring slides away from cone, after point F.

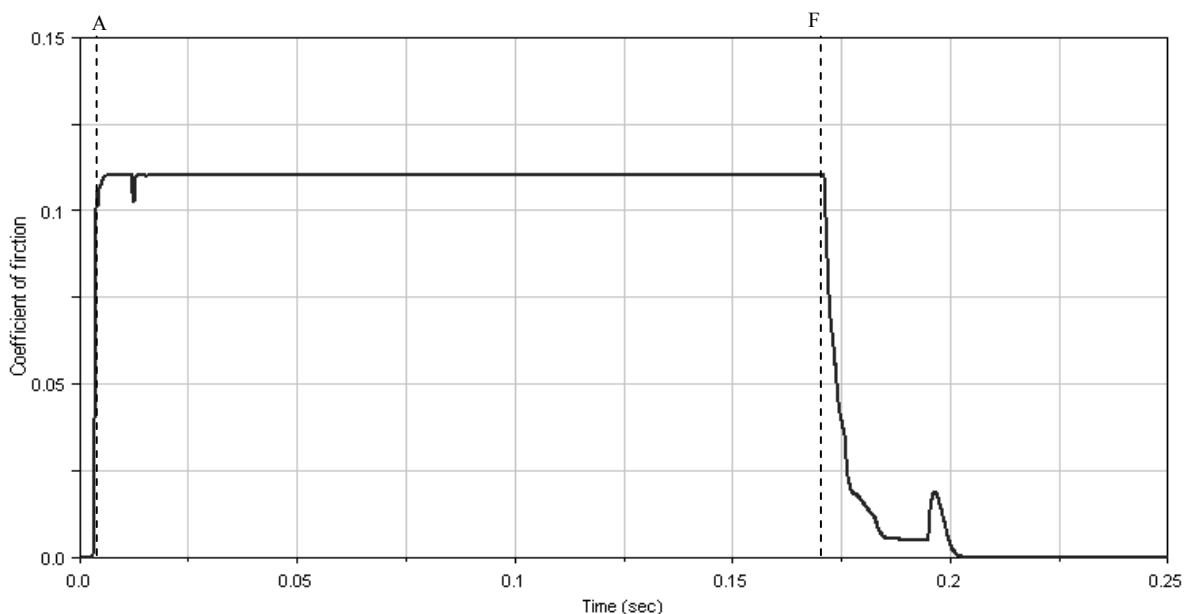


Figure 3.4-10 Coefficient of friction between cone and rings

3.5 Separating Modules

After engaging in the analytic model with the same simulation conditions but different situations, the thesis found out that it would bring different simulation results, shown in Figure 3.5-1 and Figure 3.5-2. It can be found that the results, no matter displacement of sleeve or relative rotational velocity, are the same before sleeve finishing engaging with outer ring, and different after that.

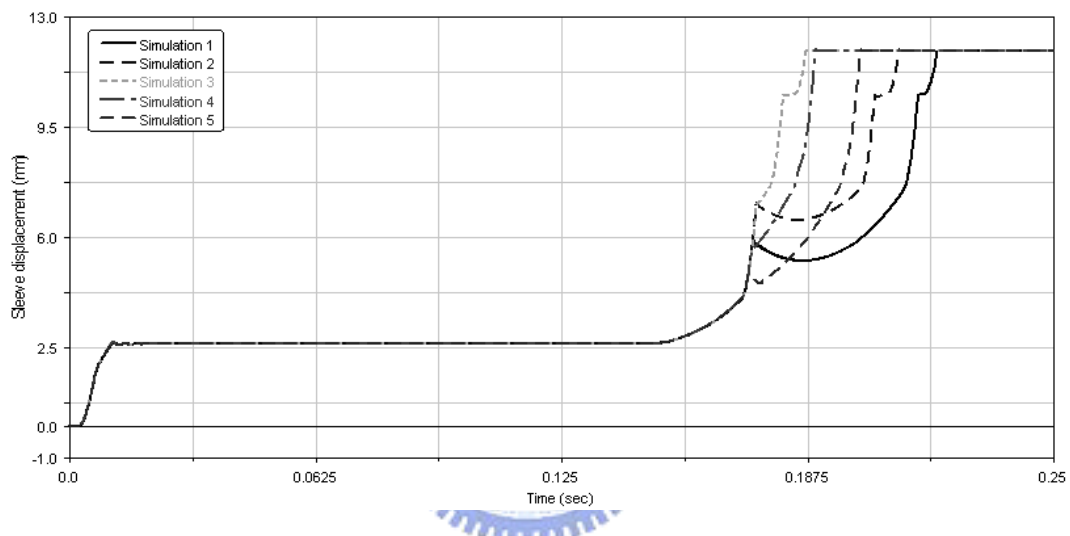


Figure 3.5-1 Distance of sleeve movement with the same conditions in different situation

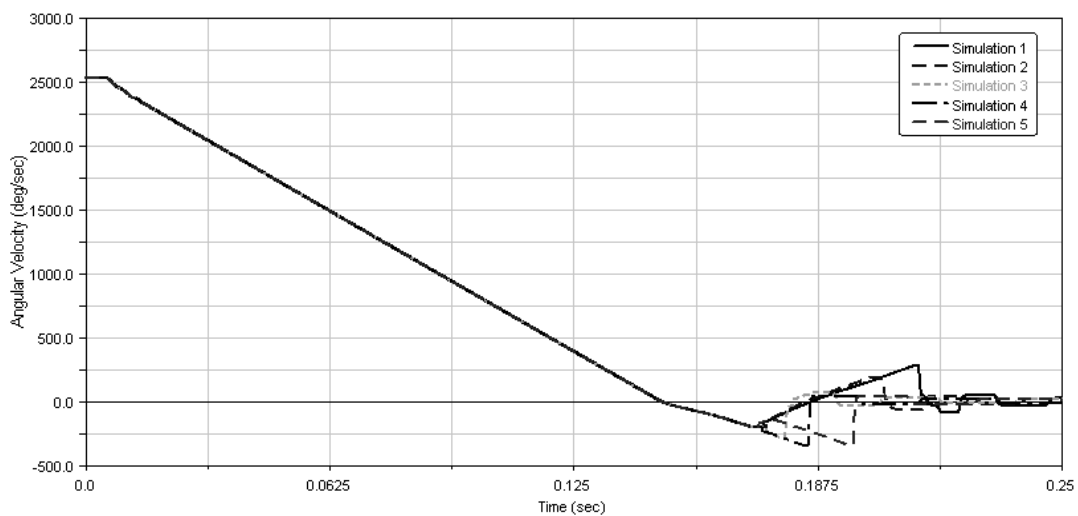


Figure 3.5-2 Relative rotational velocity with the same conditions in different situation

Considering that the phenomena of synchronization occur irregularly in very short time, and the gear shifting mechanism is very complex, separating the entire process on shifting is a better method for analyzing it. Another reason for separating entire model is that the mesh between sleeve and clutch gear is a random process, separation can focus on the procedure of random process and individual discuss it.

In this section, the entire analytic model will be separated into two parts; the first part is from starting of simulation until sleeve pass through outer ring, the second part is from sleeve pass through outer ring until finish shifting. Both these two parts are constructed on ADAMSTM, called synchronized module and mesh module, respectively.

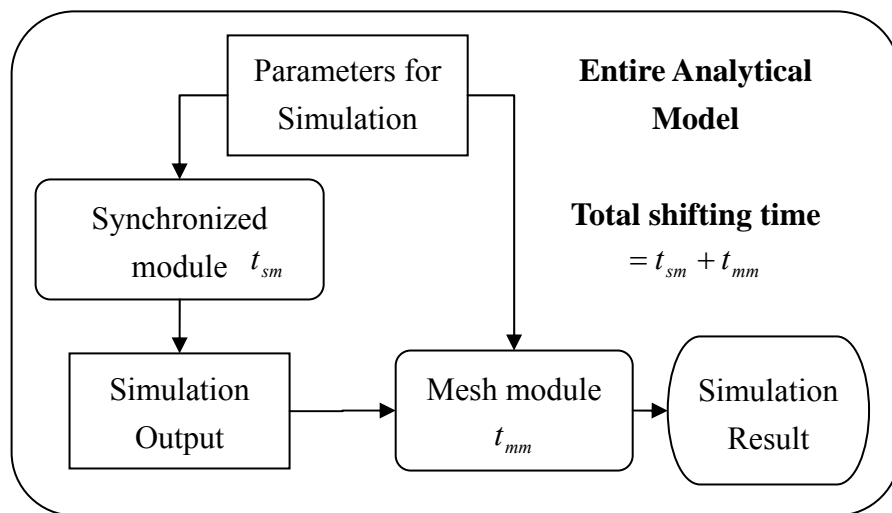


Figure 3.5-3 Procedure on separating modules

The line of demarcation on these two modules are according to Figure 2.3-14 while $x = 0$. The shifting process belongs to synchronized module when $x > 0$, and belongs to mesh module if $x < 0$ until finish gear ratio shifting.

The shifting time is also divided into two parts, so that the total shifting time equals to time on synchronized module plus time on mesh module, where t_{sm} is time on synchronized module and t_{mm} is time on mesh module.

Figure 3.5-3 mentions about the procedure of connecting these two modules. Simulation

parameters will be assigned to synchronized module first, then the simulation outputs from synchronized module and some parameters that were assigned to synchronized module will be assigned to mesh module, and further gains the final simulation result. As far as these input parameters or simulation output, these will be concerned in the following sections.

3.5.1 Synchronized Module

3.5.1.1 Module Description

Synchronized module, which was used for simulating the action before sleeve engaging with clutch, was cut apart from entire model. This module is just like entire model except for adding a sensor to stop the simulation. The sensor can sense the movement of sleeve and stop the simulation until sleeve move forward to finish engage with outer ring at $x = 0$ on Figure 2.3-14. Lessening variable parameters to simply the discussion and analysis is the reason for choosing $x = 0$.

The parameters, assigned to this module, are the same as Table 3.3-4. There are two outputs, which are linear velocity of sleeve v_s and rotational velocity of clutch gear ω_c , on this module. These parameters will be assigned to next module for proceeding different mesh possible.

3.5.1.2 Simulation Results

Gaining linear velocity of sleeve and rotational velocity of clutch gear for assigning to mesh module are the main purpose on the module. The simulation results and simulation interval on this module is exactly the same as it on entire model except less analysis time, because of the sensor, so the simulation results will not be mentioned in this section again.

The parameters, assigned to the module, were listed as Table 3.4-5 for simulating the shifting from 1st gear ratio to 2nd gear ratio. The linear velocity of sleeve and angular velocity of clutch gear on this module were shown on Figure 3.5-4 and Figure 3.5-5, respectively. These two final velocities, which are $v_s = 1131.8802\text{mm/sec}$ and $\omega_c = -206.64783^\circ/\text{sec}$, will be assigned to mesh module for proceeding the random processes of engaging between sleeve and clutch gear.

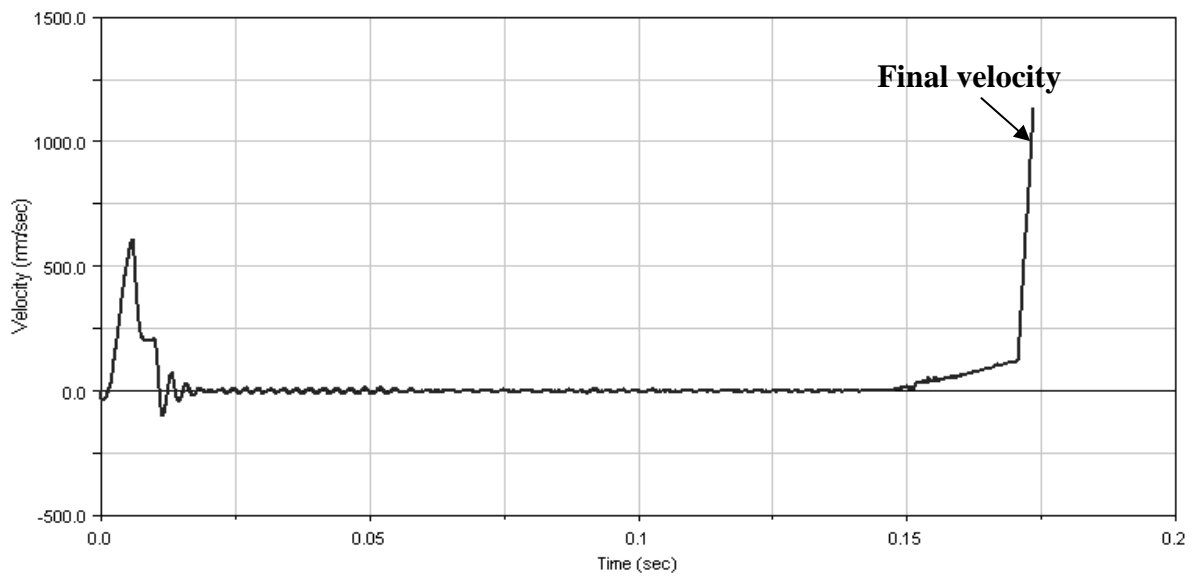


Figure 3.5-4 Sleeve velocity on synchronized module

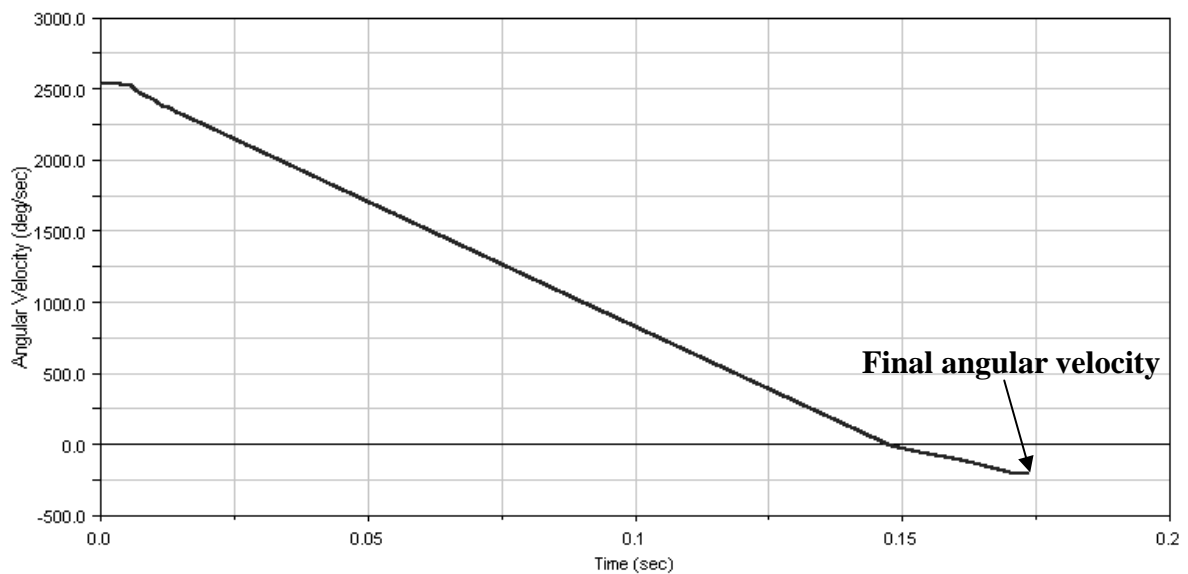


Figure 3.5-5 Angular velocity of clutch gear on synchronized module

3.5.2 Mesh Module

3.5.2.1 Module Description

After sleeve moves until arriving $x = 0$, the simulation model starts switching to mesh module. The mesh module was constructed for simulating the possibilities of engaging processes between sleeve and clutch gear. The module will change different mesh angle between sleeve and clutch gear for analyzing different mesh situation; the probability of all these angles are equally to be assumed here.

Table 3.5-1 Parameters assigned to mesh module

Description	Unit	Notation
Reflected initial applied on clutch gear	$kg \cdot mm^2$	I_r
Maximum shifting force	nt	F_{sM}
Static coefficient of friction between teeth	None	μ_{ms}
Dynamic coefficient of friction between teeth	None	μ_{md}
Velocity of sleeve	mm / sec	v_s
Rotational velocity of clutch gear	$^\circ / sec$	ω_c
Mesh angle between sleeve and clutch gear	$^\circ$	θ_m
Teeth angle on clutch gear	$^\circ$	θ_g

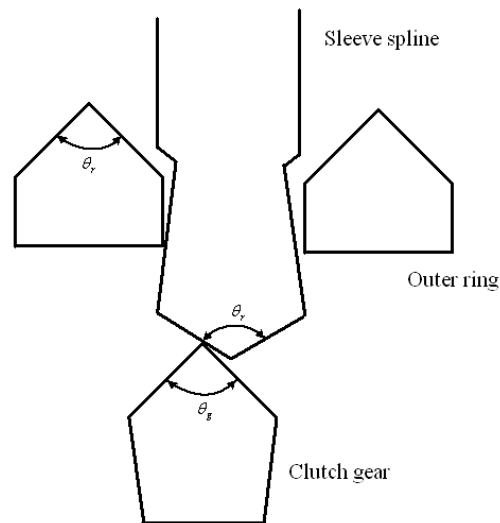


Figure 3.5-6 Geometric shape on splines of sleeve, outer ring, and clutch gear

Table 3.5-1 lists some parameters, assigned to mesh module, where θ_m is the mesh angle between sleeve and clutch gear that was defined as Figure 3.5-7, and θ_g is the teeth angle on clutch gear, and θ_r is the angle on spline chamfer of sleeve, shown in Figure 3.5-6.

Some of parameters are the same as in synchronized module, and some are originated from the simulation result in the synchronized module except θ_m . The angle θ_m was set for simulating different mesh possibility in this module. It will be set from 80° to 90° on simulation because the angle between splines on sleeve is 10° .

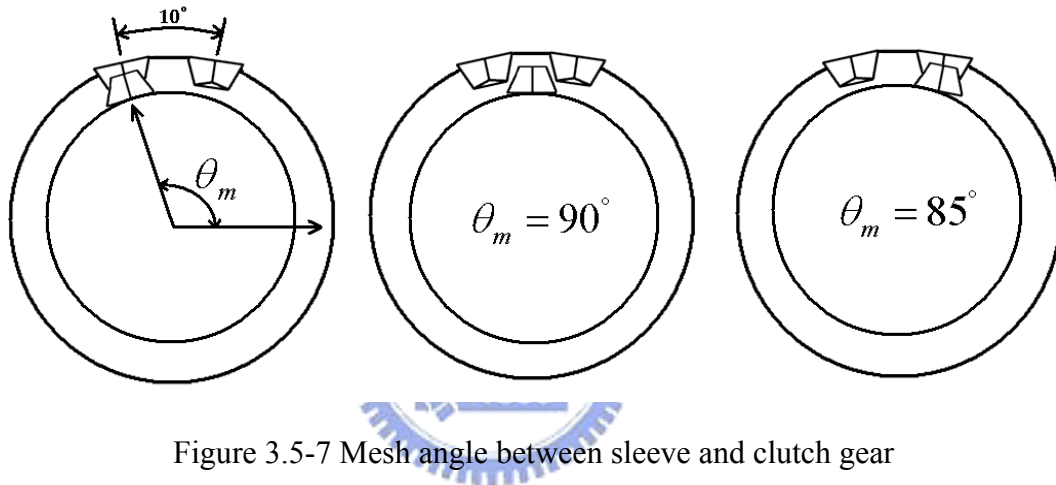


Figure 3.5-7 Mesh angle between sleeve and clutch gear

3.5.2.2 Simulation Results

The parameters, assigned to mesh module, were shown in Table 3.5-2.

Table 3.5-2 Parameters assigned to mesh module for shifting from 1st to 2nd

I_r	μ_{ms}	μ_{md}	ω_c	F_{sM}	θ_g
$1.9423 \times 10^4 \text{ kg} \cdot \text{mm}^2$	8.5E-2	5E-2	$206.6478^\circ / \text{sec}$	120 nt	90°

For simulating this module, θ_m is set from 80° to 90° with a interval of 0.25° , and the calculation interval for this module is 0.00001 seconds.

The scale view on displacement of sleeve for different mesh angle between sleeve and clutch gear was shown in Figure 3.5-8. Certain mesh angle leads into the forward and

backward movement of sleeve, but sleeve only moves forward in some others mesh angle. The detail specification of these phenomena will be mentioned later.

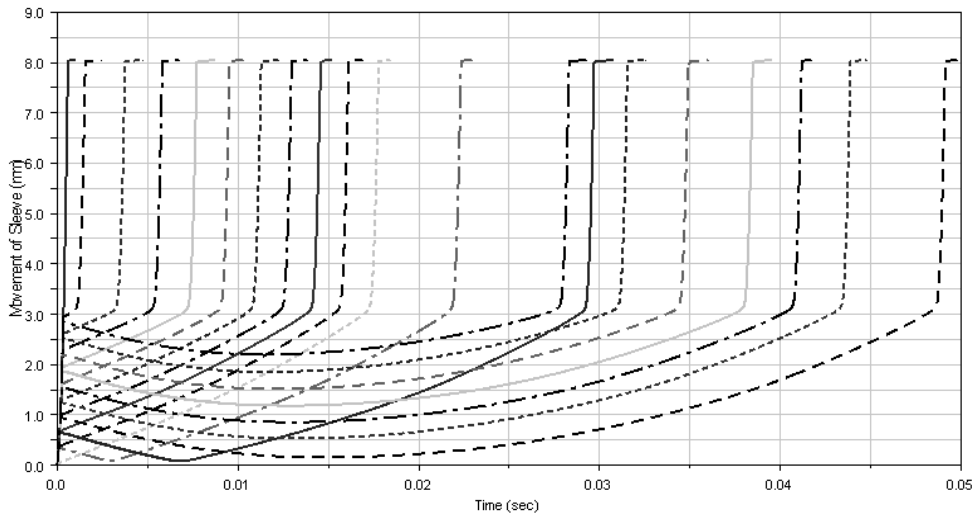


Figure 3.5-8 Scale view on displacement of sleeve for different mesh angle

The mesh time with different mesh angle was shown in Figure 3.5-9. It can be clearly found out that the mesh time is variable with angle. In this simulation case, shifting from 1st to 2nd gear ratio, the maximum mesh time is 0.0489sec, and minimum mesh time is 0.00005 sec. There is a huge difference between different mesh angles, which were simulated in different mesh possible angle.

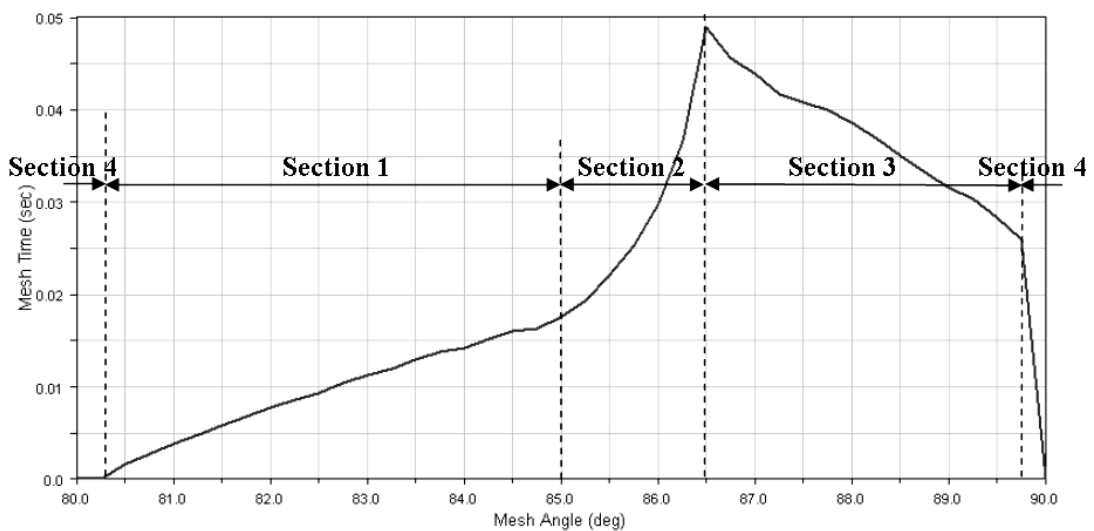


Figure 3.5-9 Mesh time with different mesh angle

The mesh processes on different angle are divided into four sections, which can be associated with Table 2.3-1, and discussed as below.

Section 1

In this section, the first contact point between sleeve and clutch gear is located at the reverse direction of rotational velocity on clutch gear, just like event A and B on Table 2.3-1. The description of this section was shown as Figure 3.5-10. Sleeve moves forward to slide along the chamfer on clutch gear, and pushes clutch gear rotating for speed-up. The range on the section in this simulation conditions is located on 80.5° to 85° .

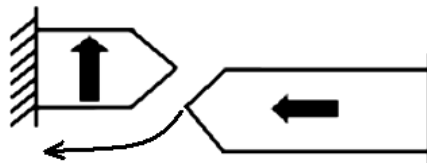


Figure 3.5-10 Mesh description of section 1

Section 2

The next section was shown as Figure 3.5-11, which is like event E on Table 2.3-1; in this section, sleeve contacts with clutch gear on its rotational direction. Because of the relative rotational velocity between clutch gear and sleeve, sleeve moves backward until crossing over the teeth of clutch gear, and then it slides along the chamfer of teeth for the final mesh. The range of section 2 on the simulation situation is between 85.25° to 86.25° .

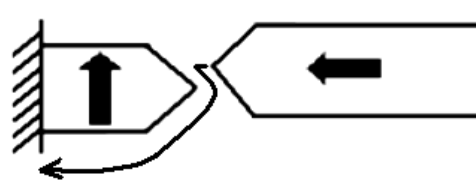


Figure 3.5-11 Mesh description of section 2

Section 3

In section 3, sleeve contacts with clutch gear first located on its rotational direction without crossing teeth of clutch gear, shown as Figure 3.5-12. The moving force, acted on

sleeve, was used to provide a torque, which was yielded from contact force for slowing down the rotational velocity of clutch gear. The range of section 3 on the simulation situation starts from 86.5° till 89.75° .

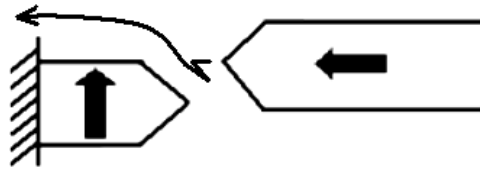


Figure 3.5-12 Mesh description of section 3

Section 4

The last section on was shown as Figure 3.5-13, and event C on Table 2.3-1. In this section, sleeve just engages with clutch gear exactly that spends on the less mesh time among all these four sections.

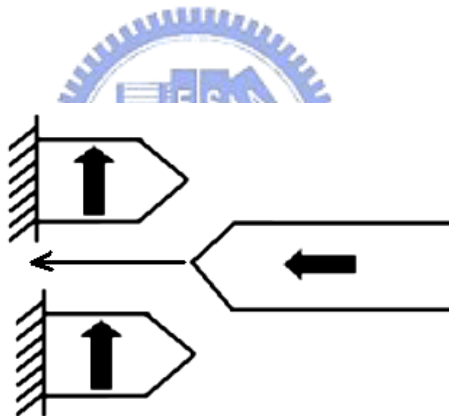


Figure 3.5-13 Mesh description of section 4

Among the four sections, if the simulation conditions, which include sleeve force, reflected inertia, teeth and spline angle, linear velocity of sleeve, and rotational velocity of clutch gear, are changed, the line of demarcation between all these sections will be different.

Because the assumption of the probability on these angles are the same, the average shifting time can be considered as the time from synchronized module plus the average time on mesh module. The average shifting time is 0.19479sec which equal to time of synchronized module 0.1736sec plus average of all time on mesh module 0.02119sec.

The simulation result, mentioned on 3.4.2 , just is one of possibilities that has been talked in this section.

3.5.2.3 Mesh Specification

Table 3.5-3 List of descriptions

Mesh process	Probability	Remark
Section 1	47.5 %	Sleeve moves forward without moving backward
Section 2	12.5 %	Sleeve moves backward and crosses spline of clutch gear
Section 3	35 %	Sleeve moves backward without crossing spline of clutch gear
Section 4	5 %	Sleeve engages with clutch gear exactly

The simulation results on these four sections will be mentioned in this section. Because the interval is very small, and the amount of simulation results is huge, the thesis only picks some of them for discussing the simulation results.

As the assumption of equally happened probability, the probability of each section can be obtained from the simulation results, listed on Table 3.5-3.

Section 1, which has the largest probability, occupies nearly half of mesh possible. Besides, the least probability among these four sections is section 4, which describes sleeve engaging with clutch gear exactly, and only has five percent probability.

The displacement of sleeve on mesh module was shown in Figure 3.5-8, which gathers all these four section and provides the state of affairs on sleeve in different sections. The discrimination between every section can be particular described respectively in the following figures.

Figure 3.5-14 shows the displacement of sleeve from section 1 through section2. There can be clearly realized that if the angle is smaller than 85.25° , the sleeve moves only forward

to engage with clutch gear. Nevertheless, while mesh angle is larger than or equal to 85.25° , sleeve will occur backward phenomenon and cross spline for a further contact with the opposite chamfer.

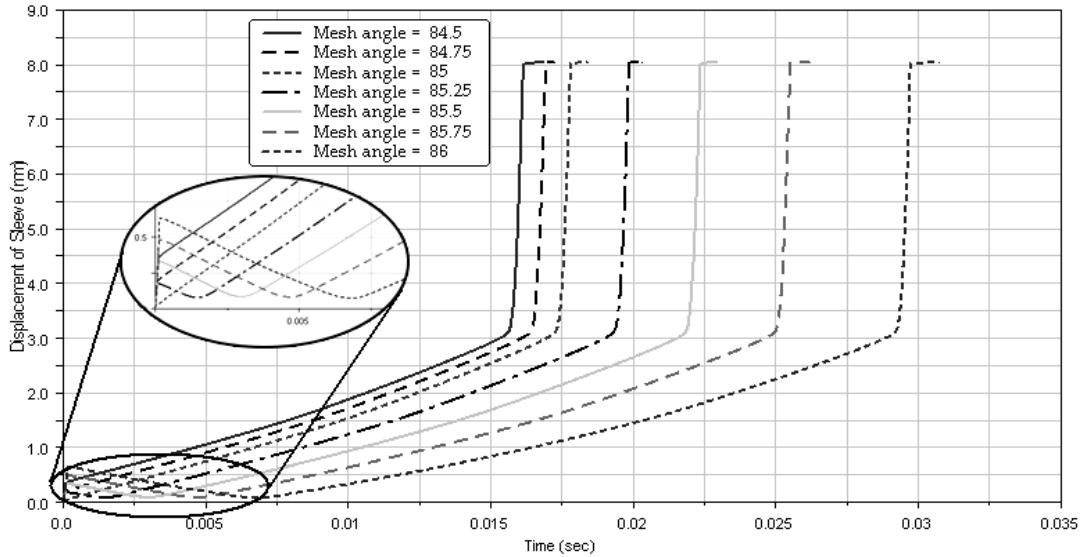


Figure 3.5-14 Displacement of sleeve on sections 1 and 2

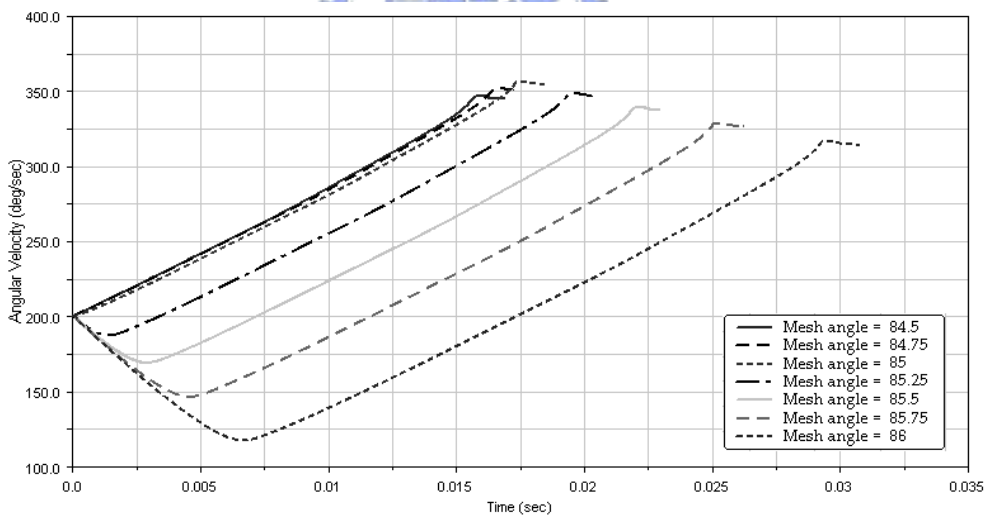


Figure 3.5-15 Relative rotational velocity on sections 1 and 2

The relative rotational velocity between sleeve and clutch gear was shown in Figure 3.5-15. In section 1, the moving force acts on sleeve to speed up the rotation of clutch gear. However, in section 2, sleeve contacts with clutch gear on its rotational side; moreover, the contact force leads into the deceleration of clutch gear and backward moving of sleeve. After sleeve crossed over spline of clutch gear, sleeve moves forward again for engaging with

clutch gear just like in section 1.

The results on displacement of sleeve and relative rotational velocity between section 2 and section 3 were shown in Figure 3.5-16 and Figure 3.5-17 respectively.

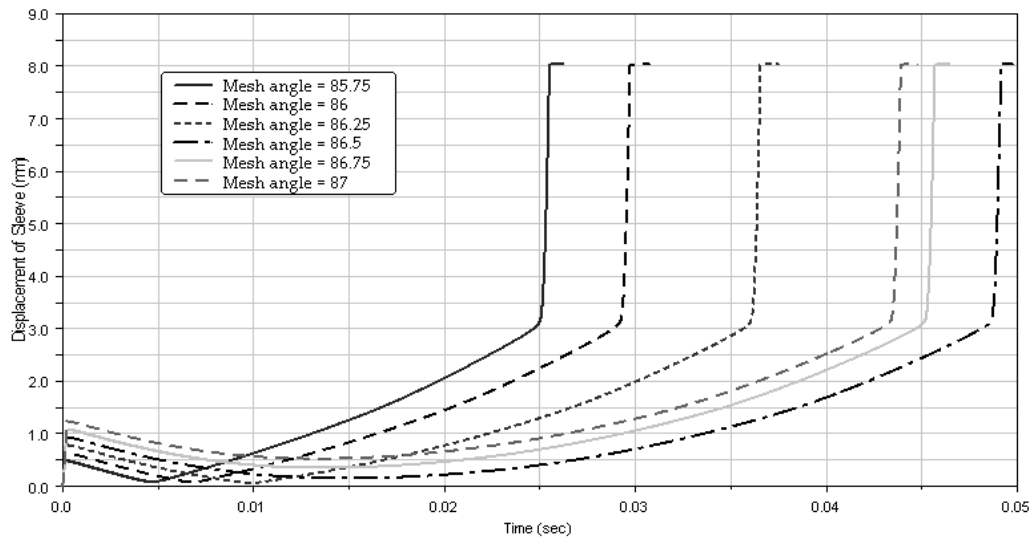


Figure 3.5-16 Displacement of sleeve on sections 2 and 3

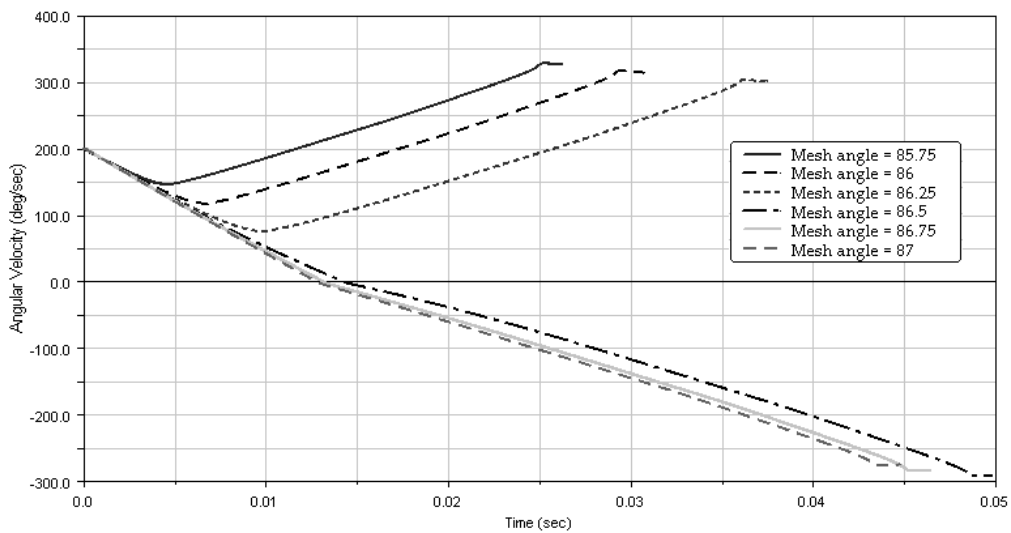


Figure 3.5-17 Relative rotational velocity on sections 2 and 3

In section 3, sleeve moves backward while contacts with clutch gear, because of the rotational velocity of clutch gear. Differing from section 2, sleeve did not move backward enough to cross the spline, so sleeve starts moving forward to engage with clutch gear afresh after a few backward movements. Whereas clutch gear that rotates in reverse direction until

finish engagement is due to the moving force and contact force between sleeve and clutch gear.

The probability and range of each section that was discussed before results from the simulation condition on this thesis. Different simulation condition, such as sleeve force, v_s , ω_c , chamfer angle on clutch gear, reflected inertia, will bring out different consequence. Nevertheless, the mesh process and situation from other different simulation condition will be the same as four sections, mentioned in this thesis.

Comparing with the average time to the shifting time on Figure 3.4-3, showing the engagement process on the simulation result, is one of possibilities meshing between sleeve and clutch gear. Besides, different shift situation, and conditions, will bring out different cases on this final lockup, the engagement between sleeve and clutch gear; the influence, resulting from different parameters about synchronization and engagement, will be discussed in the following chapter.



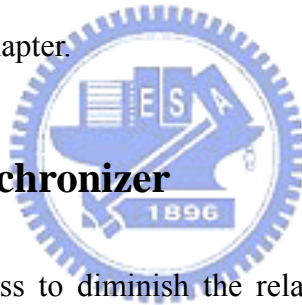
CHAPTER 4

PARAMETERS ANALYSIS

4.1 Introduction

After the construction and confirmation on simulation model of shifting, this chapter will do some parameter analysis to realize the influence between parameter and synchronization and engagement. The chapter will discuss durability of synchronization first, and then talk about parameter analysis on synchronized and mesh modules respectively. Furthermore, the results in this chapter can not only help for understanding the variation of simulation results with parameters, but also assist the discussion and provide a clearer understanding about the optimization in the next chapter. The simulation case, shifting from 1st to 2nd, is the same as in previous chapter as in this chapter.

4.1 Durability on Synchronizer



Synchronization, the process to diminish the relative rotational velocity between input shaft and output shaft, always leads to abrasion on rings surface because of the cone torque, yielded from the contact force between cone and rings. At that time that the phenomenon happened, cone torque will be lower than index torque, and result in synchronized failure on the process of synchronization as mentioned in the previous chapter. Therefore, the phenomenon will reduce the quality and durability of synchronizer, which is an important criterion that has to pay attention on by the designer and engineer who engage in the research of gearbox.

4.1.1 Lubrication and Wear

On the first process of synchronization, there exists a thin film between cone and rings; a

lubricant film separated these surfaces and no asperities are in contact to result the wear between cone and rings. While sleeve moves to contact with outer ring, lubricant was drained out leading in the contact of cone and rings for synchronization. Consequently, the coefficient of friction on cone surface starts rising from low to high, and then it decreases to low after finishing synchronization. Moreover, the contact force is the main force that wears the tiny long grooves on inner and outer ring.

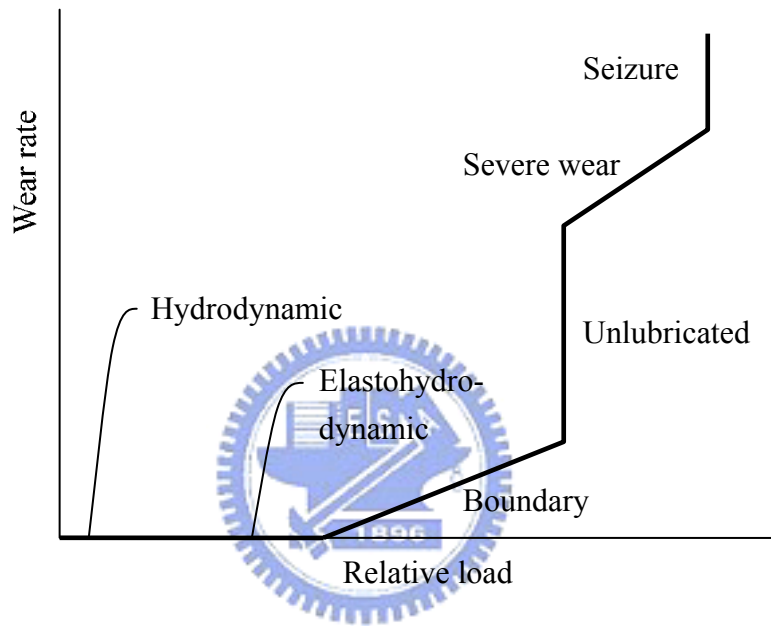


Figure 4.1-1 Wear rate for various lubrication regimes (Hamrock et al., 1999)

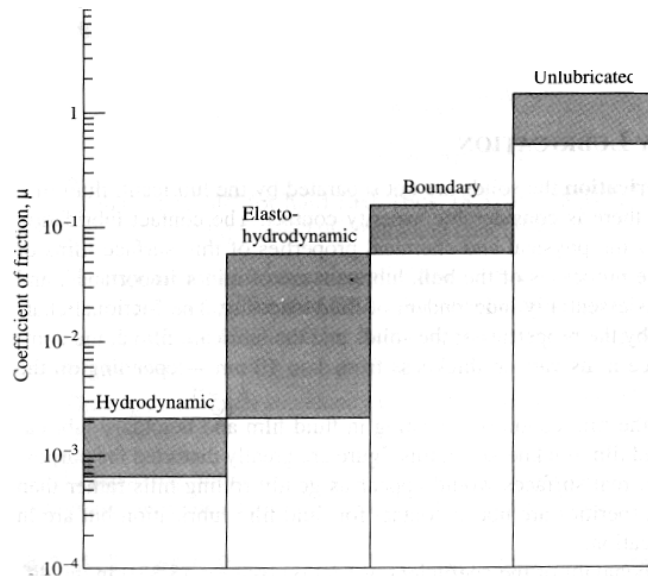



Figure 4.1-2 Showing coefficient of friction for various lubrication conditions (Hamrock et al., 1999)

There are four different regimes, which include hydrodynamic lubrication, elastohydrodynamic lubrication, boundary lubrication, and partial lubrication, at different lubricant situation; the wear rate was shown in Figure 4.1-1, whereas coefficient of friction was shown in Figure 4.1-2 on each lubrication except partial lubrication. Hydrodynamic lubrication is generally characterized by conformal surfaces with fluid film lubrication. Elastohydrodynamic lubrication is a form of hydrodynamic lubrication where nonconformal surfaces are completely separated by lubricant film and no asperities are in contact. As for boundary lubrication, lubrication condition where considerable asperity interaction occurs between solids and lubrication mechanism is governed by properties of thin surface films that are of molecular proportion (Hamrock et al., 1999). Since the surface that between cone and rings does not conform to each other very well, the situation before synchronization belongs to nonconformal surfaces.



In the normal situation of synchronization, the regime is elastohydrodynamic lubrication that brings merely a lower coefficient of friction on cone surface. While the synchronization starts, the gaps between cone and rings decrease and lead into boundary lubrication, which provides a higher coefficient of friction to engage in synchronization. After the finish of synchronization, lubricant refills the gaps between cone and rings, and then reinstates to elastohydrodynamic just like the situation before synchronization.

Nevertheless, at the situation of existing wear on rings, the variation on coefficient of friction differs from normal situation. The regime is elastohydrodynamic lubrication before synchronization just like the normal situation. However, the coefficient of friction on cone surface does not rise as fast as without abrasion, because the tiny long grooves were worn and could not drain lubricant out as fast as without abrasion. Consequently, the lower coefficient of friction provides a lower cone torque that leads into a longer synchronized time and probably results in synchronized failure.

Wear may be viewed as the progressive loss of substance from the operating surface of a body occurring because of loading and relative motion at the surface. Wear can be classified by the physical nature of the underlying process, such as abrasion, adhesion, erosion, fatigue, and corrosion. Abrasion is likely the most important criterion that result in the wear on inner and outer ring.

Since the three laws of wear are wear increase with sliding distance, wear increase with normal applied load, and wear increase as hardness of sliding surface increases, the synchronized time will be diminished and the wear on contact surfaces will increase as the force acting on sleeve increase. Such phenomenon will lead into a higher temperature on contact surface, and results in a serious wear between cone and ring, which is the main reason that result in diminishing on coefficient of friction and synchronized failure as mentioned before.



4.1.2 Variation in Coefficient of Friction on Cone

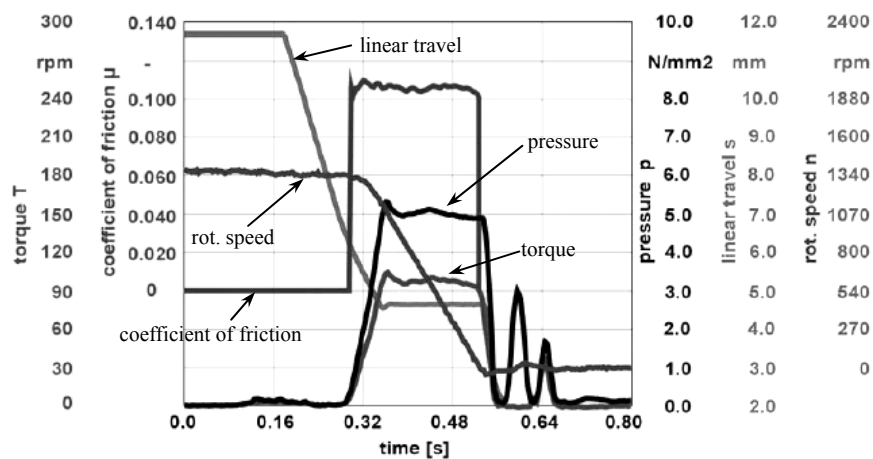


Figure 4.1-3 Cycle #500 of endurance test (Sigl and Höhn, 2003)

Because the wear influences the situation of increasing on coefficient of friction, the coefficient of friction will rise slower than the result shown in Figure 3.4-10. An experiment showed the phenomenon after a higher operation cycle in Figure 4.1-4. The experimental

result can compare with Figure 4.1-3, which is an experimental result from a lower operation cycle relative to a higher operation cycle.

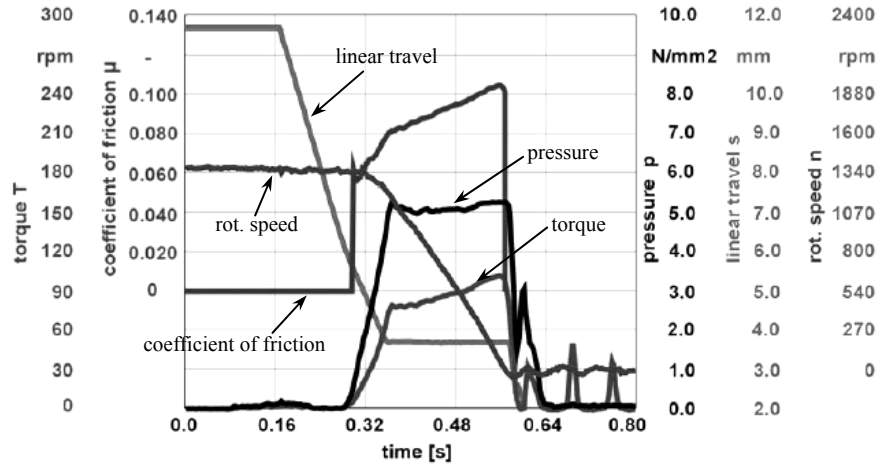


Figure 4.1-4 Cycle #100,000 of endurance test (Sigl and Höhn, 2003)

It can clear notice that the coefficient of friction in Figure 4.1-3 rising faster than in Figure 4.1-4. The vary coefficient of friction causes from the process that lubricant was drained out of gaps between cone and rings. Furthermore, the cone torque in Figure 4.1-4 also differs from Figure 4.1-3 since the cone torque equals to the multiple of coefficient of friction. While the cone torque became lower as a lower coefficient of friction, if only cone torque does not rise to equal or higher than index torque, the synchronized failure happened.

4.2 Synchronization Analysis

This section probes for the influence from parameters to simulation result. Time, mentioned in this section, equals to the interval from the start of simulation to the end of simulation on synchronized module. The simulation stops while both x in Figure 2.3-14 and relative rotational velocity between sleeve and transmission approaches zero. As for the sensitivity, will be mentioned in this section, was calculated by ADAMSTM automatically as Eq. (4.2-1), where S_i is the sensitivity, O_i is objective and DV_i is design variable.

$$S_i = \frac{1}{2} \left(\frac{O_{i+1} - O_i}{DV_{i+1} - DV_i} + \frac{O_i - O_{i-1}}{DV_i - O_{i-1}} \right) \quad (4.2-1)$$

4.2.1 Sleeve Force

Table 4.2-1 Parameter study on sleeve force

Trial	Sleeve Force (N)	Time (sec)	Sensitivity
1	100	0.20202	-0.0015150
2	125	0.16415	-0.0012603
3	150	0.13901	-0.00086964
4	175	0.12067	-0.00063906
5	200	0.10705	-0.00054447

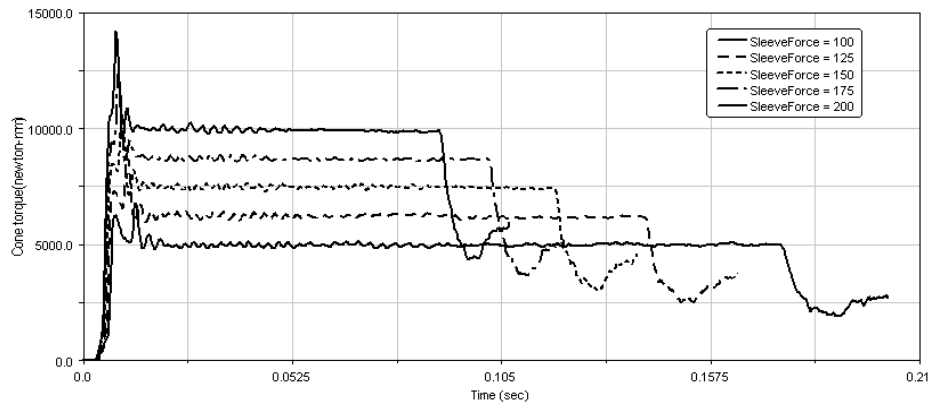


Figure 4.2-1 Cone torque versus time at different sleeve force

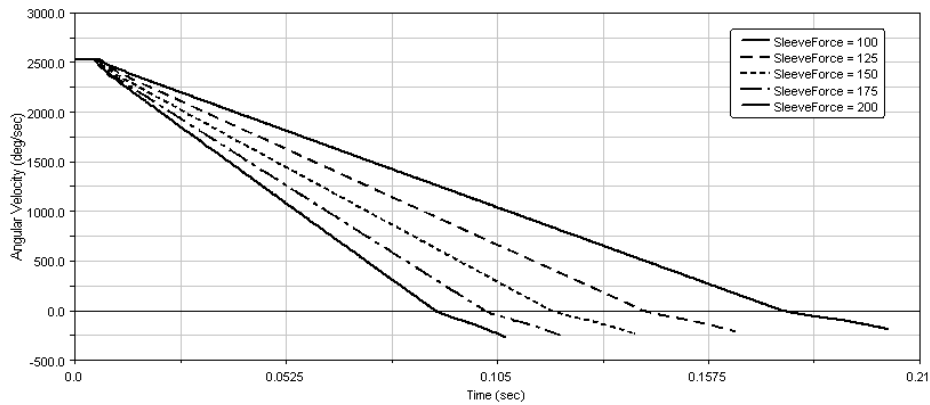


Figure 4.2-2 Relative rotational velocity versus time at different sleeve force

The first parameter, selected for discussing the influence on synchronized time, is sleeve force; the simulation result was shown on Table 4.2-1. Different operators will lead into different sleeve force, so a reasonable interval of sleeve force to engage in parameter analysis on sleeve force for realizing the influence of sleeve force on synchronization was chosen, despite there are different sleeve force exerting from driver on MT, and from actuator on AMT.

According to this analysis, the higher the sleeve force is, the short time it will be; besides, it can be found from the sensitivity, while the sleeve force is lower, the extent of time decrease also become lower. In Figure 4.2-1, a larger sleeve force will bring a higher cone torque to synchronize the relative rotational velocity, so it results in different synchronized time in Figure 4.2-2.

4.2.2 Cone Angle



Cone angle would influence the value of cone torque, and then influences the synchronized time and different synchronization, as Eq. (2.3-6). Besides, in order to avoid self-lock and let cone releases from contacting with rings after synchronization, cone angle must match Eq. (2.3-10). Five different cone angles were selected by the thesis to discuss the influence of it on synchronization, and the result was listed in the following table.

Table 4.2-2 Parameter study on cone angle

Trial	Cone Angle (degree)	Time (sec)	Sensitivity
1	7.0	0.16101	0.018967
2	7.5	0.17049	0.019080
3	8.0	0.18009	0.019081
4	8.5	0.18957	0.018918
5	9.0	0.19900	0.018869

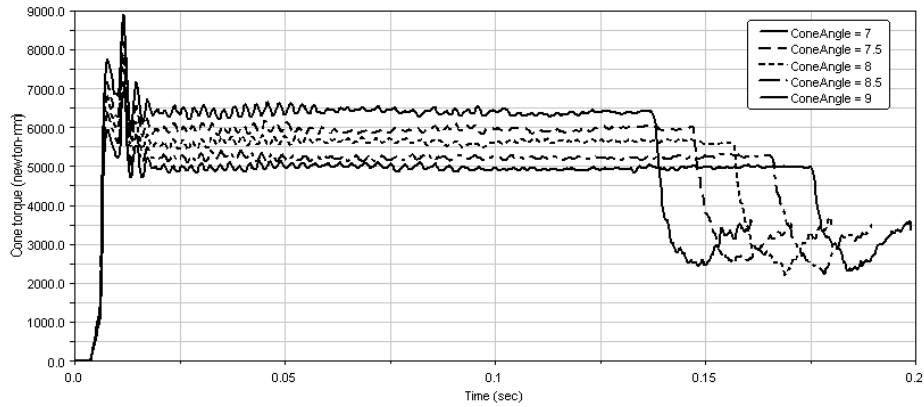


Figure 4.2-3 Cone torque versus time at different cone angle

While the cone angle increases gradually, cone torque rises with it just like Eq. (2.3-6). It can be known from Figure 4.2-3 that the lower the cone angle is, the higher the cone torque will be. Nevertheless, since cone angle was restricted by coefficient of friction in Eq. (2.3-10), the cone torque increase, resulting from cone angle, has its limit. As for relative rotational velocity, which was shown in Figure 4.2-4, does not have such large difference relative to the influence from sleeve force.

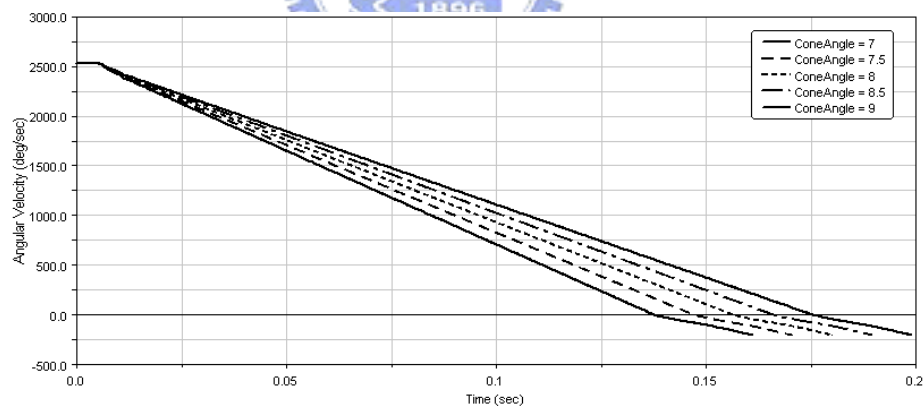


Figure 4.2-4 Relative rotational velocity versus time at different cone angle

4.2.3 Stiffness of Annular Spring

The values, choosing in this subsection, are due to Generative Structure Analysis on previous chapter, which provides to understand the rough range in stiffness of annular spring. The simulation results and parameter values are listed in the following table.

Table 4.2-3 Parameter study on stiffness of annular spring

Trial	Stiffness (N/mm)	Time (sec)	Sensitivity
1	15	0.20164	0.00012441
2	30	0.20350	0.00012488
3	45	0.20538	0.00015938
4	60	0.20829	0.00020780
5	75	0.21162	0.00022219

Table 4.2-3 says that the stiffness of annular spring does not influence a lot on synchronized time, so no matter cone torque, relative rotational velocity, and sleeve movement, shown on Figure 4.2-5 to Figure 4.2-7 respectively, all express very little difference in different stiffness. However, there is a little difference on sleeve movement while sleeve moves to contact with outer ring and finishes the engagement with outer ring.

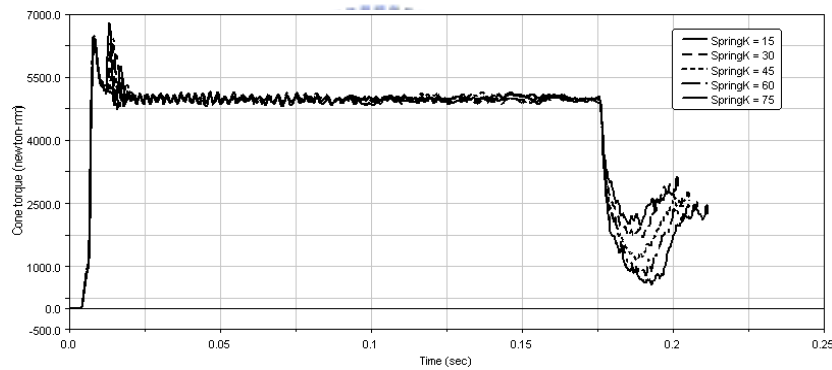


Figure 4.2-5 Cone torque versus time at different stiffness of annular spring

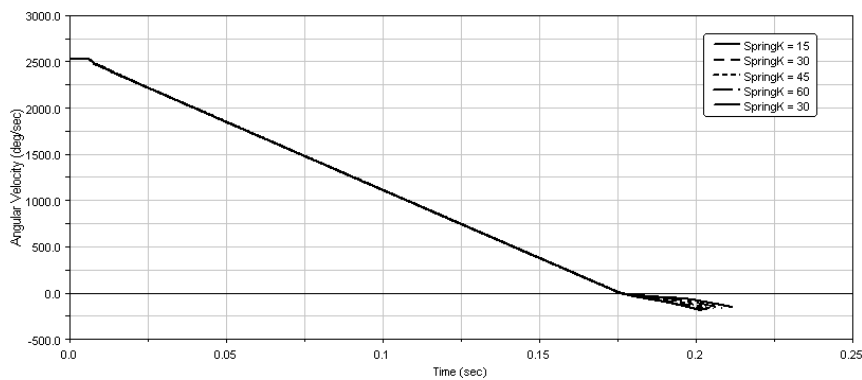


Figure 4.2-6 Relative rotational velocity versus time at different stiffness of annular spring

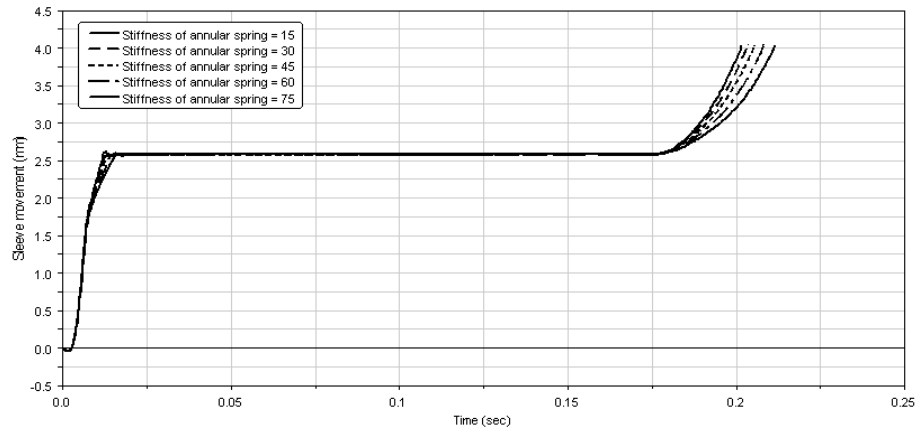


Figure 4.2-7 Sleeve movement versus time at different stiffness of annular spring

On the process of sleeve finishing engagement with outer ring, the rising velocity are different because of the stiffness and the geometric shape on larger spline in Figure 2.3-5, which provides a force for pushing sleeve to move toward clutch gear. The higher the stiffness of annular spring is, the higher pushing force can be yielded.

Figure 4.2-8 shows the scale view on sleeve movement while sleeve starts to contact with outer ring. It shows that the different stiffness will lead into different moving velocity of sleeve, which is due to resistant force from annular spring to sleeve. Since annular spring pushes outer ring moving forward cone to drain lubricant out, the different situation that results from different stiffness would relate to coefficient of friction on cone surface.

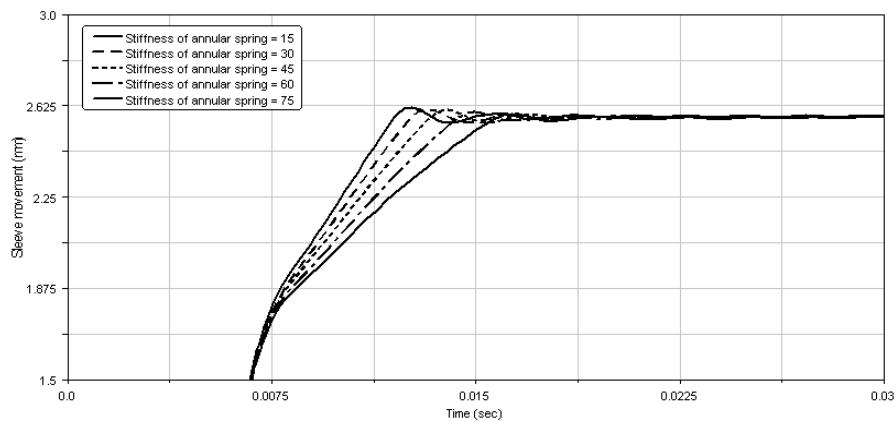


Figure 4.2-8 Scale view of sleeve movement in Figure 4.2-7

4.2.4 Coefficient of Friction on Cone Surface

4.2.4.1 Changeable μ_c with constant sleeve force

While wear occurs on inner and outer ring, the coefficient of friction that was provided to yield cone torque becomes lower. According to literatures, the coefficient of friction is always about 0.1 to 0.11 without abrasion. In this subsection, coefficient of friction from 0.06 to 0.11 was chosen by the thesis for discussing the influence of coefficient of friction on synchronization.

Table 4.2-4 Parameter study on coefficient of friction

Trial	Coefficient of friction	Time (sec)	Sensitivity
1	0.06	0.26102	-1.6283
2	0.07	0.24473	-1.5008
3	0.08	0.23100	-1.2467
4	0.09	0.21980	-1.0302
5	0.10	0.21040	-0.88884
6	0.11	0.20202	-0.83728

Figure 4.2-9 and Figure 4.2-10 show the cone torque and coefficient of friction in different coefficient of friction respectively. Since the abrasion results in that lubricant can not be drained out as fast as the situation without abrasion, the coefficient of friction can only rise to a lower coefficient of friction then gradually rise to the maximum instead of rising to maximum directly, just as shown in Figure 4.2-10.

Cone torque cannot rise to a normal value because of the phenomenon on coefficient of friction resulting from abrasion. Such difference on cone torque would lead into sleeve moves to engage with outer ring without finishing synchronization, and bring abnormal collision between spline on sleeve and clutch gear, as cone torque is lower than index torque while splines of sleeve contact with teeth of outer ring.

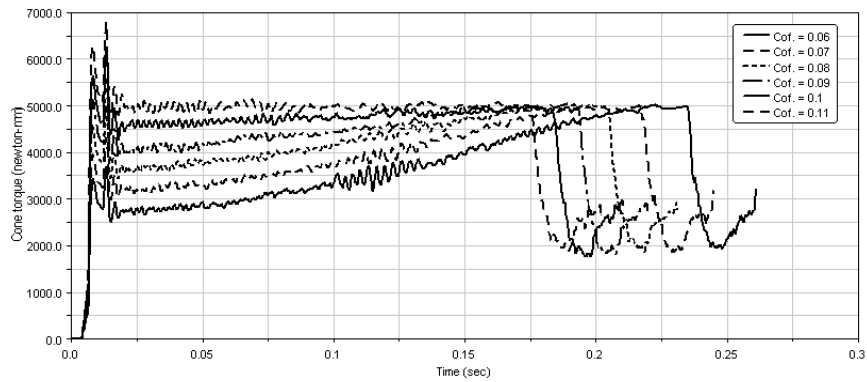


Figure 4.2-9 Cone torque versus time at different coefficient of friction

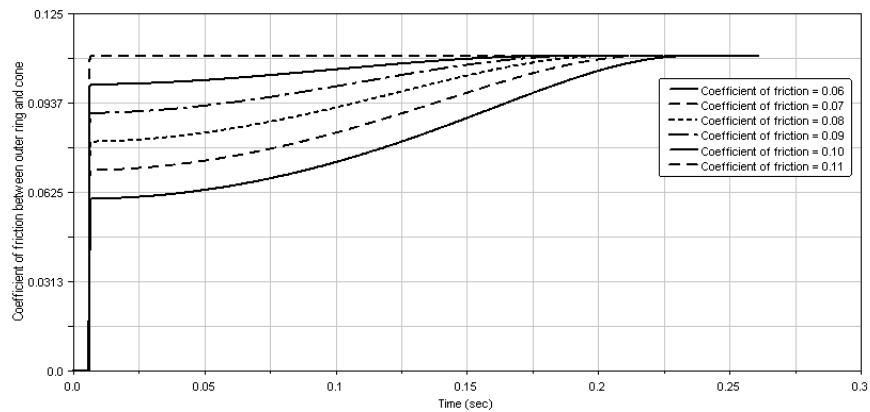


Figure 4.2-10 Coefficient of friction versus time at different coefficient of friction

As for relative rotational velocity, it also relates to cone torque, so that the lower torque will spend more time on synchronization. Besides, the variable cone torque makes the plot of relative rotational velocity yield a tiny curved line in lower coefficient of friction instead of approximate straight line in normal coefficient of friction.

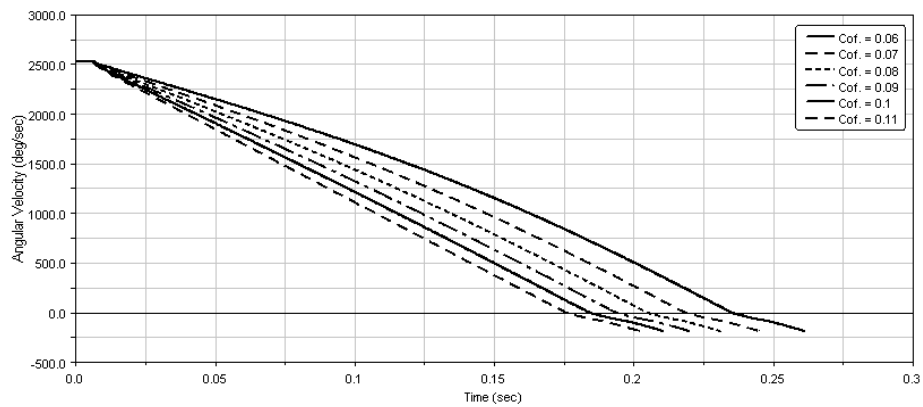


Figure 4.2-11 Relative rotational velocity versus time at different coefficient of friction

4.2.4.2 Changeable sleeve force with $\mu_c = 0.61$

Table 4.2-5 Parameter study on sleeve force at $\mu_c = 0.61$

Trial	Sleeve Force (N)	Time (sec)	Sensitivity
1	100	0.25941	-0.0020481
2	120	0.21845	-0.0017597
3	140	0.18902	-0.0012863
4	160	0.16700	-0.00098224
5	180	0.14973	-0.00078332
6	200	0.13567	-0.00070334

This subsection talks about the phenomenon in a lower coefficient of friction with different sleeve force, from 100nt to 200nt. Since a higher sleeve force will result in a higher contact force between sleeve and outer ring, which brings a higher index torque, sleeve force will influence whether the synchronization can finish or not. The simulation results list in Table 4.2-5.

As the increase of sleeve force in a lower coefficient of friction, the cone torque will rise and synchronized time will diminish, shown in Figure 4.2-12. Since cone torque rises with sleeve force, index torque also increases with sleeve force; consequently, while index torque is higher than cone torque before finishing synchronization, the synchronized failure will be happened. Cone torque, index torque, and difference between them were shown in Figure 4.2-12, Figure 4.2-13, and Figure 4.2-14 respectively.

The cone torque, increasing as coefficient of friction increases that was shown in Figure 4.2-15, is due to lubricant that was drained out of gaps between cone and rings. Because cone torque acts on outer ring, and teeth of outer ring contacts with splines of sleeve for yielding index torque, cone torque will influence the value of index torque. For this reason, index torque would rise with cone torque.

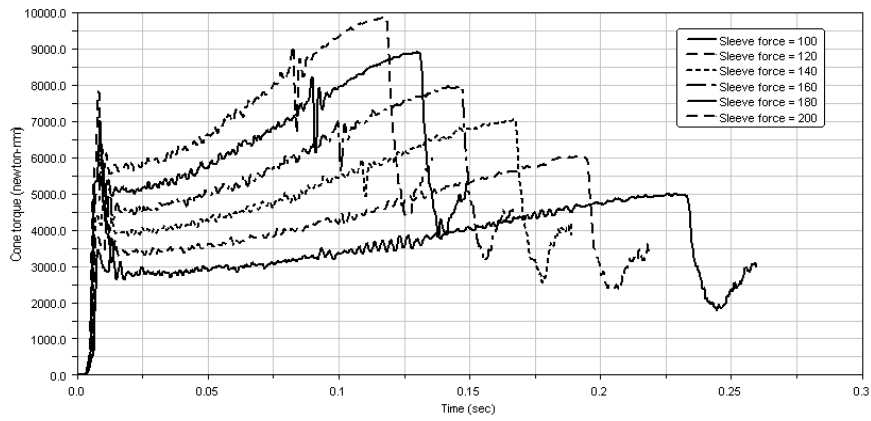


Figure 4.2-12 Cone torque versus time at different sleeve force while $\mu_c = 0.61$

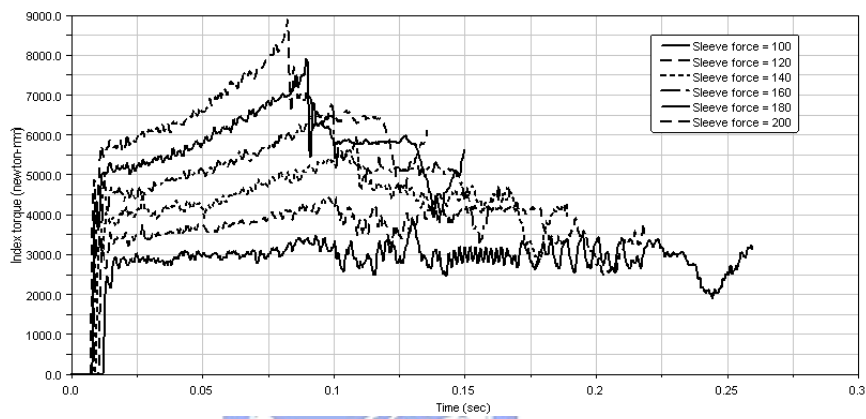


Figure 4.2-13 Index torque versus time at different sleeve force while $\mu_c = 0.61$

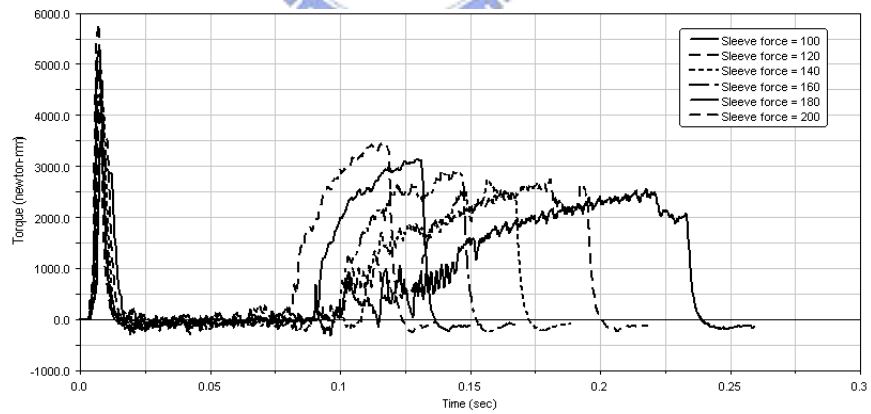


Figure 4.2-14 Difference between cone and index torque

In Figure 4.2-14, considering that while sleeve moves to contact with annular spring, annular spring will push outer ring to yield cone torque, when sleeve did not contact with teeth of outer ring yet, there is a sudden increase at the begin of the simulation. After that, cone and index torque increase together that lead into a small difference between them until

there yield an apparent difference. After a larger difference was yielded on annular spring, index torque starts to decrease, whereas cone torque keeps increasing.

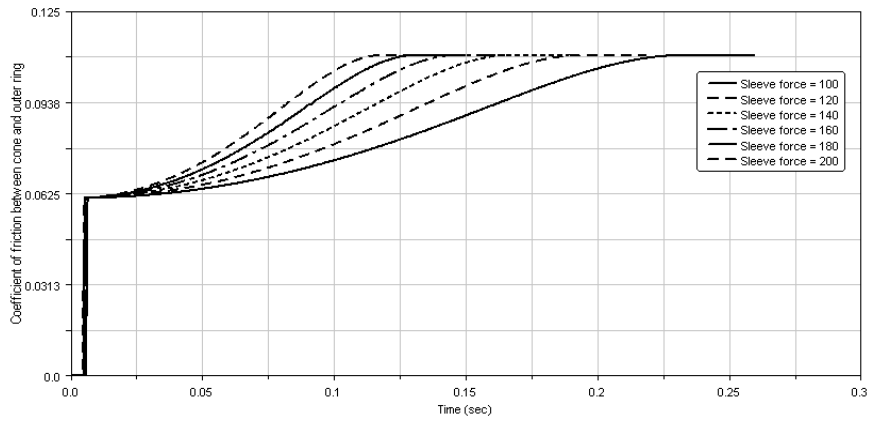


Figure 4.2-15 Coefficient of friction versus time at different sleeve force while $\mu_c = 0.61$

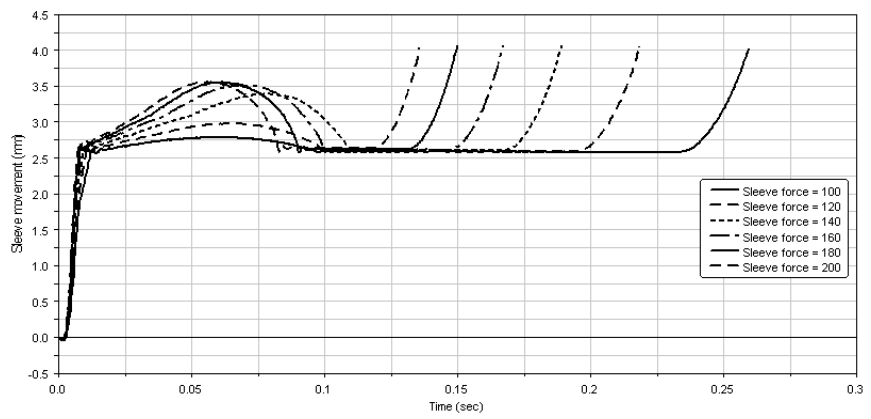


Figure 4.2-16 Sleeve movement versus time at different sleeve force while $\mu_c = 0.61$

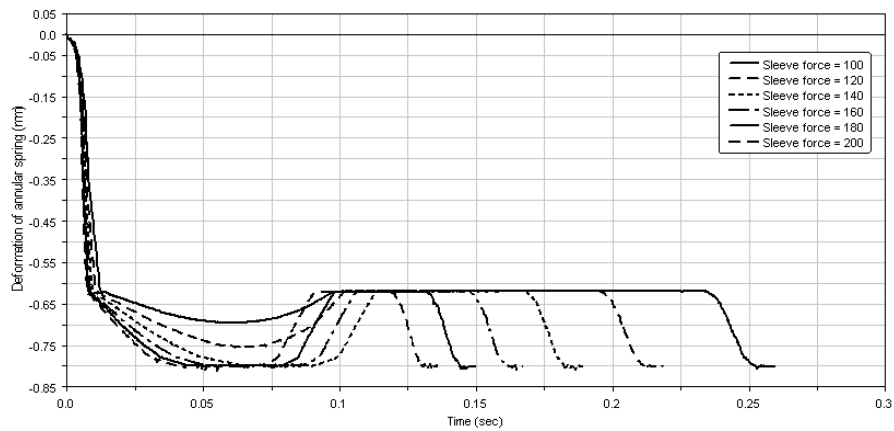


Figure 4.2-17 Deformation of annular spring versus time at different sleeve force while $\mu_c = 0.61$

The movement of sleeve and deformation of annular spring were shown in Figure 4.2-16 and Figure 4.2-17. When index torque is larger than cone torque, there is not enough force to resist sleeve from moving forward clutch gear, so sleeve keeps moving as in Figure 4.2-16. Since deformation of annular spring relates to the position of sleeve, it yields a larger deformation that differs from the normal simulation, as shown in Figure 3.4-7.

When sleeve moves to the position that annular spring achieving middle region in Figure 2.3-5, the resist force from annular spring to sleeve diminishes. Furthermore, cone torque starts to be larger than index cone that makes not only sleeve move backward until the projection of outer ring contact with the restriction on hub, but also sleeve and outer ring keep in the position until finish synchronization.

As the increase of sleeve force or the decrease of cone torque and increase of index torque, cone torque and annular spring friction force act to sleeve probably not high enough to obstruct sleeve moving backward. Consequently, sleeve will moves to engage clutch gear instead of moving backward and keeping at the synchronized position until the relative rotation velocity approaches zero. That is the reason that why the abnormal collision happened.

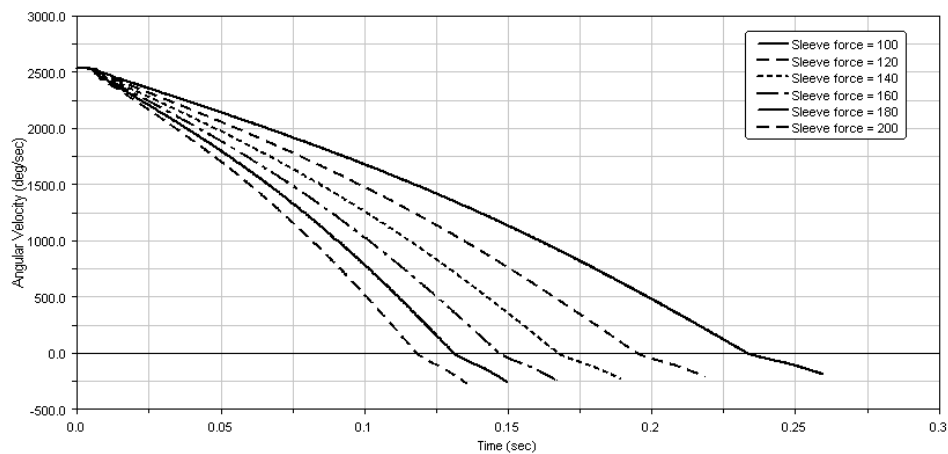


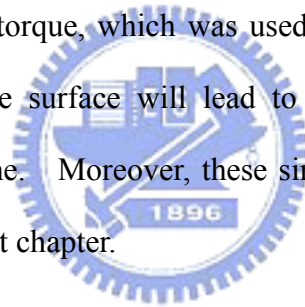
Figure 4.2-18 Relative rotational velocity versus time at different sleeve force while $\mu_c = 0.61$

The relative rotational velocity in a lower coefficient of friction with changeable sleeve force was shown in Figure 4.2-18. Since the cone torque does not stay in a stable value, the relative rotational velocity diminishes like a curve, as mentioned in the previous subsection.

4.2.5 Remark

In this section, the simulation about influence on different parameters with the synchronized time can be noticed. Where sleeve force, cone angle, stiffness of annular, and coefficient of friction on cone surface, were chosen on parameter study, such parameters all would affect the synchronized result in different case.

Stiffness of annular spring will result in different force acting on sleeve and outer ring and take one step ahead the cone torque, which was used to synchronization. Cone angle and coefficient of friction on cone surface will lead to different synchronized torque, which influence the synchronized time. Moreover, these simulation results will be referred to the optimization process in the next chapter.



4.3 Engagement Analysis

After talking about the influence of parameter on synchronization in the synchronized module, this section will mention the influence of parameter on engagement with time in the mesh module. Tooth angle on clutch gear and sleeve are the two main parameters that will be studied in this section.

4.3.1 Tooth Angle

90° tooth angle is according to the layout, which uses to construct the simulation model in the previous chapter. Some different tooth angles, which are 60°, 70°, 80°, 90°, 95°, and 100°,

will be chosen by the thesis to find out the influence of these different values on engagement time in this subsection. The result was shown in Figure 4.3-1.

The peak value and the engagement time are different from tooth angle. These values were shown in Table 4.3-1 and Figure 4.3-2 after arrangement, which can be easily found out that not only the maximum time increases, but also the RMS increases as tooth angle increase. Consequently, tooth angle will yield a certain influence of extent on engagement time.

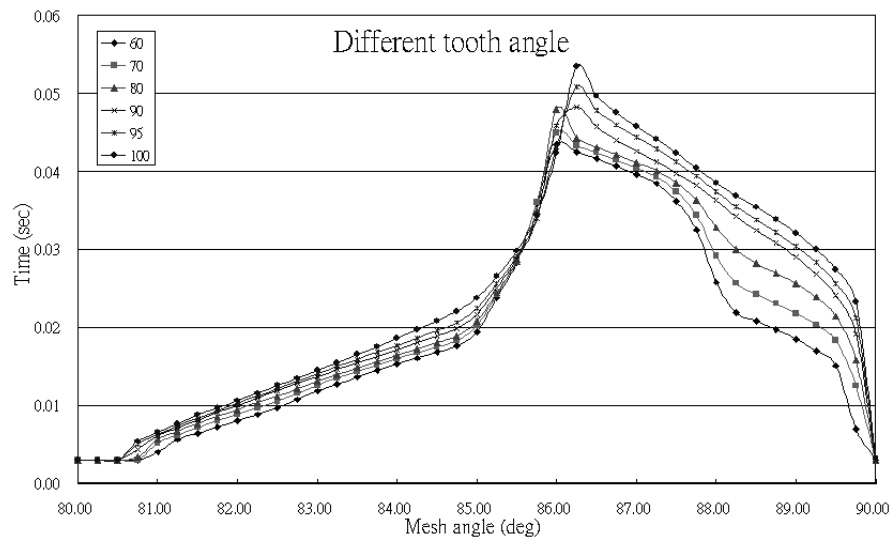


Figure 4.3-1 Mesh time versus different mesh angle with different tooth angle

Table 4.3-1 Simulation results in different tooth angle

Tooth angle (deg)	Max. time	Min. time	RMS	Average
60	0.0434	0.003	0.0225	0.0186
70	0.045	0.003	0.0237	0.0199
80	0.048	0.003	0.0249	0.0211
90	0.0483	0.003	0.0262	0.0223
95	0.0509	0.003	0.0271	0.0231
100	0.0535	0.003	0.0281	0.024

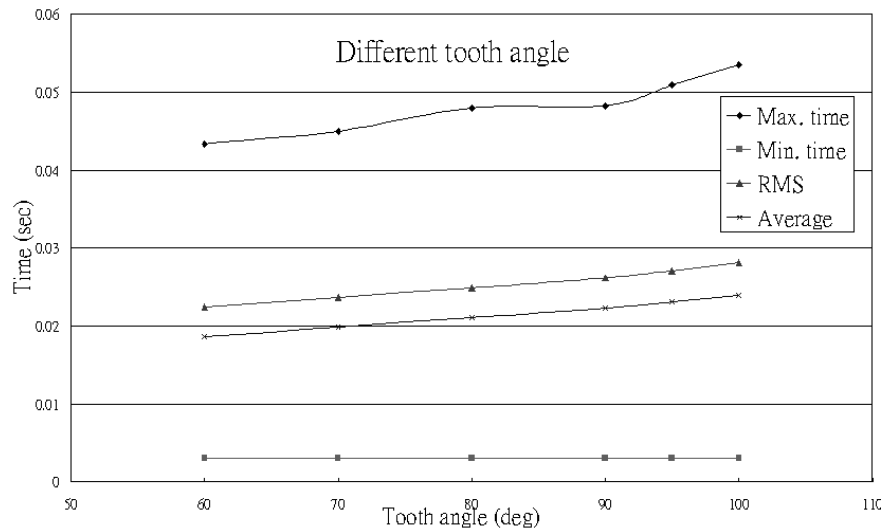


Figure 4.3-2 Plot the data in Table 4.3-1

4.3.2 Sleeve Force

On the study of the influence of sleeve force on engagement time, tooth angle 90°, 100°, and 80° were chosen to take a further understanding that the engagement result from sleeve force and tooth angle in the thesis. The simulation results were shown from Figure 4.3-3 to Figure 4.3-8.

First, in Figure 4.3-3, while the sleeve force that acts on engagement increases, the peak of engagement time will not only rise but also move toward the same rotational direction of clutch gear. Comparing with different angle and force, the peak, while tooth angle equals to 80°, is the lowest as sleeve force equals to 116 N. Nevertheless, while sleeve force diminishes to 26 N, 80° tooth angle will yield the highest maximum time comparing to other two angles. In short, a larger tooth angle will yield a higher engagement time at a higher sleeve force, and a lower engagement time at a lower sleeve force, which is reverse for a small tooth angle.

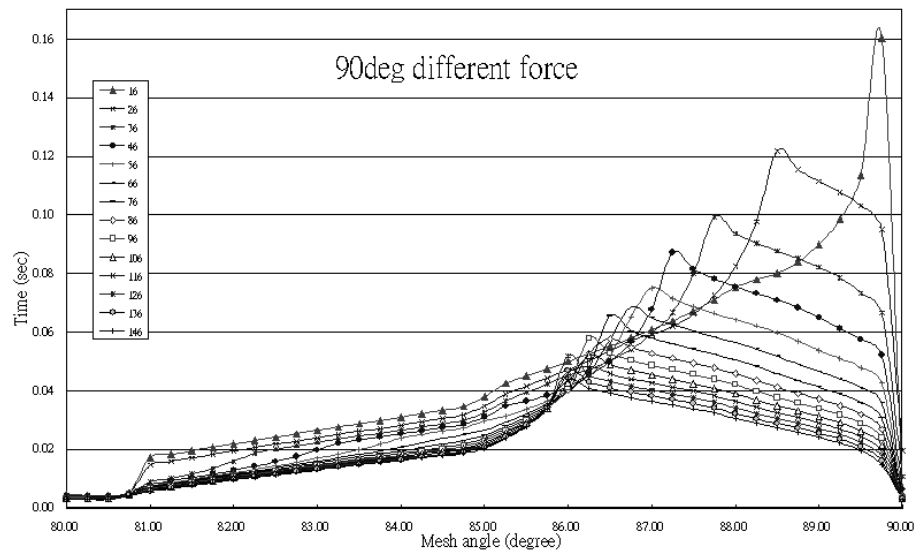


Figure 4.3-3 Mesh time versus different sleeve force while tooth angle = 90°

Table 4.3-2 Simulation results in different sleeve force while tooth angle = 90°

Sleeve force (N)	Max. time	Min. time	RMS	Average
16	0.16	0.0043	0.0561	0.0455
26	0.122	0.0041	0.0567	0.0456
36	0.0993	0.0039	0.0498	0.0406
46	0.0871	0.0037	0.0443	0.0363
56	0.0751	0.0036	0.0397	0.0328
66	0.0685	0.0035	0.0361	0.03
76	0.0656	0.0034	0.0334	0.0279
86	0.0577	0.0033	0.031	0.0261
96	0.058	0.0032	0.0293	0.0247
106	0.0521	0.0031	0.0276	0.0234
116	0.0483	0.003	0.0262	0.0223
126	0.0519	0.003	0.0253	0.0215
136	0.0468	0.0029	0.0241	0.0206
146	0.0438	0.0029	0.0231	0.0198

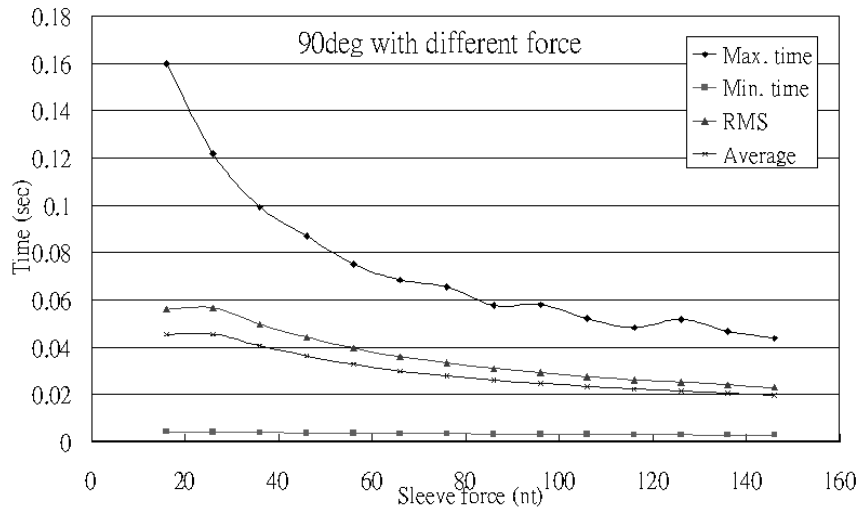


Figure 4.3-4 Plot the data in Table 4.3-2

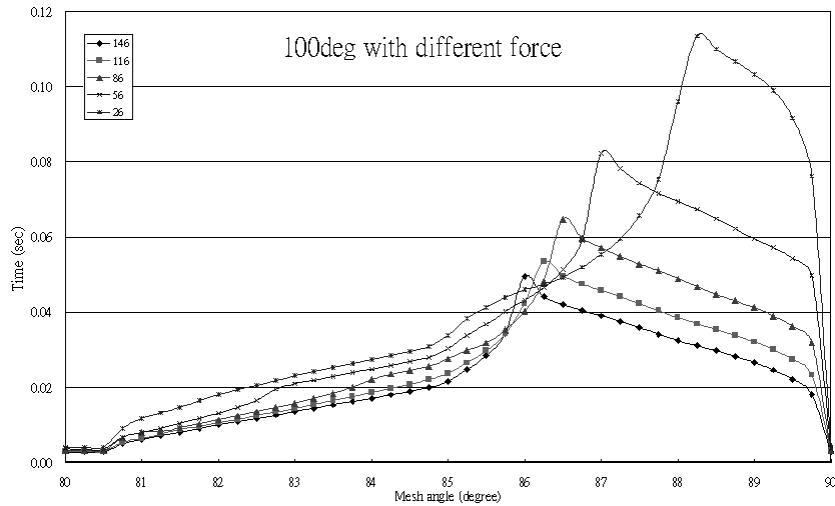


Figure 4.3-5 Mesh time versus different sleeve force while tooth angle = 100°

Table 4.3-3 Simulation results in different sleeve force while tooth angle = 100°

Sleeve force (N)	Max. time	Min. time	RMS	Average
26	0.113	0.0041	0.0544	0.0437
56	0.0823	0.0036	0.0427	0.0356
86	0.0648	0.0033	0.0335	0.0284
116	0.0535	0.003	0.0281	0.024
146	0.0495	0.0029	0.0248	0.0213

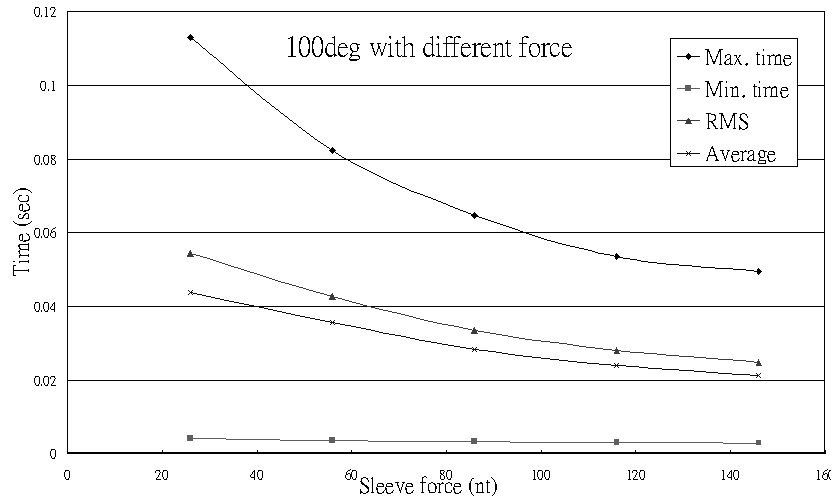


Figure 4.3-6 Plot the data in Table 4.3-3

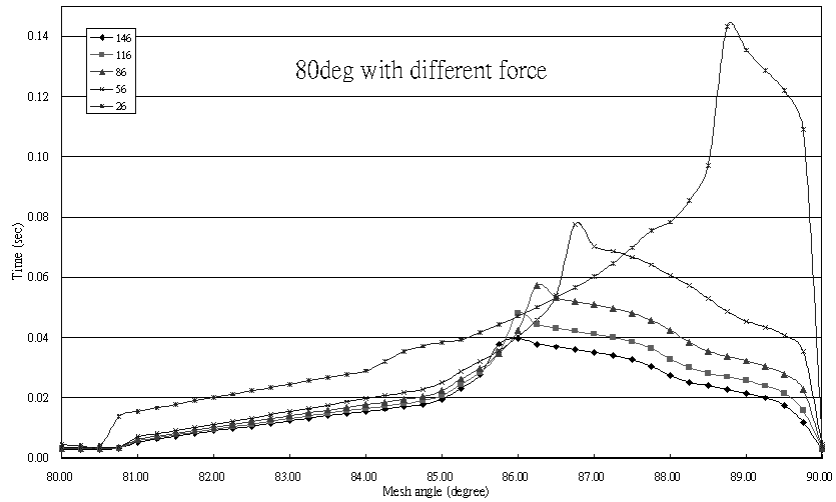


Figure 4.3-7 Mesh time versus different sleeve force while tooth angle = 80°

Table 4.3-4 Simulation results in different sleeve force while tooth angle = 80°

Sleeve force (N)	Max. time	Min. time	RMS	Average
26	0.143	0.0041	0.0608	0.048
56	0.0777	0.0036	0.0375	0.0305
86	0.0573	0.0033	0.0295	0.0246
116	0.048	0.003	0.0249	0.0211
146	0.0396	0.0029	0.0218	0.0187

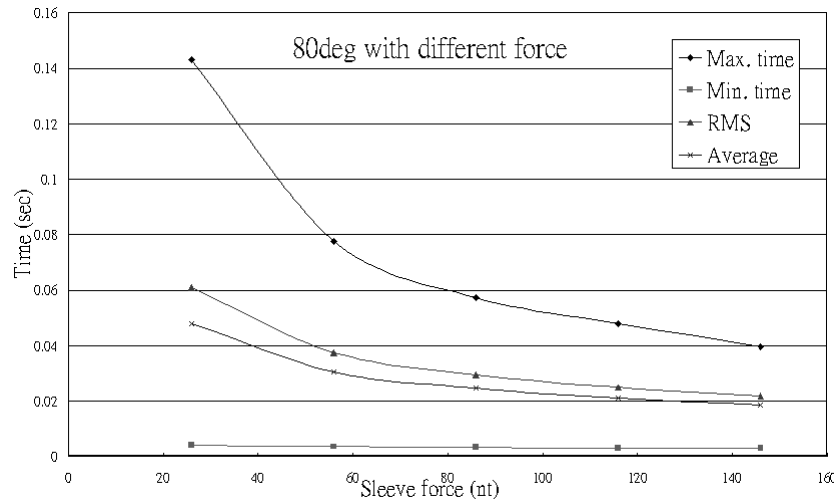


Figure 4.3-8 Plot the data in Table 4.3-4

4.3.3 Remark

Since the mesh module is a random process, in that the engagement position can not be control by designer or driver, the result in the section can provide a roughly general concept of the influence on theses parameter with synchronized performance. Besides, thus result can further provide an aspect of modifying and designing on synchronizer.

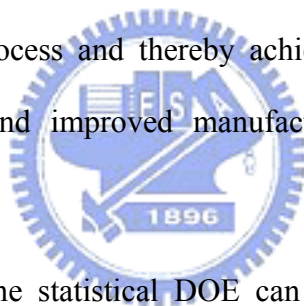
CHAPTER 5

OPTIMIZATION BY TAGUCHI METHOD

5.1 Overview of Taguchi Method

5.1.1 Introduction

In this chapter, the Taguchi method, a powerful problem solving technique for improving process performance, is utilized to optimize a synchronizer. The quality engineering methods was developed from Dr. Taguchi, employing design of experiments (DOE), is one of the most important statistical tools of Total Quality Management (TQM) for designing high quality systems at reducing cost. DOE is a powerful statistical technique for determining the optimal factor setting of a process and thereby achieving improved process performance, reduced process variability and improved manufacturability of products and processes (Rowland et al., 2000).



Dr. Taguchi shows how the statistical DOE can help industrial engineers design and manufacture products that are both of high quality and low cost. Moreover, his approach primarily focuses on eliminating the causes of poor quality and on making product performance insensitive to variation.

Dr. Taguchi has developed a mathematical model, in which loss is a quadratic function of the deviation of the quality of interest from its target value, shown as Figure 5.1-1. The quadratic loss function can meaningfully approximate the quality loss in most situations. When a critical quality characteristic deviates from the target value, it causes a loss. In other words, variation from target is the antithesis of quality. Quality simply means no variability or very little variation from target performance. An improvement drives cost down; lowest cost can only be achieved at zero variability from target. Continuously pursuing variability

reduction from the target value in critical quality characteristics is the key to achieve high quality and reduce cost (Taguchi, 1986; Rowland et al., 2000; Antony and Antony, 2001).

Besides, Taguchi's quadratic loss function is the first operational joining of cost of quality and variability of product that allows design engineers actually to calculate the optimum design based on cost analysis and experimentation with the design.

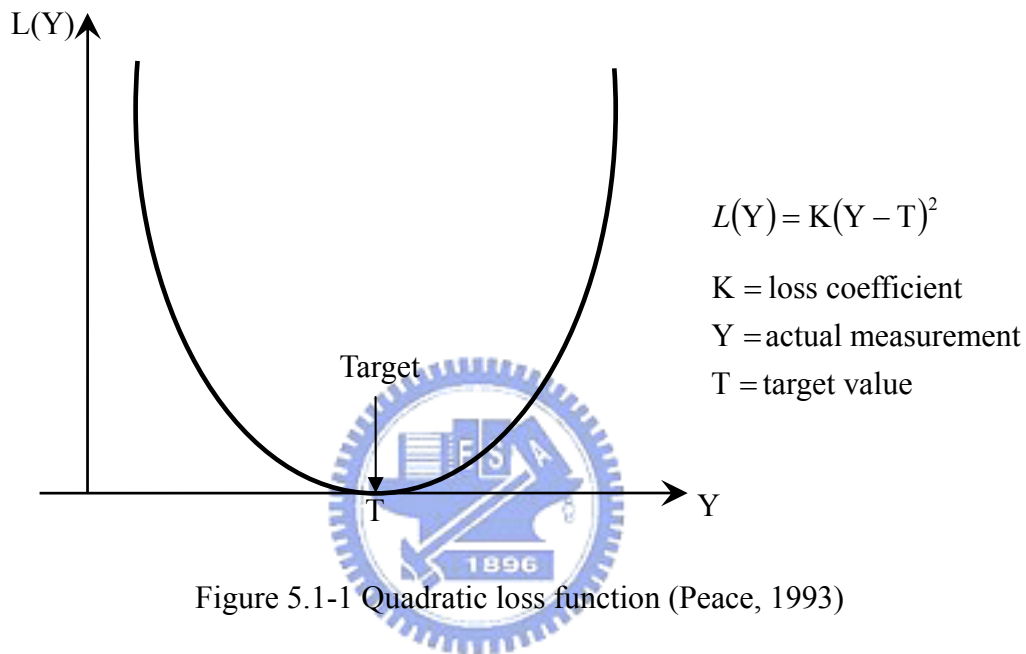


Figure 5.1-1 Quadratic loss function (Peace, 1993)

Traditionally, studying the design parameters one at a time or by trial and error until a first feasible design is found as a common approach to design optimization. However, this leads either to a very long and expensive time spends for completing the design or to a premature termination of the design process due to budget or schedule pressure. The result, in most cases, is a product design, which is far from optimal. By varying design parameters one at a time, for example, the study of 12 design parameters at 4 levels would require 16,777,216, which is equal to 4^{12} , possible experimental evaluations. The time and cost to conduct such a detailed study during advanced design is prohibitive. Naturally, one designer would like to reduce the number of experimental evaluations to a practical point, yet reach a near optimal solution (Antony and Antony, 2001).

Therefore, Dr. Taguchi uses parametric design approach, and provides the design engineer with a systematic and efficient method for determining near optimum design parameters for performance and cost by advocating the use of orthogonal array designs to assign the factors, which are chosen for the experiment. Moreover, the power of the Taguchi method is that it integrates statistical methods into the engineering process.

5.1.2 Steps

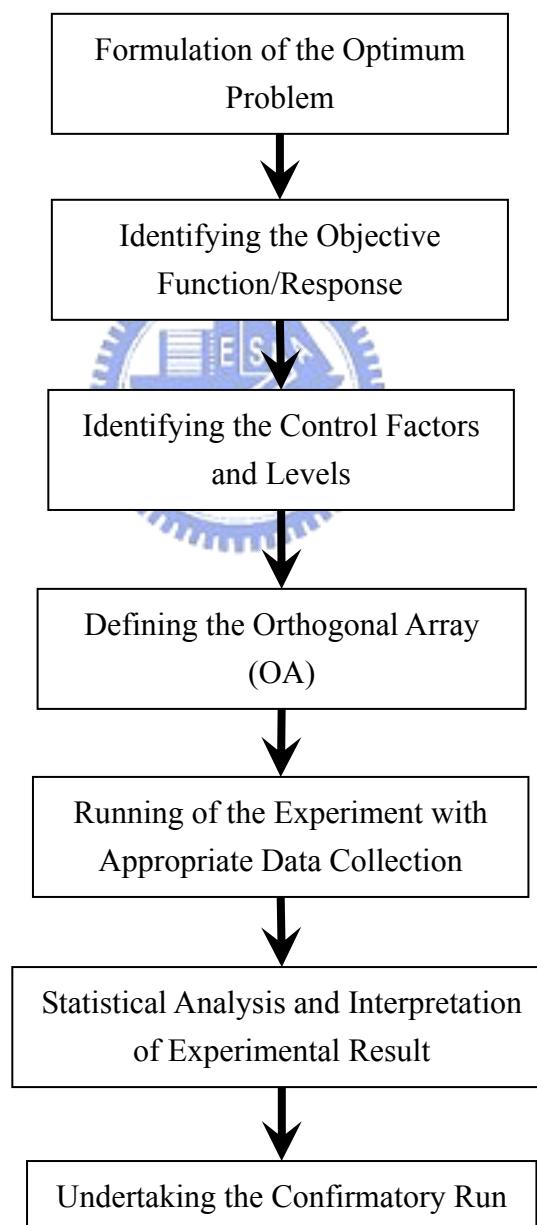


Figure 5.1-2 Flowchart of the Taguchi method

Figure 5.1-2 provides a brief overview of a number of distinct steps followed by Taguchi's approach to parameter design; the details of these steps were described in the following.

Step 1: Formulation of the optimum problem

The first step in the Taguchi method is to determine the quality characteristic to be optimized, since the success of any experiment is dependent on a full understanding of the nature of the problem. The quality characteristic is a parameter whose variation has a critical effect on product quality, and it is the output or the response variable to be observed.

Step 2: Identifying the objective function/response

Constructing the objective function/response is the main purpose in this step. The function establishing in this step will influence the response and following statistical analysis. Therefore, this is an important step, which needs to be confirmed before starting experiment, because the influence will result in different result and effect.

Step 3: Identifying the control factors and levels

Control factors are those parameters that can be set and maintained. This step needs to identify the control factors and their respective levels thought to have significant effects on the quality characteristic. The levels, which refer to the specified value of a setting, for each test parameter must be chosen at this point. The numbers of levels, with associated test values, for each test parameter define the experimental region.

Step 4: Defining the orthogonal array

The next step is to design the matrix experiment and define the data analysis procedure. First, the appropriate orthogonal arrays for the noise and control parameters to fit a specific study are selected. Taguchi provides many standard orthogonal arrays and corresponding linear graphs for this purpose.

Step 5: Running of the experiment with appropriate data collection

Then, the following step is to conduct the matrix experiment and record the results. The Taguchi method can be used in any situation where there is a controllable process. The controllable process can be an actual hardware experiment, systems of mathematical equations, or computer models that can adequately model the response of many products and processes.

Step 6: Statistical analysis and interpretation of experimental result

After the experiments have been conducted, the optimum test parameter configuration within the experiment design must be determined. To analyze the results, the Taguchi method uses a statistical measure of performance called signal-to-noise (S/N) ratio borrowed from electrical control theory. The S/N ratio developed by Dr. Taguchi is a performance measure to choose control levels that best cope with noise. Besides, Analysis of Mean (ANOM) and Analysis of Variance (ANOVA) can use to analyze the factors about how these factors influence experimental results, the objective function.

Step 7: Undertaking the confirmatory run

Using the Taguchi method for parameter design, the predicted optimum setting need not correspond to one of the rows of the matrix experiment. This is often the case when highly fractioned designs are used. Therefore, as the final step, an experimental confirmation is run using the predicted optimum levels for the control parameters being studied.

5.1.3 Response

Energy transformation or response is the most important device that uses to measure the feasibility and cost of objective function. Measurable characteristics are those results that can be measured on a continuous scale. Examples include dimensions, weight, pressure, and clearance; within the framework of measurable characteristics, engineer can subdivide this

classification further into nominal-the-best, smaller-the-better, and larger-the-better characteristics.

The signal-to-noise ratio is one of the major contributions in quality engineering by Dr. Taguchi. The signal-to-noise ratio is often written as S/N ratio or represented by the Greek letter η , whose unit is decibel. The Figure 5.1-3 to Figure 5.1-5 show the S/N ratio on all three responses, whereas Eqs. (5.1-1), (5.1-2), and (5.1-3) show the S/N ratio on smaller-the-better, larger-the-better, and nominal-the-best, respectively.

$$\eta = -10 \times \log \left(\frac{1}{n} \sum_{i=1}^n y_i^2 \right) db \quad (5.1-1)$$

$$\eta = -10 \times \log \left(\frac{1}{n} \sum_{i=1}^n \frac{1}{y_i^2} \right) db \quad (5.1-2)$$

$$\eta = 10 \times \log \left(\frac{\frac{1}{n} (S_m - V_e)}{V_e} \right) db \quad (5.1-3)$$

$$\text{where } S_m = \frac{\left(\sum_{i=1}^n y_i \right)^2}{n} \quad V_e = \frac{\sum_{i=1}^n y_i^2 - S_m}{n-1} \quad (5.1-4)$$

where y_i is the response of each experimental case, V_e is experimental variance, and S_m is sum of the square of the mean.

From the context of ratios stations, engineer should want the S/N to be as larger as possible. To achieve an improvement in the process or product, engineer would likewise wish to increase its signal-to-noise. For the smaller-the-better response, this could mean reducing

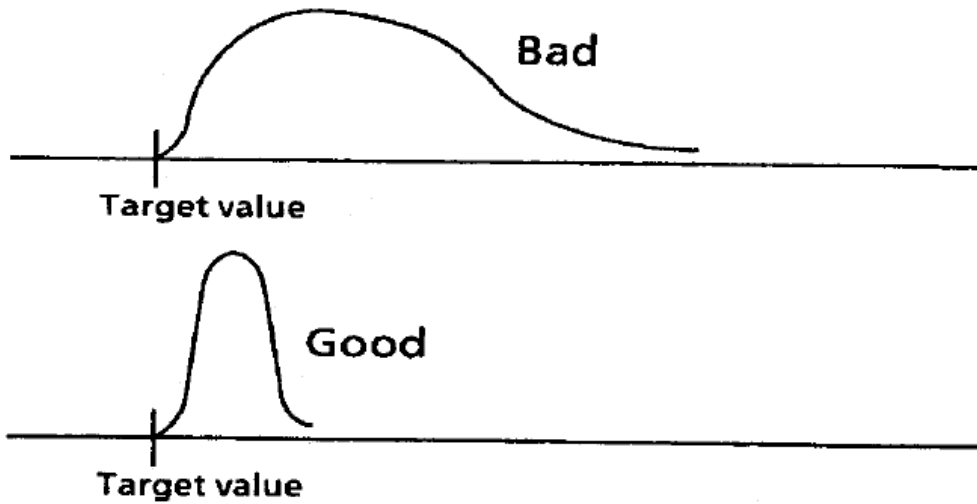


Figure 5.1-3 Smaller-the-better analysis (Phadke, 1989)

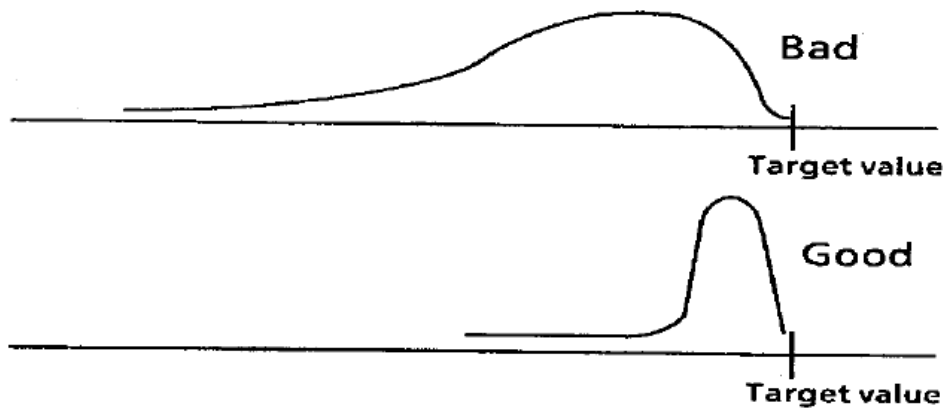


Figure 5.1-4 Larger-the-better analysis (Phadke, 1989)

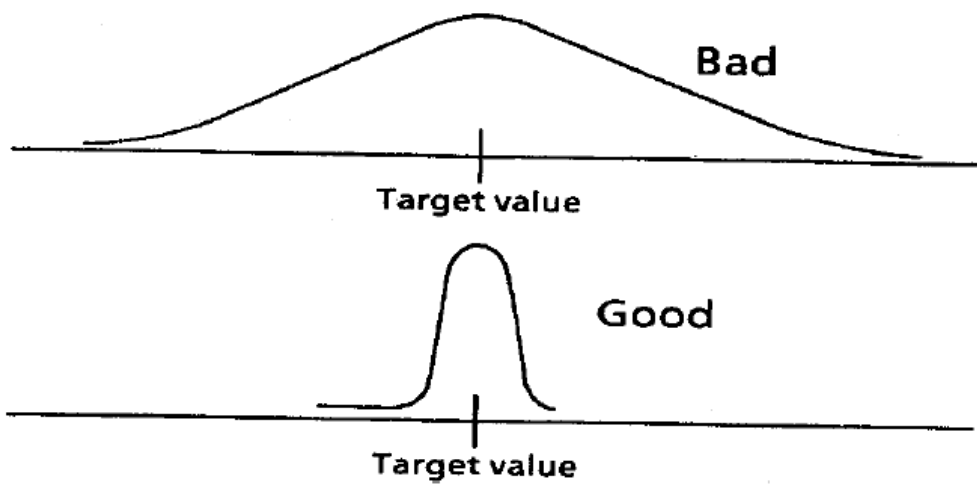


Figure 5.1-5 Nominal-the-best analysis (Phadke, 1989)

the average results or improving the consistency from one unit to the next. The goal in conducting parameter design experiments involving a smaller-the-better response should be to identify those factor settings that will produce the most consistently small response values.

An improvement in the process or resulting product is signified by an increase in the signal-to-noise ratio. With the smaller-the-better response, this meant a decrease in the average results or an improvement in the consistency from one unit to the next. For the larger-the-better response, the S/N increases as the average results increase. Improved consistency or reduced variability between units will again raise the S/N. The goal in conducting parameter design experiments involving a larger-the-better response should be to identify those factor settings that will produce the most consistently large response values.

5.2 Formulation of the Problem

5.2.1 Objective Function/Response



After the construction on simulation model of synchronization, this chapter uses the simulation model to engage in parameter study and optimization. Not enough enduring lifespan is the most important problem that bothers vehicle driver as well as synchronizer designer a lot. Therefore, it will focus on the phenomenon in the thesis, and use Taguchi method to find out the influence that effect from shorter lifespan on several selected parameters. In the following process, it only uses the synchronized module to simulating out the synchronization results while shifting from 1st to 2nd in the thesis, because the mesh module is a random process, and it does not influence if the synchronization finish or not.

Cone surface provides cone torque that synchronizes different rotational velocity between output shaft and input shaft. The synchronization would lose efficacy and lead into engagement without finishing synchronization and abnormal collision between spline on

sleeve and teeth on clutch gear, if cone torque is not higher than index torque. Because lower cone torque always yields from lower coefficient of friction that causes from abrasion, as mentioned in the previous chapter, the objective function will focus on the influence from lower coefficient of friction and whether synchronization can accomplishment or not.

Besides, the coefficient of friction on cone surface results from lubricant that was drained out through threads on outer and inner ring. The more the lubricant drained out, the higher coefficient of friction will be yielded from the contact surface between rings and cone and yield higher cone torque. Furthermore, a higher sleeve force will result in different circumstance, draining out process and increasing coefficient of friction. Consequently, it will engage in two different sleeve forces to realize and make sure the results from higher and lower sleeve force in the thesis.

Sleeve force namely 100 N and 200 N was selected by the thesis to simulate the synchronization. The objective functions describe as the following equations.

$$y_1 = \frac{100}{\mu_1} \tag{5.2-1}$$

$$y_2 = \frac{200}{\mu_2} \tag{5.2-2}$$

where y_1 and y_2 are the objective function on 100 N and 200 N sleeve force, μ_1 and μ_2 are the lowest coefficient of friction that make synchronization can finish on 100 N and 200 N sleeve force respectively.

The experiment would simulate from a lower coefficient of friction rising to a higher coefficient of friction by a gradually increasing, with an interval 0.001, until the synchronization finish in a certain case. The synchronization finish or not that was judged by the movement of sleeve, and the relative rotational velocity between output shaft and input shaft. As sleeve moves to $x = 0$ in Figure 2.3-14, and relative rotational velocity is lower than or approach to zero simultaneously, the simulation stops and the coefficient of friction at

that case is the lowest coefficient of friction that can make synchronizer achieve synchronization without any abnormal collision, which is μ_1 and μ_2 on Eqs. (5.2-1) and (5.2-2).

Considering that the higher the sleeve is and the lower μ_1 and μ_2 are, the synchronizer will have higher potential to stand a higher difference of coefficient of friction, which equal to a lower coefficient of friction, on cone surface. That is the reason why sleeve force divides by the lowest coefficient of friction that can finish the synchronization on Eqs. (5.2-1) and (5.2-2) in the thesis. Therefore, the higher the objective functions are, the higher sufficiency the synchronizer has for finishing the synchronization in a lower coefficient of friction on cone surface. In accordance with the objective function above, larger-the-better analysis was used by the thesis to derive the S/N ratio for discussing the optimization in Taguchi method.

5.2.2 Factors and Levels



After determining the objective function and the quality characteristic by which it will measure the ability to achieve a synchronizer with standing lower coefficient of friction on cone surface in the thesis, it needs to select the independent variables that may have a significant impact on this measurement. The quality characteristic can be thought as the dependent variable, and each of the influences that affects it as an independent variable. Dr. Taguchi and others adopting his methodology typically use the term of factors instead of independent variables, and here will generally conform to this convention (Edwin, 1991).

There are many factors, which are also called parameters, can influence the simulation results on the shifting process of synchronization. Some of these factors, including noise factors and control factors, are already listed in Table 3.3-4 in the previous chapter. In this sub-section, some factors that can be easily controlled and probably have a higher influence on the simulation of synchronization with variation of cone surface will be selected in the

thesis.

Stiffness of annular spring k , cone angle θ_c , teeth angle on sleeve spline and outer ring θ_r , mean cone radius of first cone surface R_{m1} , and mean cone radius of second cone surface R_{m2} was picked by the thesis, as the control factors are chosen in the process of Taguchi method. Seeing that these five factors, except stiffness of annular spring, would all influence the quantity of cone torque, these factors can change the value of cone torque, which relate to whether cone torque is higher than index torque or not. Furthermore, the stiffness of annular spring could influence the circumstance that lubricant was drained out of the gap between cone and rings, and lead into the variation on coefficient of friction.

After finishing the selection of the factors that are going to be changed in the optimization, levels of each factor, which is also named degree of freedom, is the next step that has to decide. Degree of freedom is a measure of the amount of information concerning an item of interest that can be obtained. A general definition is “the number of comparisons that need to be made without being redundant to derive a conclusion.” Within the scope of experimentation, this definition translates into “the number of comparisons between factor or interaction levers that need to be made to determine which level is better and specifically how much better it is.”

Four levels that were defined for each factor in this research were listed in Table 5.2-1. The levels on each factor just like the design variable in optimization; the possibility of these levels has to follow its constrain from the design of the system that use to optimize. Consequently, stiffness of annular spring set from 15 N/mm to 60 N/mm, the cone angle is set from 7° to 8.5° as Eqs. (2.3-9) and (2.3-10), teeth angle on sleeve spline and outer ring is set from 85° to 100° , and mean cone radius on cone surface is set according to the geometric size of synchronizer. These factors and levels will be used to simulate out synchronized results for further discussion of the optimization by Taguchi method.

Table 5.2-1 Control factors and their level of settings for the experiment

Control factor			Level 1	Level 2	Level 3	Level 4
A	k	Stiffness of annular spring (N/mm)	15	30	45	60
B	θ_c	Cone angle (°)	7	7.5	8	8.5
C	θ_r	Spline angle (°)	85	90	95	100
D	R_{m1}	First mean cone radius (mm)	30.5	31	31.5	32
E	R_{m2}	Second mean cone radius (mm)	27	27.5	28	28.5

5.2.3 Orthogonal Array

The foundation for designing an experiment using Taguchi method is the orthogonal array. Although the more classical types of designs, such as the full factorial and any of the wide variety of fractional factorials, could be employed, the orthogonal array has traditionally been associated with Taguchi experiment techniques. This custom does not just because it personifies the nature of experiment as embraced by Dr. Taguchi and has been the primary tool for experiment using this technique, but also the orthogonal array is so efficient in obtaining only a relatively small amount of data and being able to translate it into meaningful and verifiable conclusions. Furthermore, the designs of experiments utilizing orthogonal arrays are basically simple to understand and the guidelines are easy to follow (Taguchi, 1986; Taguchi, 1993).

The choice of a suitable orthogonal array design is critical for the success of an experiment and depends on the total degrees of freedom required to study the main and interaction effects, the goal of the experiment, resources and budget available and time constraints. Orthogonal arrays allow one to compute the main and interaction effects via a minimum number of experimental trials. Degree of freedom refers to the number of fair and

independent comparisons that can be made from a set of observations.

Since these five factors with four levels are chosen to proceed the optimization by Taguchi method, a standard $L_{16}(4^5)$ orthogonal array was selected and listed in Table 5.2-2. Here the notation “L” implies that the information is based on the Latin square arrangement of factors. A Latin square arrangement is a square matrix arrangement of factors with separable factor effects. The number 16 denotes the number of experimental trials. For the synchronization experiment, as the total degrees of freedom is five, the closest number of experimental trials that can be employed for the experiment is 16, L^{16} orthogonal array. The number inside the parentheses denotes the number of levels within each column and the number of columns available within the orthogonal array.

Table 5.2-2 $L_{16}(4^5)$ orthogonal array

	A	B	C	D	E
L_{16}	1	2	3	4	5
1	1	1	1	1	1
2	1	2	2	2	2
3	1	3	3	3	3
4	1	4	4	4	4
5	2	1	2	3	4
6	2	2	1	4	3
7	2	3	4	1	2
8	2	4	3	2	1
9	3	1	3	4	2
10	3	2	4	3	1
11	3	3	1	2	4
12	3	4	2	1	3
13	4	1	4	2	3
14	4	2	3	1	4
15	4	3	2	4	1
16	4	4	1	3	2

5.3 Results and Discussions

In this section, the simulation result for proceeding Taguchi method and further getting the influence on each factor with simulation result are presented. Besides, analysis of mean (ANOM) can decide the optimal value of every factor and the situation that these factors influence on synchronization. Moreover, analysis of variance (ANOVA) can further test the influential extent on all factors to simulation and the optimal design variables. Such results can provide not only a clear correlation between these variables that were selected for optimization, but also an evident understanding of synchronization and an aspect of improvement on synchronization performance.

5.3.1 Simulation Results

Table 5.3-1 Factors, levels, experimental results and S/N ratio for durability

	k	θ_c	θ_r	R_{m1}	R_{m2}	μ_1	y_1	μ_2	y_2	η
L ₁₆	A	B	C	D	E	-	100nt	-	200nt	S/N
1	15	7	85	30.5	27	0.071	1408.450704	0.071	2816.901408	65.016
2	15	7.5	90	31	27.5	0.067	1492.537313	0.068	2941.176471	65.4937
3	15	8	95	31.5	28	0.064	1562.5	0.065	3076.923077	65.8903
4	15	8.5	100	32	28.5	0.061	1639.344262	0.062	3225.806452	66.306
5	30	7	90	31.5	28.5	0.053	1886.792453	0.058	3448.275862	67.3874
6	30	7.5	85	32	28	0.065	1538.461538	0.071	2816.901408	65.6183
7	30	8	100	30.5	27.5	0.052	1923.076923	0.057	3508.77193	67.5495
8	30	8.5	95	31	27	0.062	1612.903226	0.068	2941.176471	66.0206
9	45	7	95	32	27.5	0.042	2380.952381	0.05	4000	69.2281
10	45	7.5	100	31.5	27	0.041	2439.02439	0.049	4081.632653	69.4286
11	45	8	85	31	28.5	0.061	1639.344262	0.074	2702.702703	65.9431
12	45	8.5	90	30.5	28	0.058	1724.137931	0.071	2816.901408	66.3599
13	60	7	100	31	28	0.031	3225.806452	0.042	4761.904762	71.5428
14	60	7.5	95	30.5	28.5	0.037	2702.702703	0.051	3921.568627	69.9584
15	60	8	90	32	27	0.045	2222.222222	0.062	3225.806452	68.2594
16	60	8.5	85	31.5	27.5	0.055	1818.181818	0.076	2631.578947	66.5082

The simulation results were shown on Table 5.3-1; the lowest coefficient of friction on each simulation case and its value of objective function were also shown on the table. Besides, the S/N ratios, which are used to go into the next discussion about ANOM and ANOVA in the following sub-section, derive from larger-the-better analysis, Eq. (5.1-2), and list on the right side of the table.

The data on the table can provide a concept that sleeve force will influence the lowest coefficient of friction without having a steady relation. Different case at different sleeve force will result in dissimilar result. The phenomena will also be discussed in the following sub-section.

5.3.2 Analysis of Mean (ANOM)

The purpose of ANOM is to provide a clear notion for understanding the tendency of the objective function influencing by different label and lever. Moreover, the result of ANOM can also decide the optimum combination of label with their respective level.

The averages of all factors and all levels from different factors have to be calculated at first, following the equations below.

$$m_{Ai} = \frac{1}{n_A} \sum_{i=1}^{L_A} \eta_{Ai} \quad (5.3-1)$$

$$m = \frac{1}{M} \sum_{j=1}^M \eta_j \quad (5.3-2)$$

where A is the name of factor, m_{Ai} is the average of the i_{th} level of factor A, η_{Ai} is the S/N ratio of the i_{th} level of factor A, n_A is the number of the i_{th} level of factor A appear on the orthogonal array, m is the average of all S/N ratio, M is the total number of cases, and η_j is the S/N ratio at the j_{th} experiment.

The calculation results were listed on Table 5.3-2, and the plots of factor effects were

shown on Figure 5.3-1, where exists an undertone line that approximately located at 67.28 S/N ratio is the overall mean value of S/N ratio for all the experimental region defined by the factor levels in Table 5.3-1.

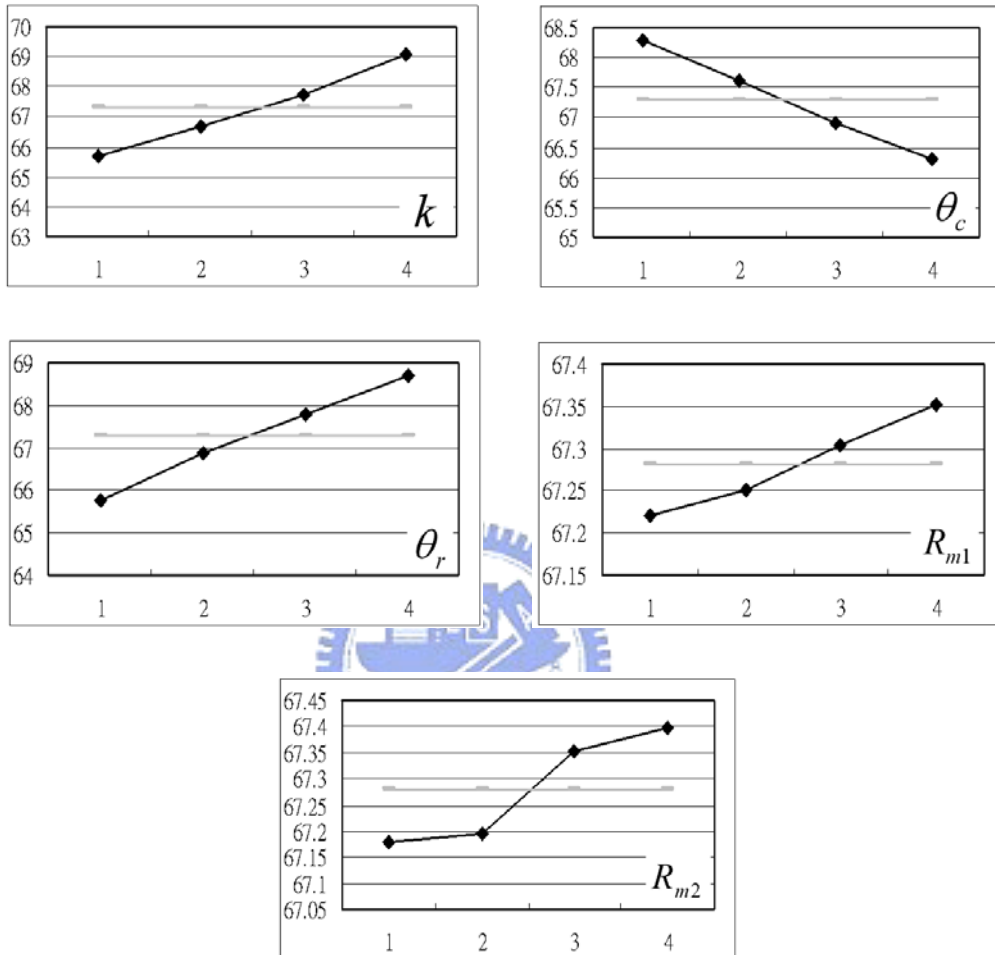


Figure 5.3-1 Plots of factor effects in different labels and levels for durability

Table 5.3-2 S/N ratio of ANOM at different labels and levels for durability

Label \ Level	A	B	C	D	E	Overall
1	65.677	68.29	65.77	67.22	67.181	67.2819
2	66.644	67.62	66.88	67.25	67.195	
3	67.74	66.91	67.77	67.3	67.353	
4	69.067	66.3	68.71	67.35	67.399	

The result from proceeding ANOM can obtain the influence of all these factors with whether synchronization can finish or not. The tendency of every factor can be observed in Figure 5.3-1. The higher the slope was shown on the figure, the higher effect the factor will influence the objective function. Therefore, the stiffness of annular spring and spline angle of sleeve and outer ring dominate a higher influence to the performance of synchronizer as the influence from first and second mean cone radius. Consequently, the value of objective function will suffer a higher variation while the designer modifies stiffness of annular spring and spline angle than cone radius.

Besides, the ANOM can also provide information about the experimental result that the higher the S/N ratios on the figure, the better the objective function will be obtained. Take stiffness and cone angle as examples; the S/N ratio is much higher in the first level than the fourth level, which means that the synchronization performance will increase as the stiffness increase. However, while cone angle increases from first level to fourth level, the slope of ANOM on cone angle is negative, so that a lower cone angle can support a higher synchronized performance on the situation that the coefficient of friction on cone surface decrease than a higher cone angle.

A primary goal in conducting a matrix experiment is to optimize the product or process design, which is to determine the best or the optimum level for each factor. The optimum level for a factor is the level that gives the highest value of S/N ratio in the experimental region.

Form Figure 5.3-1, there can determine the optimum level for each factor as the level that has the highest value of S/N ratio. Thus, the stiffness of annular spring is 60 N/mm, cone angle is 7°, spline angle is 100°, first mean cone radius is 32 mm, and second mean cone radius is 28.5 mm, which can show as $A_4B_1C_4D_4E_4$. Based on the ANOM, there can conclude that the settings mentioning above would give the highest S/N ratio and that case

can rise the performance of synchronization while suffer a larger difference on cone surface coefficient of friction.

5.3.3 Analysis of Variance (ANOVA)

Different factors affect the synchronization relating to a different degree. The relative magnitude of the factor effects could be judged from Table 5.3-2, which gives the average S/N ratio for each factor lever and have be mention in the previous sub-section. A better feel for the relative effect of the different factors can be obtained by the decomposition of variance, which is commonly called analysis of variance (ANOVA). ANOVA is needed for estimating the error variance for the factor effects and variance of the prediction error.

Correction factor (CF):

$$CF = \frac{\left(\sum_{i=1}^n \eta_i \right)^2}{M} \quad (5.3-3)$$



Total sum of square (S_T):

$$S_T = \sum_{i=1}^n \eta_i^2 - CF \quad (5.3-4)$$

Degree of freedom (f):

$$f_i = p_i - 1 \quad (5.3-5)$$

Sum of square (S):

$$S_i = \left(\frac{(i_1)^2}{m_1} + \frac{(i_2)^2}{m_2} + \frac{(i_3)^2}{m_3} + \dots + \frac{(i_p)^2}{m_p} \right) - CF \quad (5.3-6)$$

Sum of square due to error (Se):

$$S_e = S_T - \sum_{i=1}^n S_i \quad (5.3-7)$$

Variance (V):

$$V_i = \frac{S_i}{f_i} \quad (5.3-8)$$

Variance ratio (F):

$$F = \frac{S_i}{S_e f_i} \quad (5.3-9)$$

Contribution (ρ):

$$\rho_i(\%) = \frac{S_i}{S_T} \quad (5.3-10)$$

where η is S/N ratio, i is the name of factor, p is the number of level, and m_i is the experimental number on p_{th} of factor i . Besides, sum of square was used by the thesis to compute probability in each factor.

The number of independent parameters associated with an entity like a matrix experiment, or a factor or a sum of squares is called its degrees of freedom. The estimation of error variance can be approximately obtained by polling the sum of squares corresponding to the factors having the lowest mean square. The sum of squares corresponding to the bottom half of the factors corresponding to about half of the degrees of freedom can be used to estimate the error mean square or error variance.

The variance ratio is the ratio of the mean square due to a factor and the error variance. A large value of F means the effect of that factor is large compared to the error variance. Moreover, the larger value of F , the more important that factor is in influencing the process response S/N ratio. So, the values of F can be used to rank order the factors. As for contribution, it is used to express the potential of factors that influences the quality and value of objective function.

The ANOVA result was shown on Table 5.3-3, where SOV is source of variance.

Table 5.3-3 Analysis of variance for durability

SOV	f	S	V	F	ρ (%)
A	3	25.52552	8.508508	45.59361	47.64574
B	3	8.982706	2.994235	16.04488	16.76705
C	3	18.87873	6.29291	33.72112	35.23888
D	3	0.041002	0.013667	0.022955	0.076535
E	3	0.145614	0.048538	0.260095	0.271802
(e)	(6)	(0.186616)	(0.031103)	(0.166667)	(0.348336)
Total	15	53.76019	-	-	100

Since the sum of square is low in factor D and E on the ANOVA results, these two factors as the estimation of error variance was chosen in the thesis. It can be found that stiffness of annular spring, factor A, own a higher potential to influence the experiment result, the objective function. That means a smaller change on factor can yield a larger influence on objective function than other factors. Besides, factor A also has the largest value of F, so it also means that factor A can influence objective function more than the error variance.



5.3.4 Confirmation Run and Discussions

After the discussion on Taguchi method, the thesis has already provided the correlation of sensitivity, influence and parameters for the objective function on all the factors. In this sub-section, the thesis will affirm the confirmation run if it can provide a better case that raise the performance of synchronization as anticipation. The compared result was listed on Table 5.3-4 as below.

Table 5.3-4 Optimization result for durability

	Level combination	k	θ_c	θ_r	R_{m1}	R_{m2}	μ_1	μ_2	η
Initial design	A ₁ B ₁ C ₁ D ₁ E ₁	15	7	85	30.5	27	0.071	0.071	65.0160
Optimal result	A ₄ B ₁ C ₄ D ₄ E ₄	60	7	100	32	28.5	0.031	0.041	71.6076

The optimization case can suffer a higher difference on coefficient of friction on cone

surface than the initial design. Furthermore, the higher the spline angle, the higher the performance, since that the index torque will diminish as the spline angle increase. The contact force between spline of sleeve and teeth of outer ring can be divided into two forces, one is parallel to transmission shaft, and the other is perpendicular to the first separated force, as showing in Figure 2.3-8, where the two forces are $N\cos\frac{\theta_r}{2}$ and $N\sin\frac{\theta_r}{2}$.

Index torque will decrease while the spline angle increase, so the lower index torque would have much opportunity to stay lower than cone torque. Consequently, on the condition of a larger spline angle, the synchronizer will keep work while the coefficient of friction is much lower. Besides, the larger spline angle will also obtain a higher force using to push outer ring and then yield cone torque to synchronization, so the synchronized time will also decrease while the spline angle increase.

Nevertheless, a lower index torque, yielding from a larger spline angle, will obtain another problem. The force, used to obtain index torque, will be further used to push outer ring rotating in the reverse direction for sleeve to engage with outer ring after finishing synchronization. Therefore, if the force is so small that the synchronizer will spend much more time on the engagement between sleeve and outer ring that will also increase the shifting time. For this reason, the increase of spline angle has also need to consider these problems mentioning above.

As to stiffness of annular spring, although a higher stiffness will enhance the potential that synchronizer can bear a lower coefficient of friction, excessively high stiffness probably lead into too much resistant force exerting on sleeve force. In that the problem of an excessively higher annular spring may occur to sleeve, the stiffness can not increase boundlessly.

5.3.5 Synchronized Time

After talking about the optimization on durability of synchronizer, the thesis also mentioned about the influence on the same factors and levels, listed on Table 5.2-1, with synchronized time by Taguchi method.

The simulation results, factors, levels, and S/N ratio were shown in Table 5.3-5, where the objective function is synchronized time, which is y_3 on the table, and small-the-better analysis was used by the thesis to derive the S/N ratio for discussion the synchronized time.

	k	θ_c	θ_r	R_{m1}	R_{m2}	y_3	η
						t_s	
L ₁₆	A	B	C	D	E	-	S/N
1	15	7	85	30.5	27	0.0855	21.3656
2	15	7.5	90	31	27.5	0.0897	20.9447
3	15	8	95	31.5	28	0.0939	20.5457
4	15	8.5	100	32	28.5	0.0980	20.1778
5	30	7	90	31.5	28.5	0.0819	21.7343
6	30	7.5	85	32	28	0.0876	21.1498
7	30	8	100	30.5	27.5	0.0963	20.3281
8	30	8.5	95	31	27	0.1020	19.8288
9	45	7	95	32	27.5	0.0825	21.6679
10	45	7.5	100	31.5	27	0.0897	20.9414
11	45	8	85	31	28.5	0.0939	20.5437
12	45	8.5	90	30.5	28	0.1011	19.9010
13	60	7	100	31	28	0.0833	21.5921
14	60	7.5	95	30.5	28.5	0.0889	21.0176
15	60	8	90	32	27	0.0947	20.4726
16	60	8.5	85	31.5	27.5	0.1004	19.9688

Table 5.3-5 Experimental result for discussing synchronized time

The results from proceeding ANOM, listed on Table 5.3-6 and shown in Figure 5.3-2, can provide observation about the influence of all these factors with synchronized time.

Table 5.3-6 S/N ratio of ANOM at different labels and levels for synchronized time

Label \ Level	A	B	C	D	E	Overall
1	20.758	21.590	20.757	20.653	20.652	20.763
2	20.760	21.013	20.763	20.727	20.727	
3	20.763	20.472	20.765	20.797	20.797	
4	20.762	19.969	20.759	20.86	20.868	

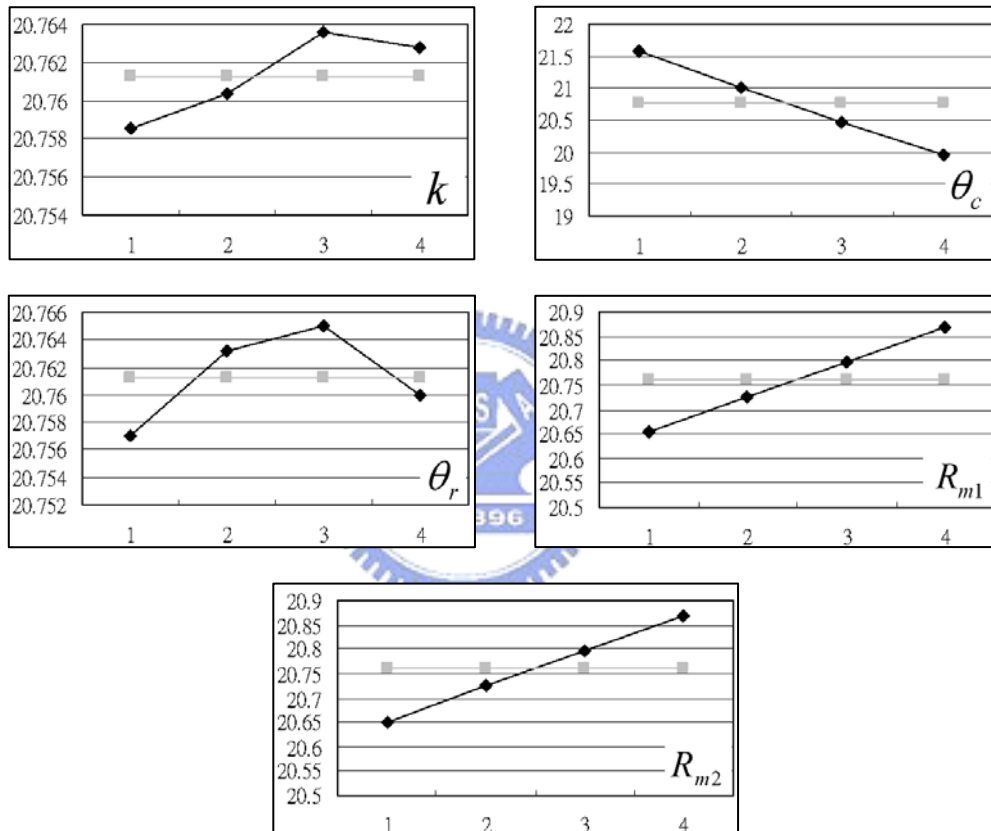


Figure 5.3-2 Plots of factors effects in different labels and levels for synchronized time

In Figure 5.3-2, the undertone line is the overall mean value of S/N ratio for all experimental regions. It can be easier found out that there is a limit on stiffness of annular spring and spline chamfer angle, which is different from the result talking about durability, among these effects on different factors. Hence, although a higher value on these two factors will bring a higher durability, the synchronized time will become worse if these two factors larger than certain value.

Table 5.3-7 Analysis of variance for synchronized time

SOV	f	S	V	F	ρ (%)
A	3	25.59648	8.532159	11.35826	34.318202
B	3	29.31476	9.771587	13.00823	39.303456
C	3	18.92329	6.307763	8.397083	25.371199
D	3	0.270277	0.090092	0.609085	0.3623715
E	3	0.48090	0.160303	0.2134	0.6447717
(e)	(6)	(0.75118)	(0.12519)	(0.16666)	(1.007143)
Total	15	75.3369	-	-	100

The different between durability and synchronized time by Taguchi method can also be found out from ANOVA. In the case of discussing synchronized time, stiffness of annular spring and cone angle occupy higher influence than other factors that are different from the case of discussing durability. Consequently, the designer or research worker can modify the factors that will influence a lot on the aspect, on which they pay much attention. Therefore, a new type of synchronizer will be produced to face and solve different kind of demands on vehicle transmission.



CHAPTER 6

CONCLUSIONS AND FUTURE WORKS

6.1 Conclusions

The analytic model is necessarily constructed for understanding the action of synchronization because of the following reasons. The first reason is to improve the performance of synchronization and operational comfort of controlling vehicle. Moreover, another reason is that these phenomena occur irregularly in very short time, and the gear shifting mechanism is complex.

The entire simulation model of synchronization and separated modules, which simulate shift from 1st gear ratio to 2nd gear ratio, were constructed in this thesis by ADAMSTM. Displacement of sleeve, relative rotational velocity, cone torque, index torque, deformation of annular spring, coefficient of friction on cone surface, and relative rotational displacement, which can help to realize the action of components during shifting process, had been observed from the entire analytic model of synchronization.

Besides, the simulation results from separated modules can assist to understand random mesh process between sleeve and clutch gear. Among these possible mesh situations had been divided into four different sections that can describe different mesh cases. The results from these sections can help to realize the phenomena of random mesh between sleeve and clutch, and assist to find out and improve shifting time.

Moreover, the parametric study chooses some parameters that probably have a larger influence on the synchronization to figure out the variation and correlation between parameters and simulation result. The results were used to help to engage in optimization by Taguchi method. The optimization found out that stiffness of annular spring, and spline angle on teeth of sleeve and outer ring will dominate a higher contribution on the objective

function, finishing synchronization in a much lower coefficient of friction on cone surface.

The results on this thesis can provide not only a clear understanding on the detail synchronization during shifting process, but also an aspect that can improve the performance of synchronizer while design or modify one.

6.2 Future Works

There are some suggestions that can provide a way on the improvement of this area in the future as listed below.

1. In the simulation model, the sleeve force was assumed as step force, which approximately according to the shifting force on the previous literature. However, in the reality use, no matter the shifting force was exerted from driver in manual transmission or actuator in automated manual transmission, the force would not just actually equal to the step function, as used in the simulation model on this thesis. Although the assumption on sleeve force is reasonable, such assumption has to be confirmed that the change of sleeve curve if it influences the simulation a lot or not.
2. Since the synchronizer uses cone torque, which results from friction, to synchronize the different relative rotational velocity, there must bring a large number heat that will influence synchronization, such as the study by Kinugasa et al. (1999). The phenomenon, neglected in this thesis, probably should incorporate into the simulation model for obtaining a higher accuracy model of synchronization.
3. As the discussions on Chapter 5 about the influence of stiffness of annular spring and spline angle, both these two parameters can influence the performance a lot. Although Chapter 5 had already provided a direction to modify synchronizer, these

two parameters both had its limit that will lead into another drawback. Stiffness of annular spring, for example, can not increase limitless despite the higher the stiffness is, the higher the performance will be. That is the same as spline angle. However, it did not mention the limit of these parameters that consider both durability and shifting time in this thesis, so the future work should be able to find out such limit in order to design a synchronizer with higher shift capacity, potential, and performance.

As long as the use of synchronizer, the device always needs to be analyzed and improved, without limits, for providing a great progress on vehicle transmission all the time (Satoh et al., 2003). In addition, hoping the simulation model and results, and optimization results can assist the following research on manual transmission gearbox in the future.



REFERENCES

ADAMS™ User Manual, Mechanical Dynamics, Inc, 2003.

Antony, J., and Antony, F. J., “Teaching the Taguchi method to industrial engineers,” MCB University Press, Work Study, Vol. 50, No. 4, 2001, pp. 141-149.

Arora, J. S., Introduction to Optimum Design, McGraw-Hill, New York, 2004.

Bansbach, E. A., “Development of a Shift by Wire Synchronized 5-Speed Manual Transmission,” SAE Special Publications, Vol. 1324, 980831, 1998, pp. 119-125, Detroit, MI, USA.

Crouse, W. H., and Anglin, D. L., Automotive Mechanics, McGraw-Hill, New York, 1985.

Edwin, B., “Taguchi Approach to Design Optimization for Quality and Cost: An Overview,” International Society of Parametric Analysis, 1991.



Fernandez, J. R., “Synchronizer,” US Patent No. 6,588,562, 2003.

Fujiwara, H., “Synchronizer Ring,” US Patent No. 4,998,445, 1991.

Hamrock, B. J., Jacobson, B., and Schmid, S. R., Fundamentals of Machine Elements, WCB/McGraw-Hill, Boston, 1999.

Hoshino, H., “Analysis on Synchronization Mechanism of Transmission,” SAE Technical Paper Series, 1999, Detroit, MI, USA.

Hoshino, H., “Simulation on Synchronization Mechanism of Transmission Gearbox,” International ADAMS User Conference, 1998.

Jackson, G. A., “Synchronizer,” US Patent No. 6,729,457 B2, 2004.

Kelly, D., and Kent, C., “Gear Shift Quality Improvement in Manual Transmissions Using Dynamic Modeling,” FISITA World Automotive Congress, 2000, Seoul, Korea.

Kim, E., Sung, D., Seok, C., Kim, H., Song, H., Lim, C., and Kim, J., “Development of Shift Feeling Simulator for a Manual Transmission,” SAE Technical Paper Series, 2002, Paris, France.

Kinugasa, T., Ishii, H., Shozaki, H., Takami, K., “Thermal Analysis of the Synchronizer Friction Surface and its Application to the Synchronizer Durability Improvement,” JSAE Review, Vol. 20, No. 2, 1999, pp. 217-222.

Komatsuzaki, K., and Okazaki, Y., “Double-Cone Synchronizer With Paper Lining for Medium Duty Trucks,” SAE Transactions, Vol. 99, No. Sect 2, 902278, 1990, pp. 928-932, Detroit, MI, USA.

Murata, S., Mori, Y., Doi, T., Takada T., and Noguchi Y., “Synchronizer and Shift System Optimization for Improved Manual Transmission Shiftability,” SAE Technical Paper Series, 891998, 1989, Dearborn, MI, USA.

Ore, T. G., Nellums, R. A., and Skotnicki, G., “Improved Synchronizers for Truck Transmissions,” SAE Technical Paper Series, 952602, 1995, Winston-Salem, NC, USA.

Peace, G. S., Taguchi Methods: A Hands-On Approach, Addison-Wesley, Massachusetts, 1993.

Phadke, M. S., Quality Engineering Using Robust Design, Prentice Hall, New Jersey, 1989.

Razzacki, S. T., “Synchronizer Design: A Mathematical and Dimensional Treatise,” SAE Technical Paper Series, 2004, Detroit, MI, USA.

Razzacki, S. T., and Holbrook, G.L., “Strutless Synchronizer,” US Patent No. 4,776,228, 1988.

Rowland, H., Antony, J., and Knowles, G., “An Application of Experimental Design for Process Optimisation,” The TQM Magazine, MCB University Press, Vol. 12, No. 2, 2000, pp. 78-83.

Satoh, K., Shintani, M., Akai, S., Hiraiwa, K., “Development of a New Synchronizer with the Lever Mechanism,” JSAE Review, Vol. 24, No. 1, 2003, pp. 93-97.

Sigl, L. S., Höhn, B. R., “Processing and Performance of PM Synchronizer Rings with Friction Linings,” European Congress and Exhibition on Powder Metallurgy, 2003, Valencia, Spain.

Socin, R. J., Walters, L. K., “Manual Transmission Synchronizers,” SAE Technical Paper Series, 680008, 1968, pp. 31-65.

Szadkowski, A., “Shiftability and Shift Quality Issues in Clutch-Transmission Systems,” SAE Special Publications, Vol. 100, No. Sect 2, 912697, 1991, pp. 618-628.

Taguchi, G., Introduction to Quality Engineering: Designing Quality into Products and Processes, Asian Productivity Organization, Tokyo, 1986.

Taguchi, G., Taguchi on Robust Technology Development, ASME Press, New York, 1993.

Youk, Y. C., “Synchronizer for a Manual Transmission,” US Patent No. 6,848,554 B2, 2005.

